PHOTON 2019

Frascati - 5 June 2019

Unveiling the gamma-ray background through its anisotropies

Michela Negro
INFN of Torino
michela.negro@to.infn.it

INFN Istituto Nazionale di Fisica Nucleare

fermi Gamma-ray Space Telescope

Vela Project

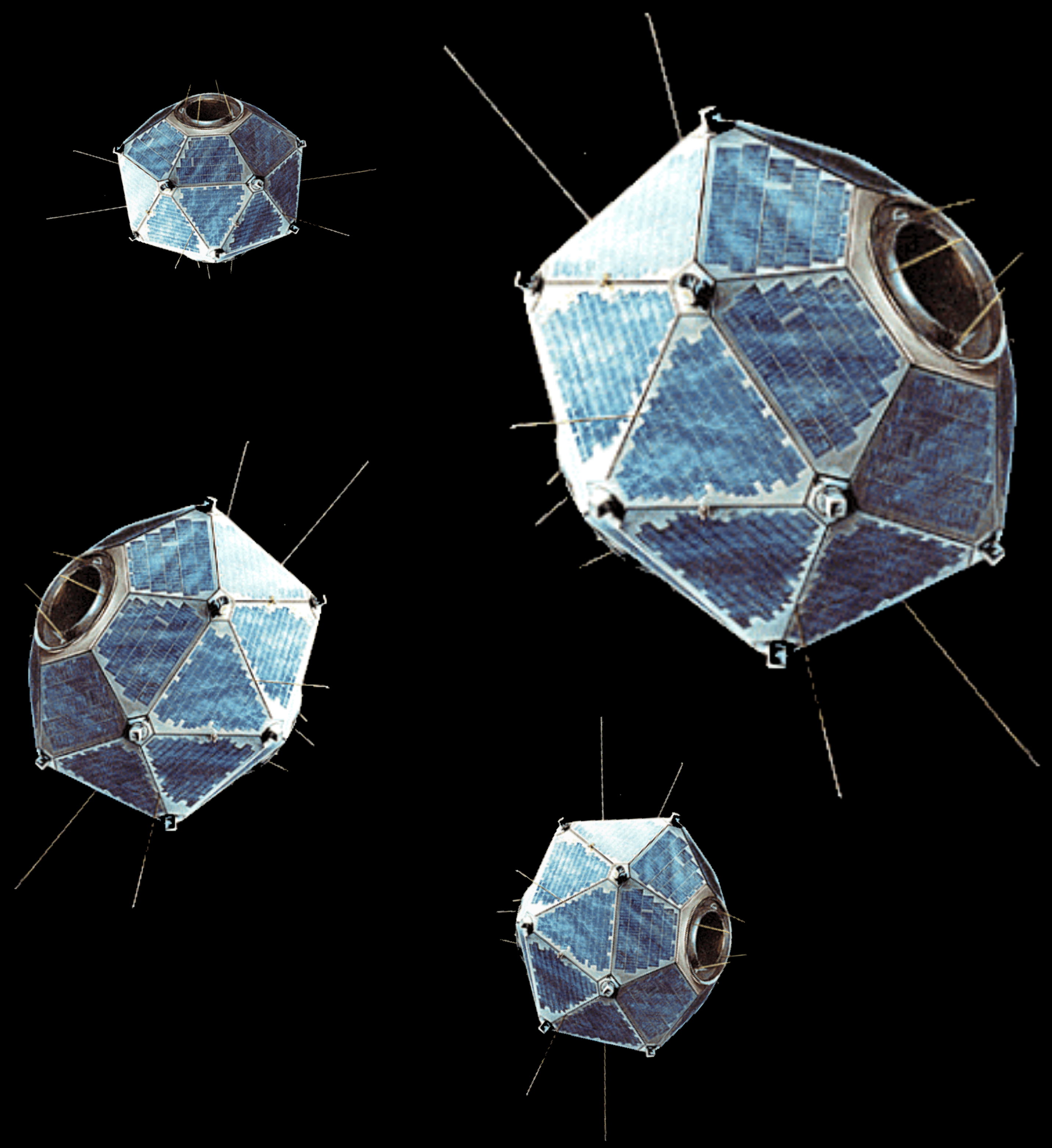

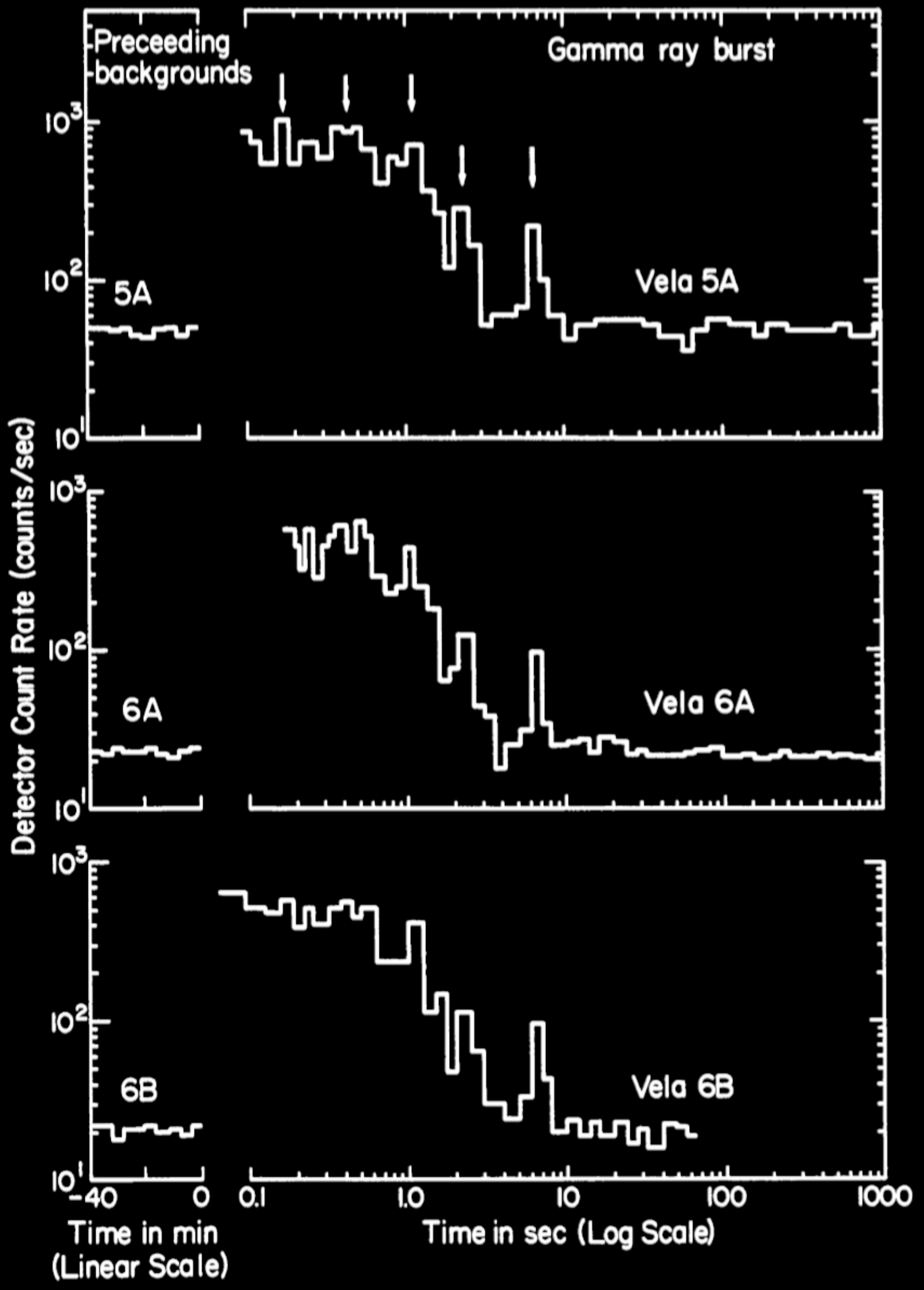

OSO-3

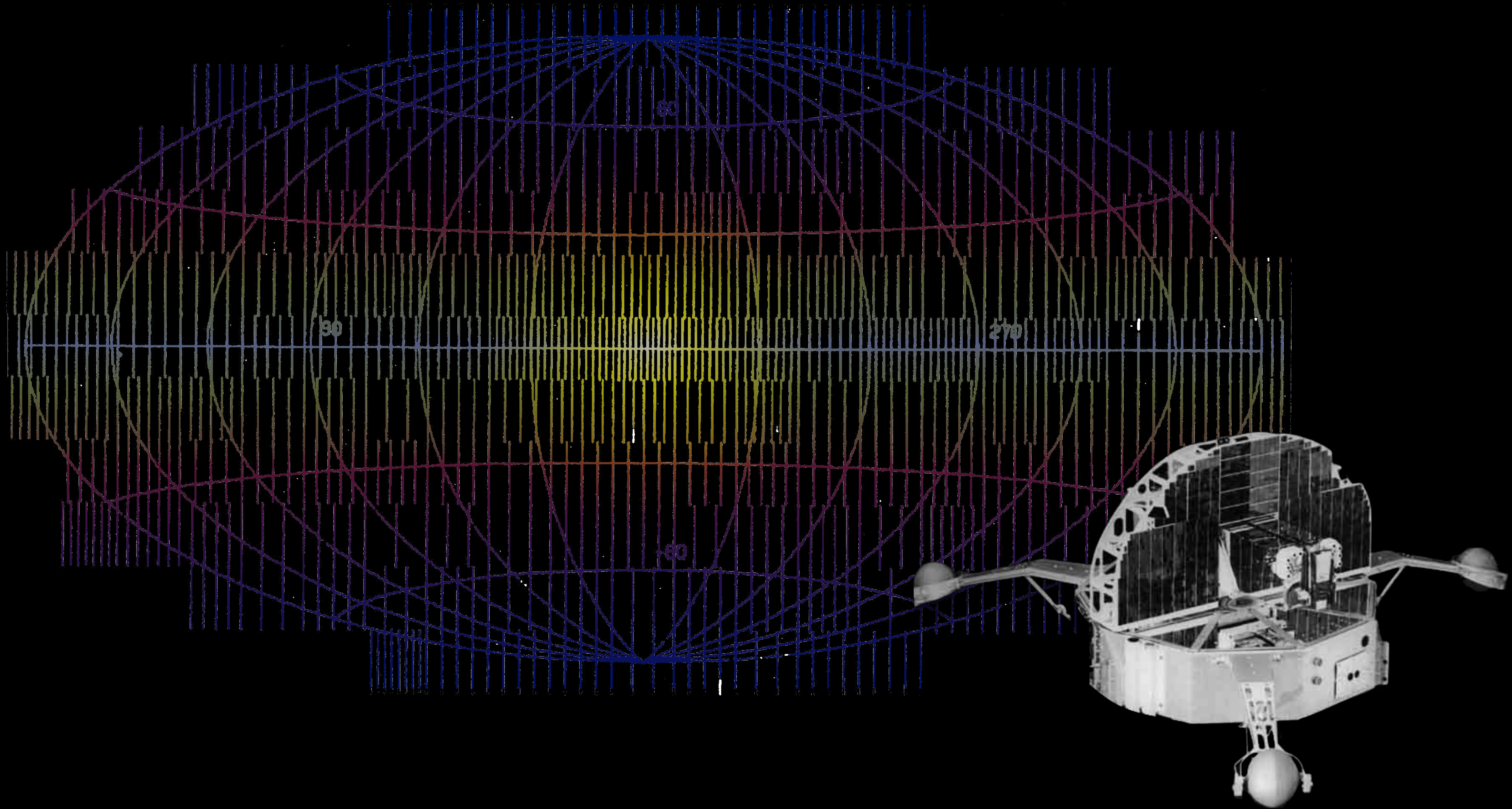

COS-B

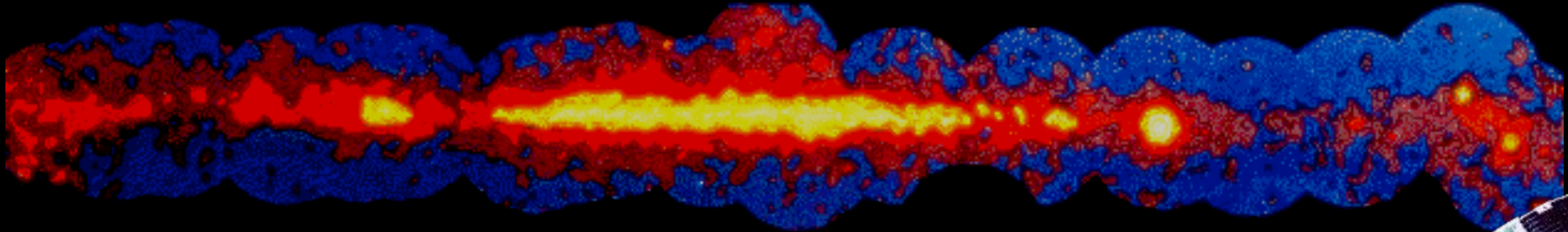

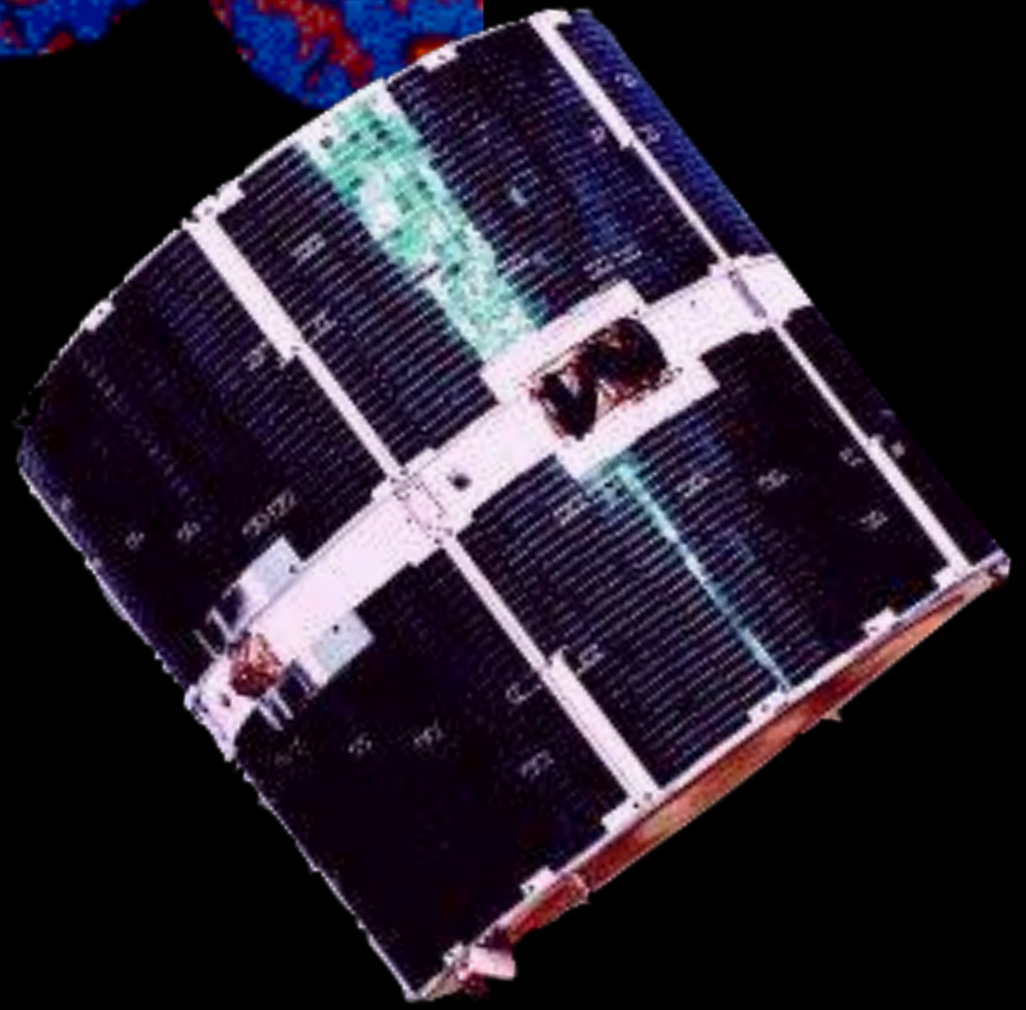

EGRET

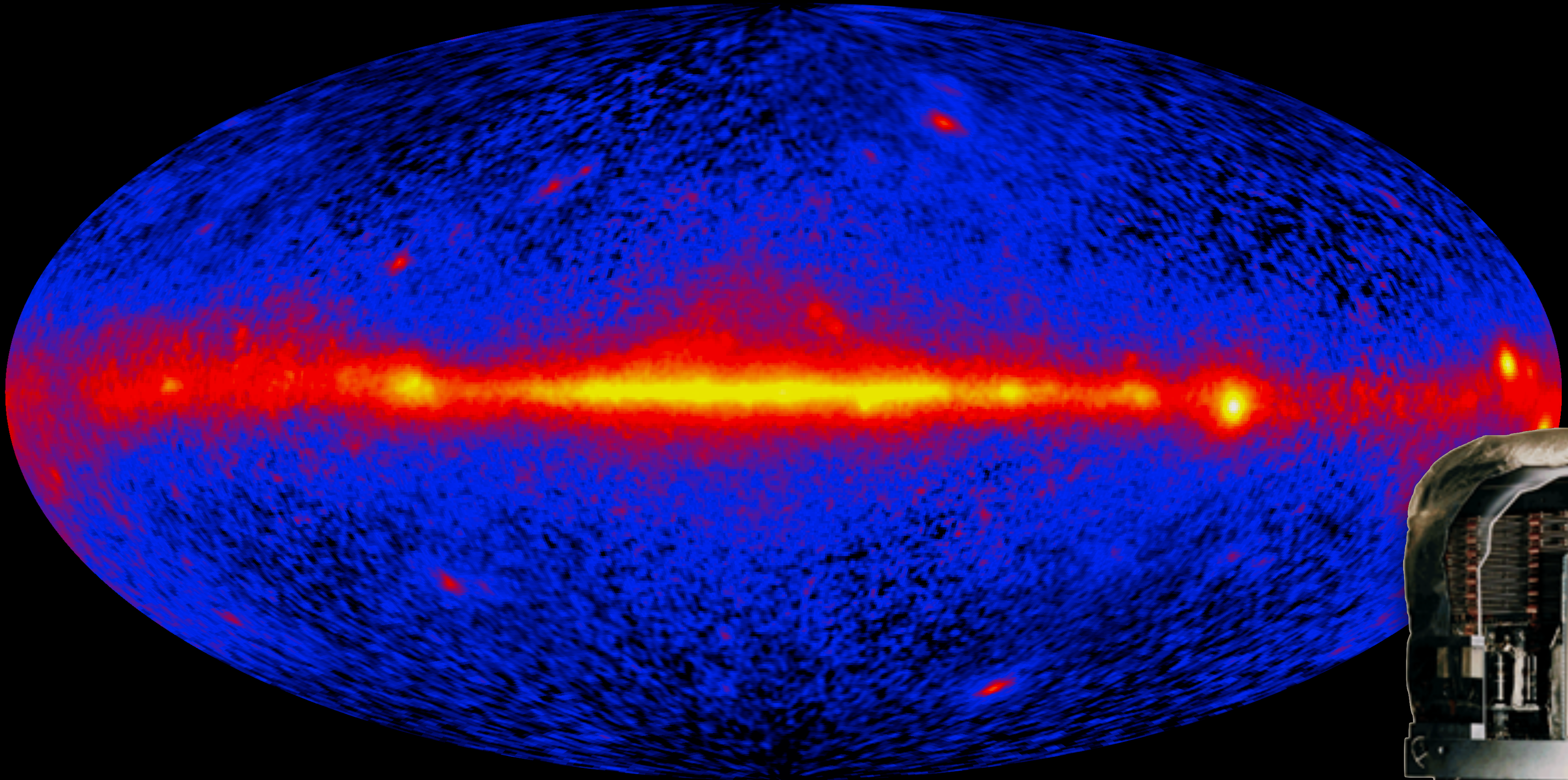

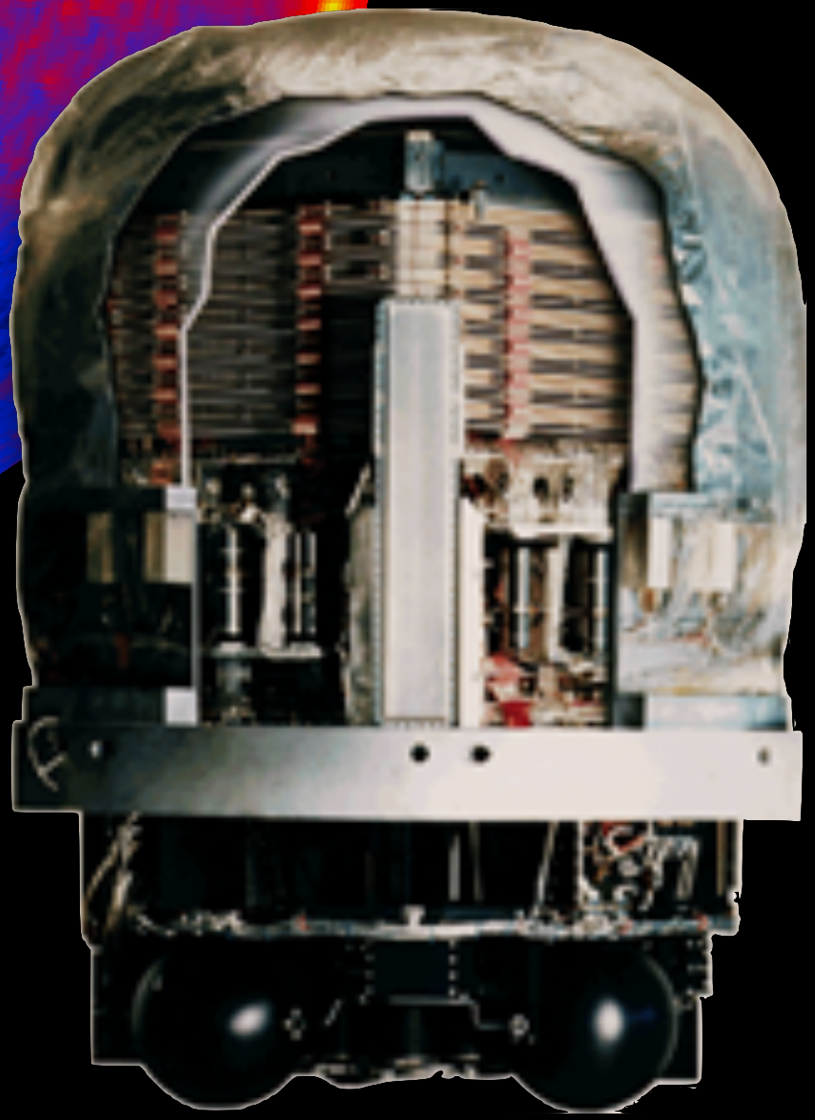

FERMI

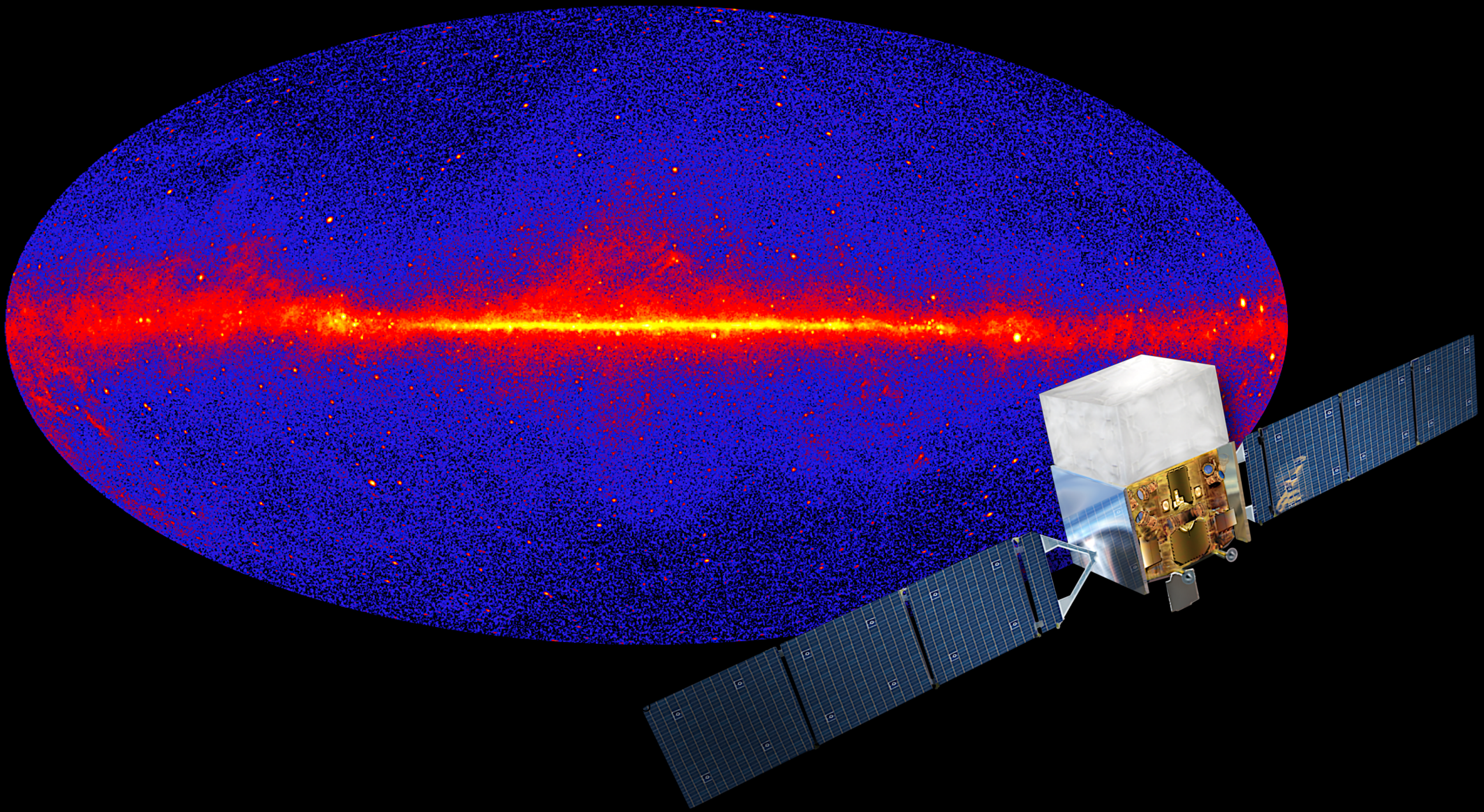

The Large Area Telescope

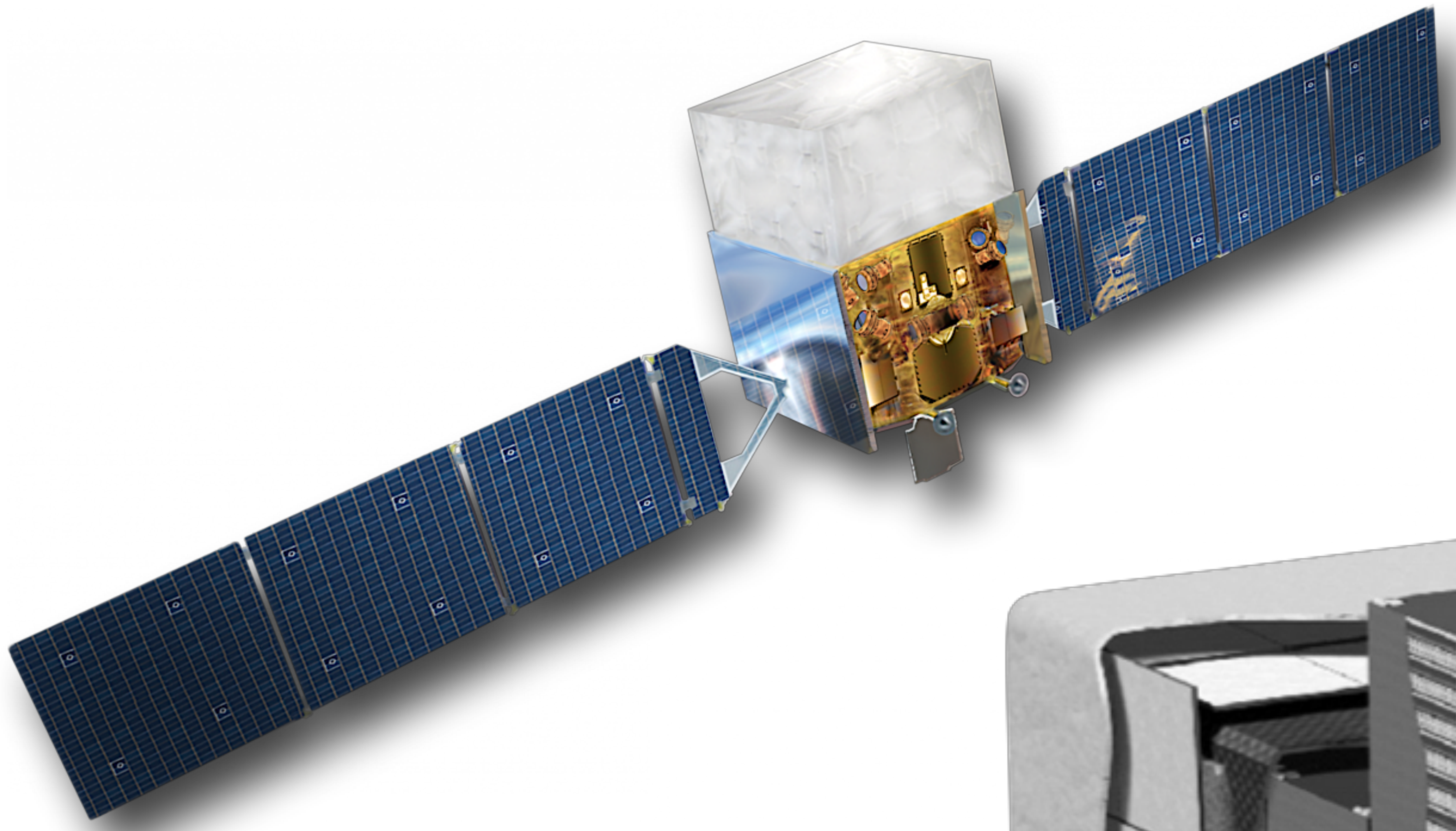

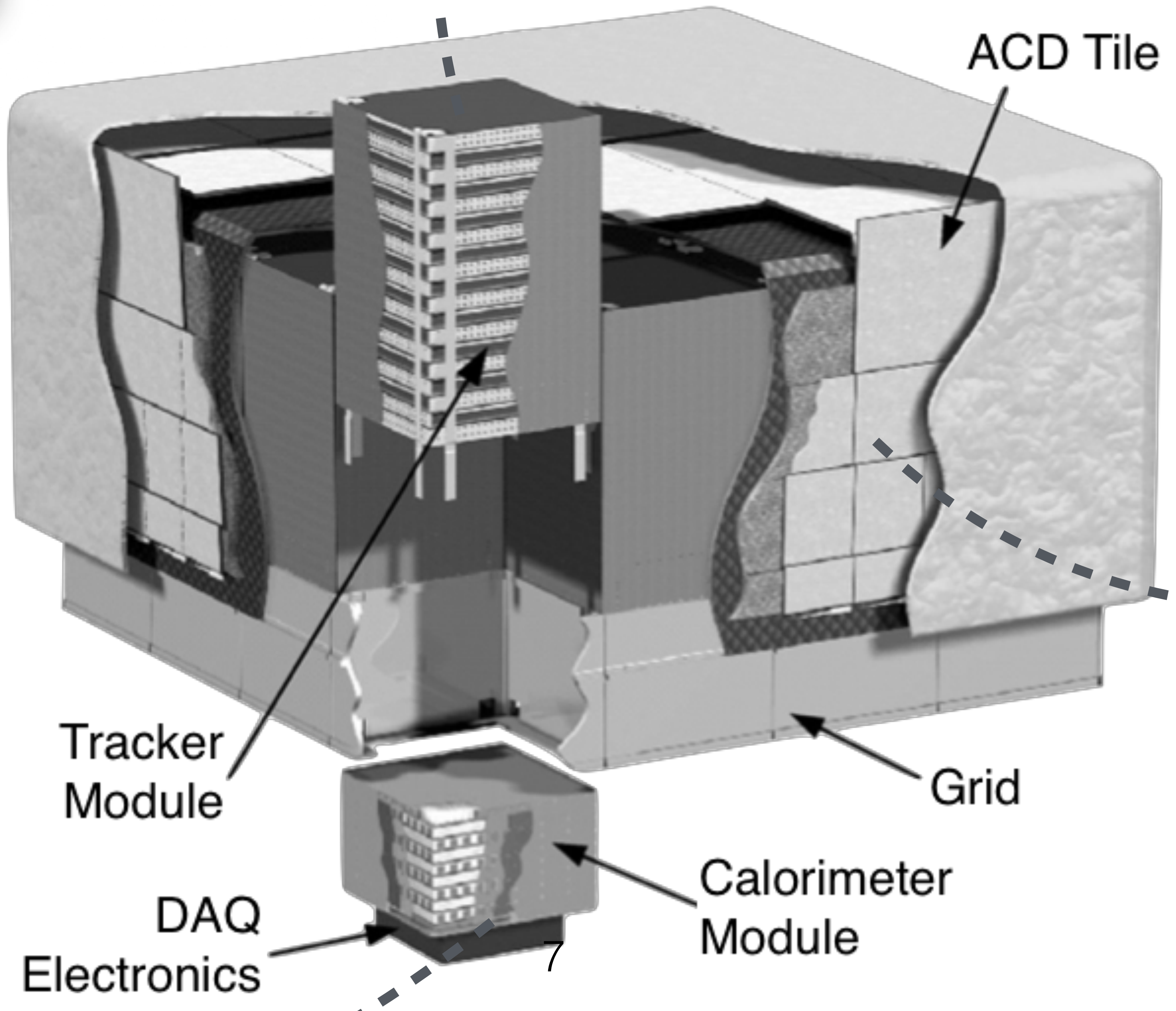

The Tracker-converter

Pair production in tungsten foils
Tracks detection in single-sided strip detectors

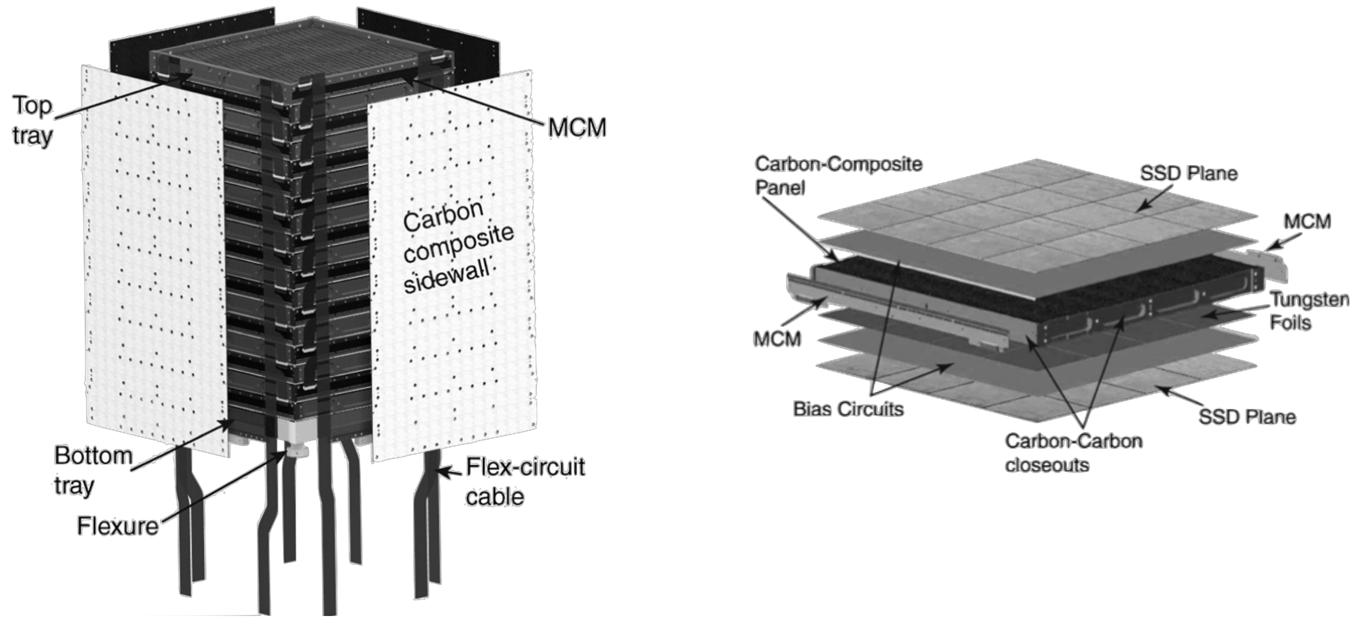

The Anti-coincidence Detector

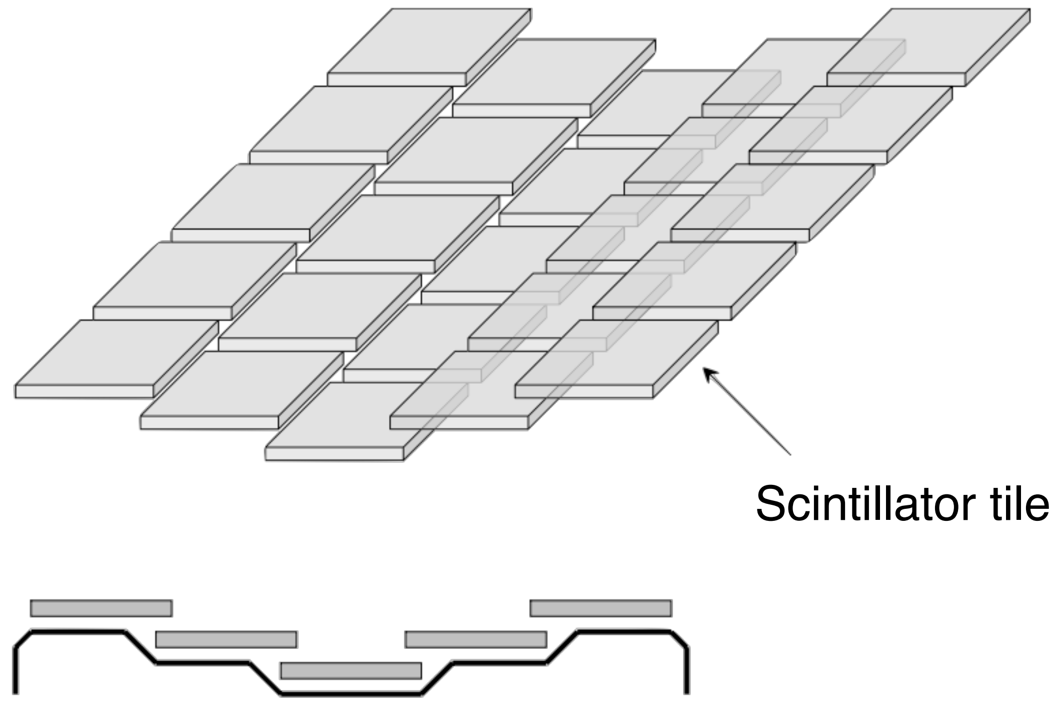

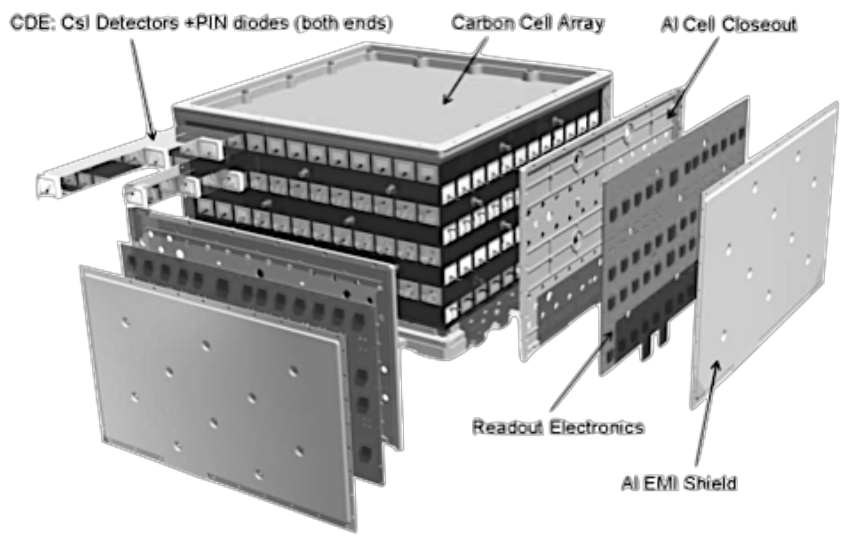

The Calorimeter

Optimized energy range:
0.1 - 300 GeV

The gamma-ray sky

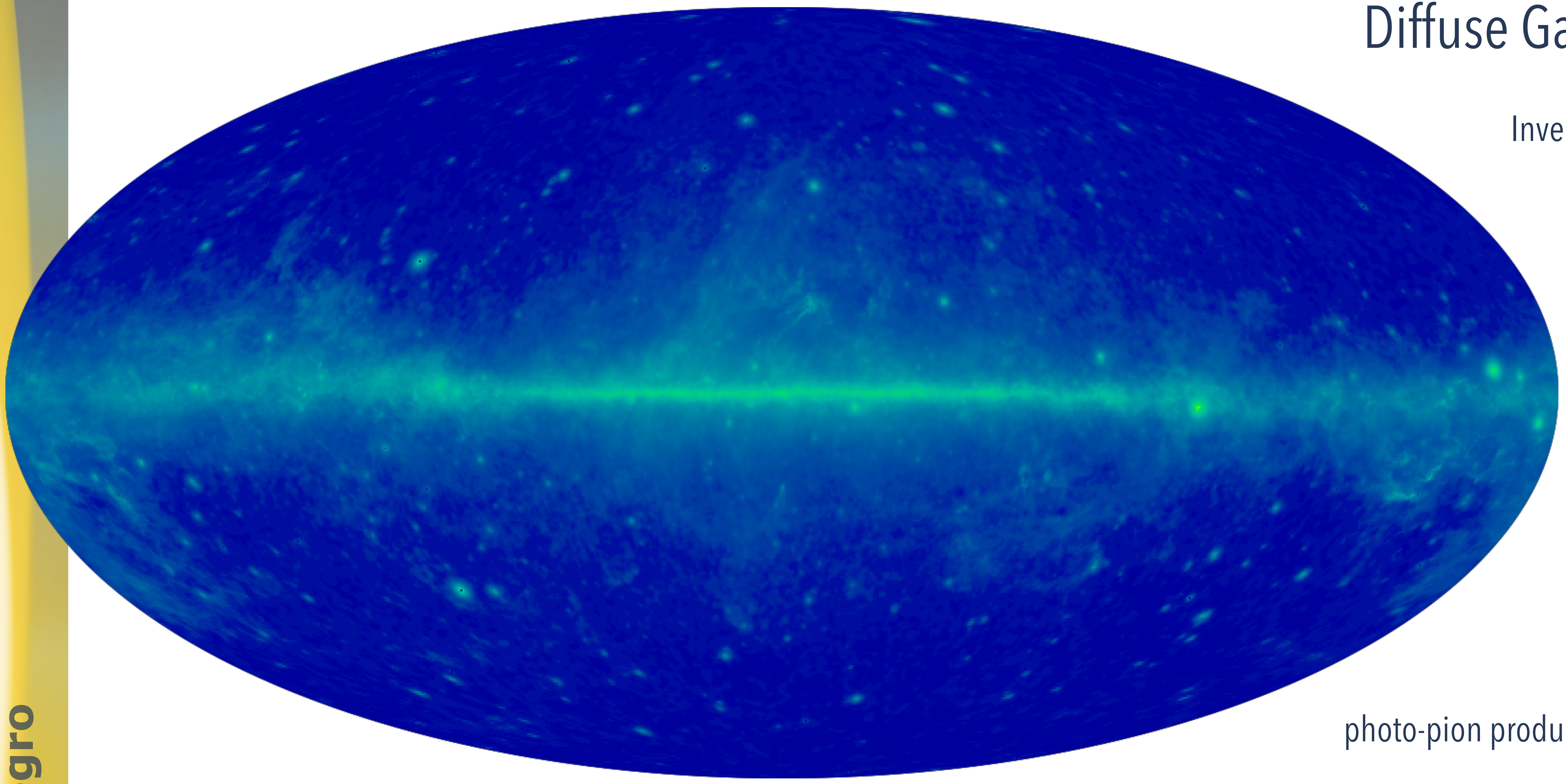

Diffuse Galactic emission

Inverse Compton process

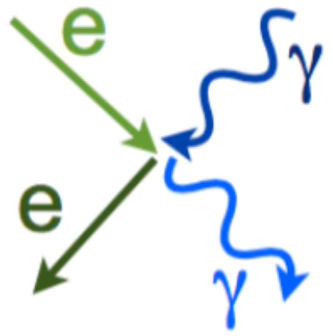

Bremsstrahlung

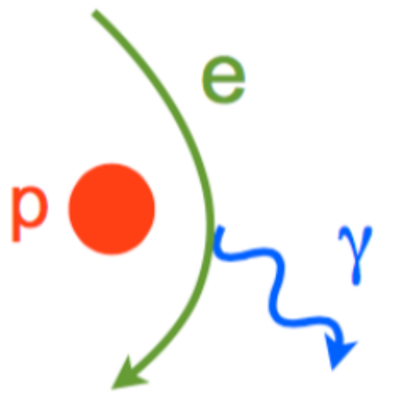

Synchrotron

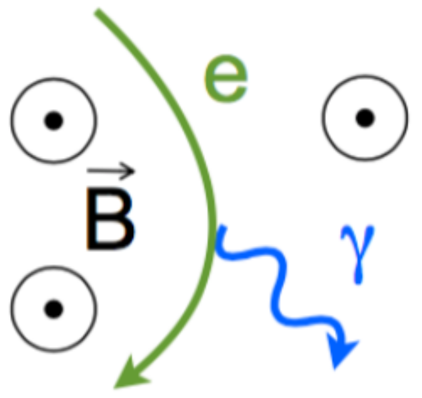

photo-pion production

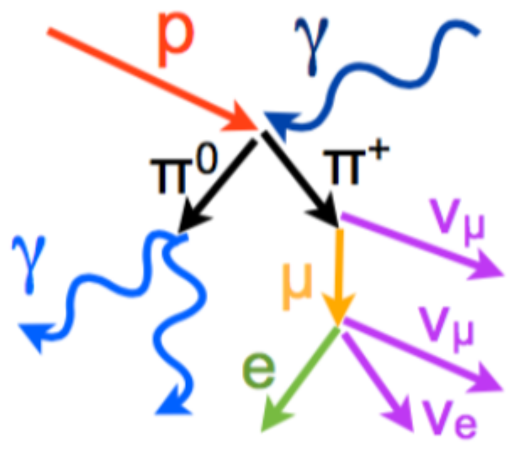

proton-proton interaction

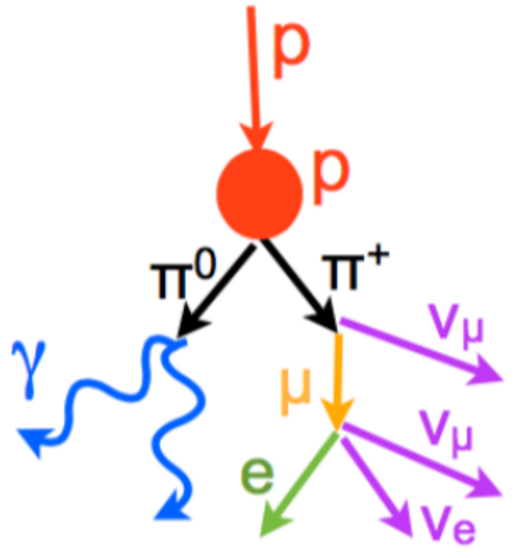

The gamma-ray sky

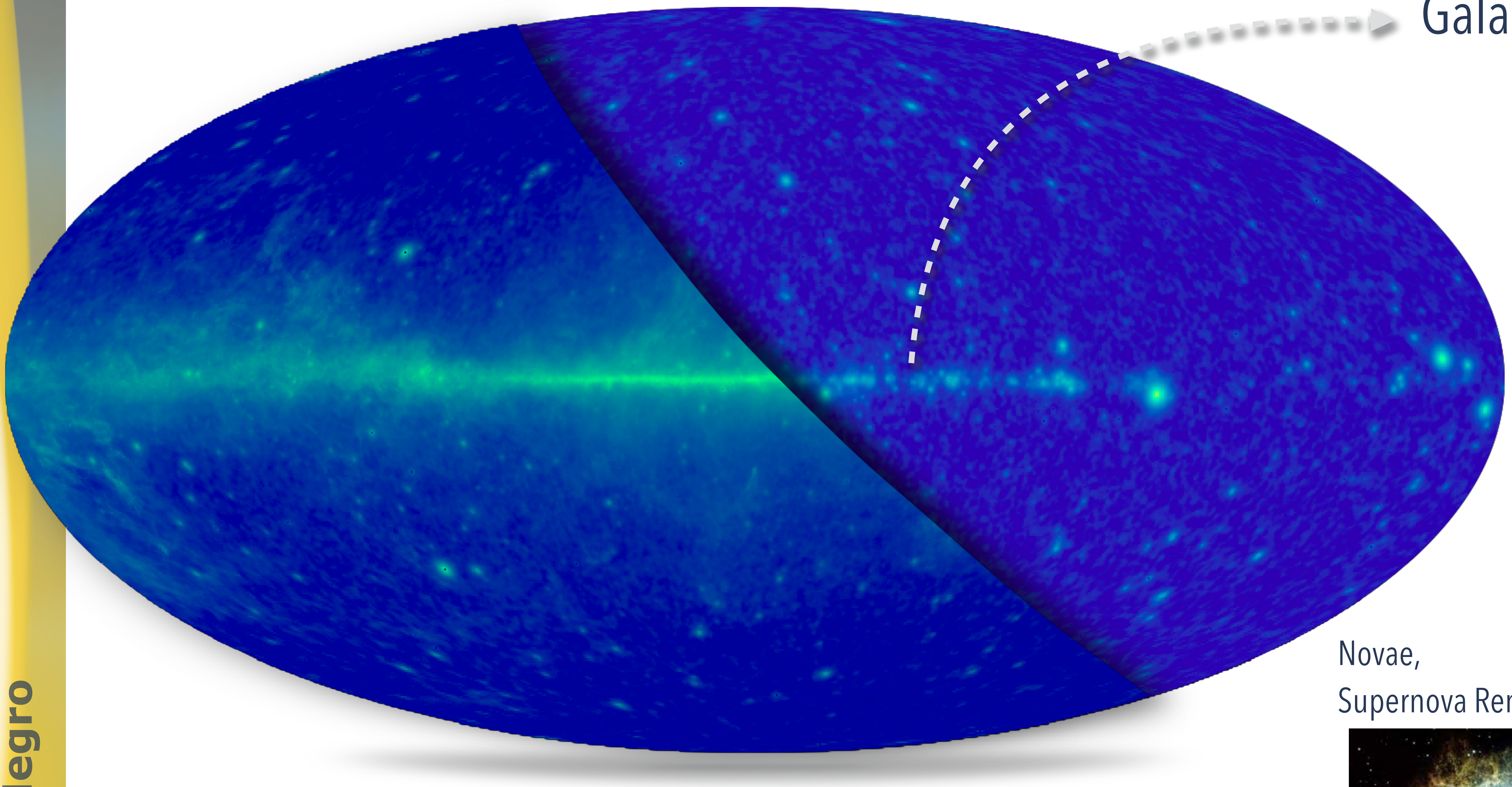

Galactic Sources

Globular clusters

Star-forming regions

Binary systems

Pulsars,
pulsar wind nebulae

Novae,
Supernova Remnants

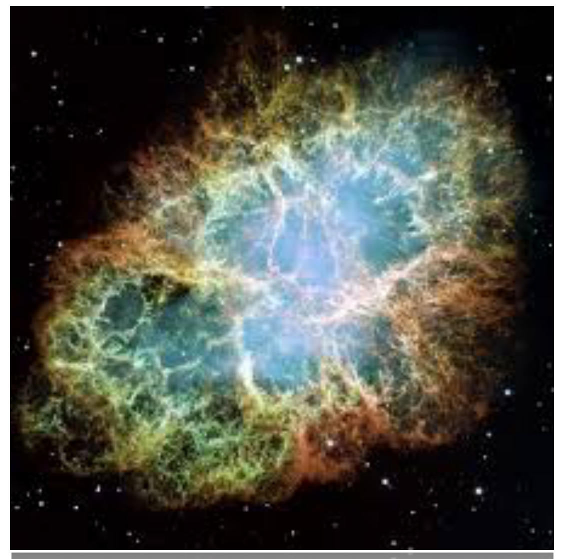

The gamma-ray sky

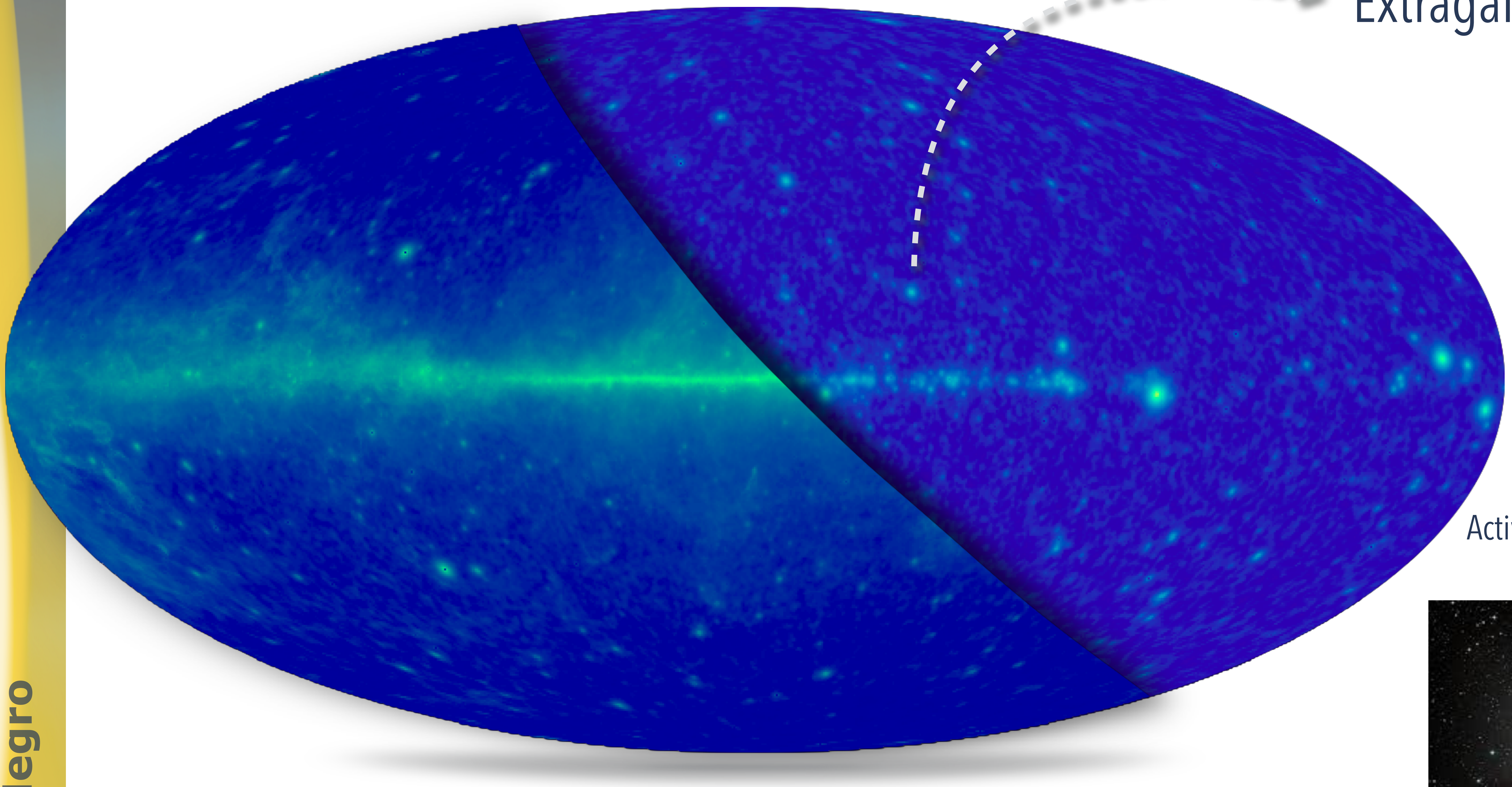

Extragalactic Sources

Star forming galaxies (SFG)

Active galactic nuclei (AGN)

The gamma-ray sky

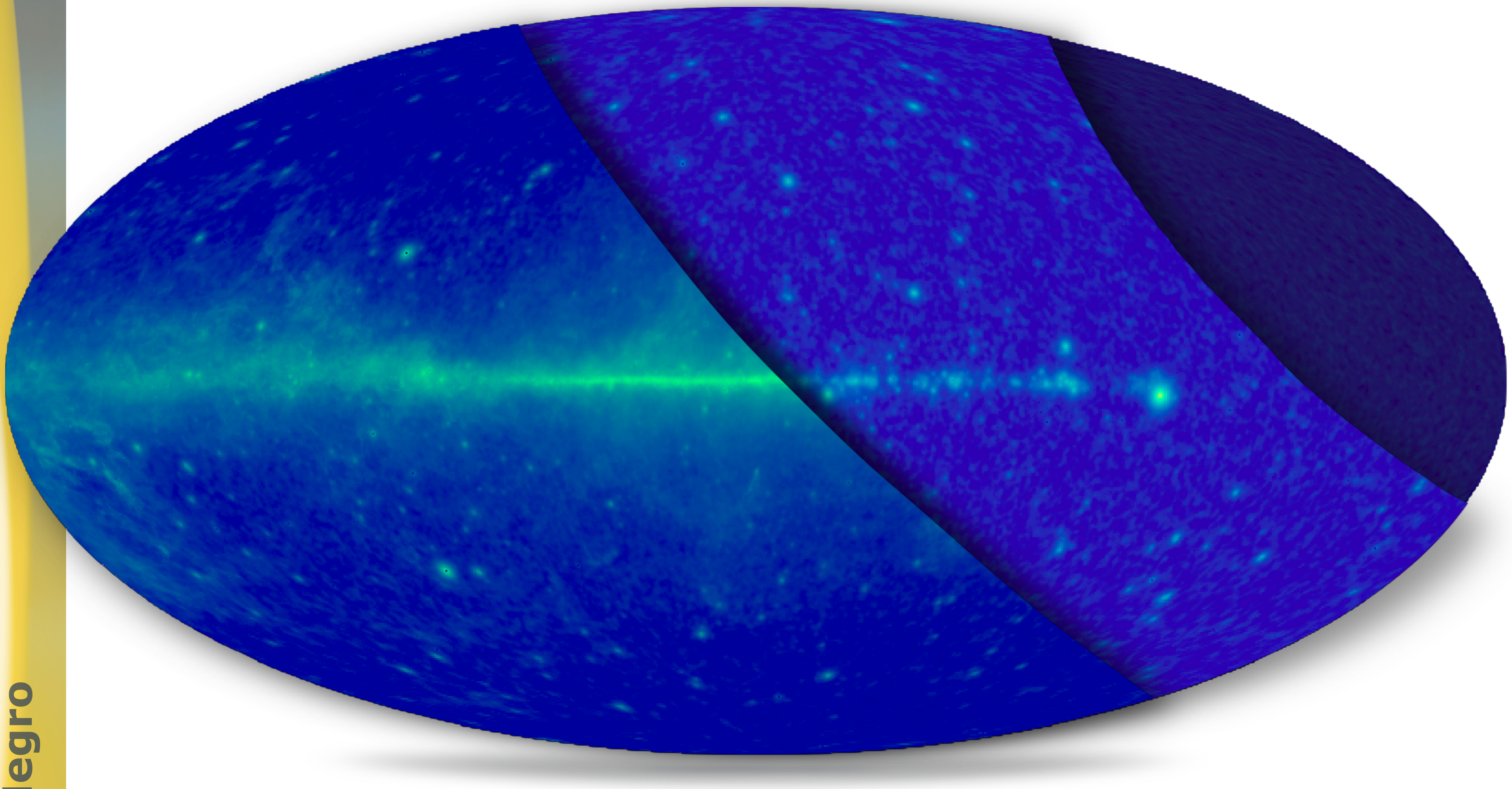

PHOTON 2019
Michela Negro

The unresolved gamma-ray background

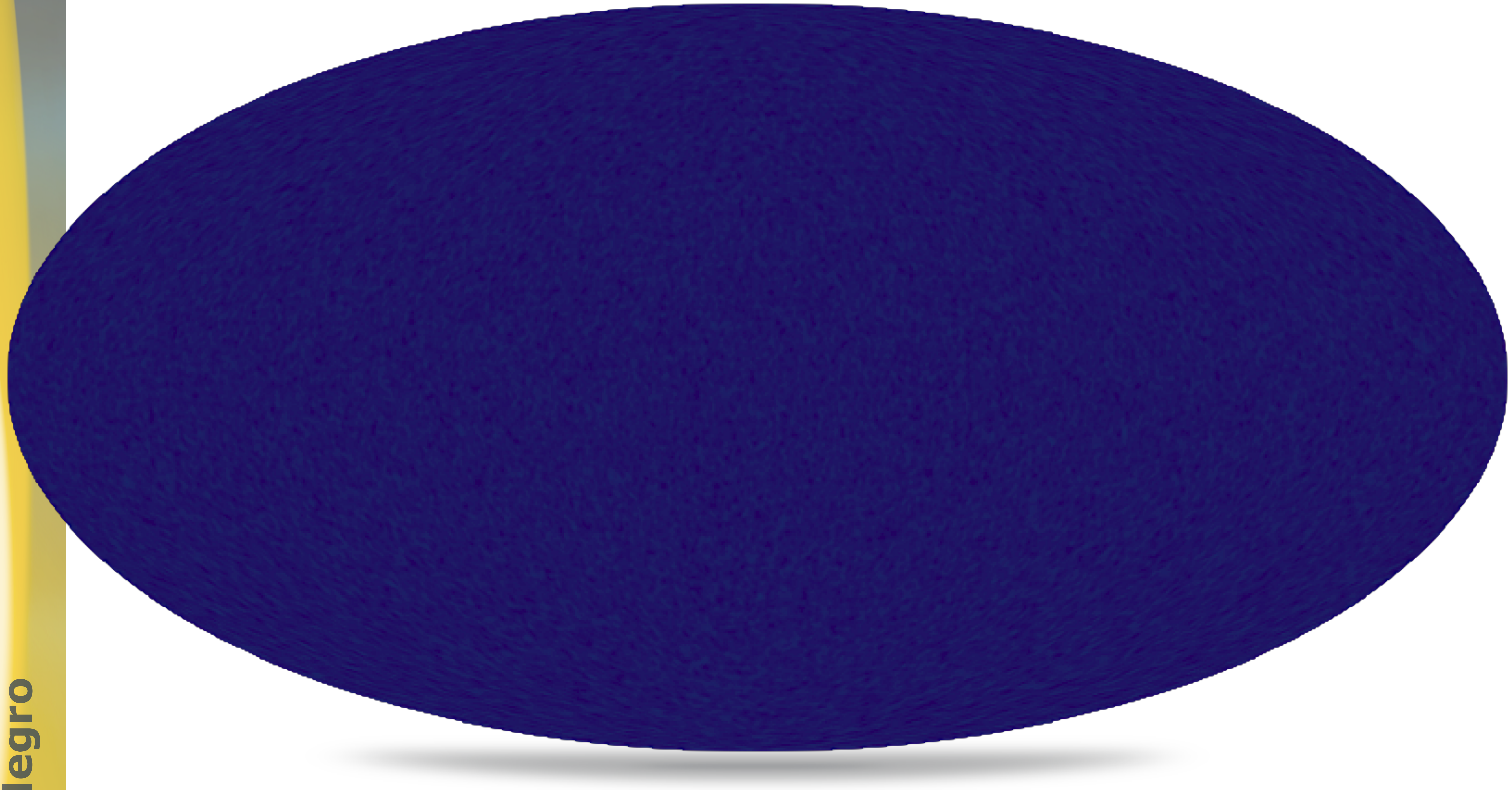

Study the UGRB

to determine its exact composition

to constrain the faint end of the luminosity functions of components

to shed light on exotic physics (WIMP-like DM)

The UGRB intensity energy spectrum

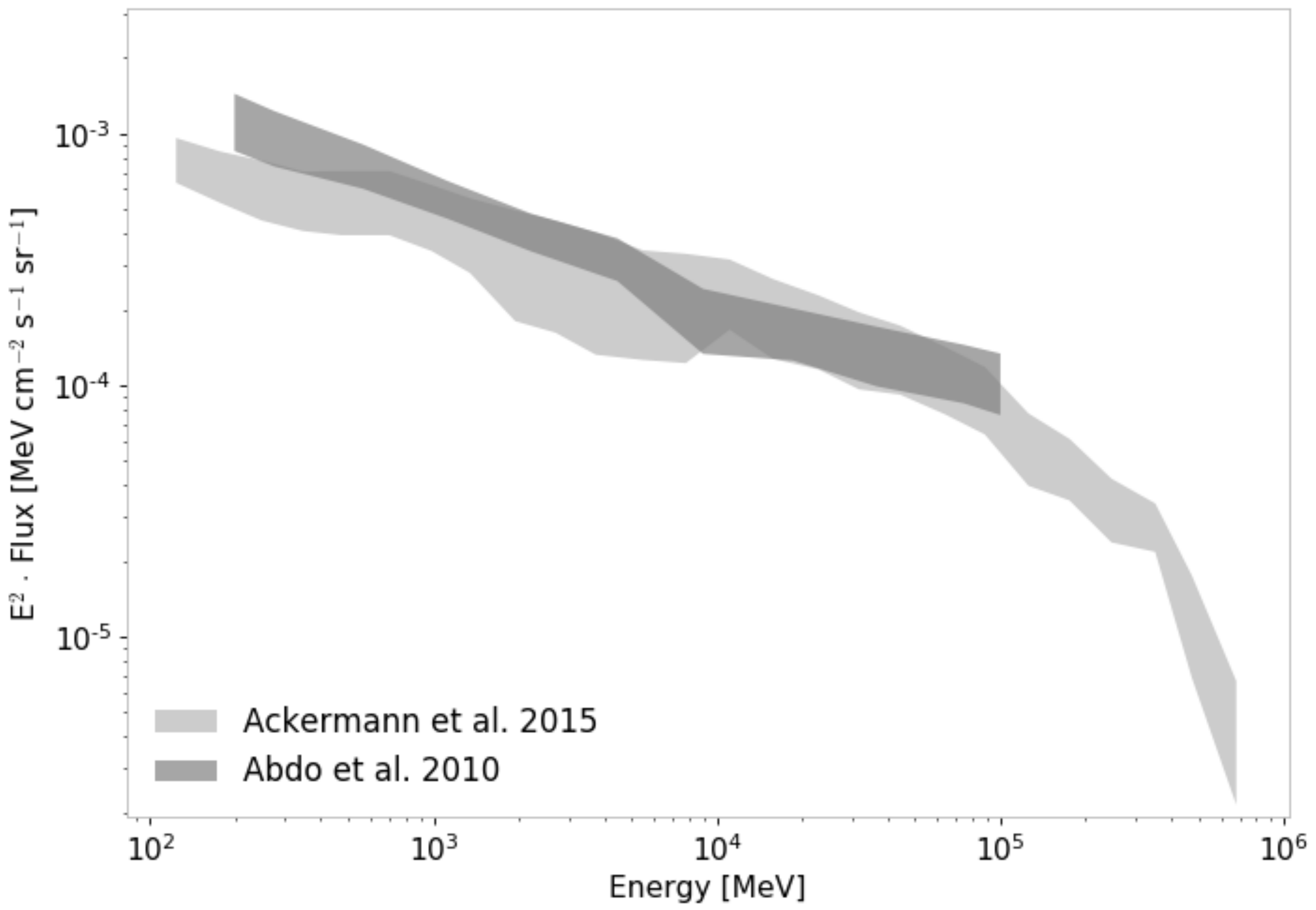

The UGRB intensity energy spectrum

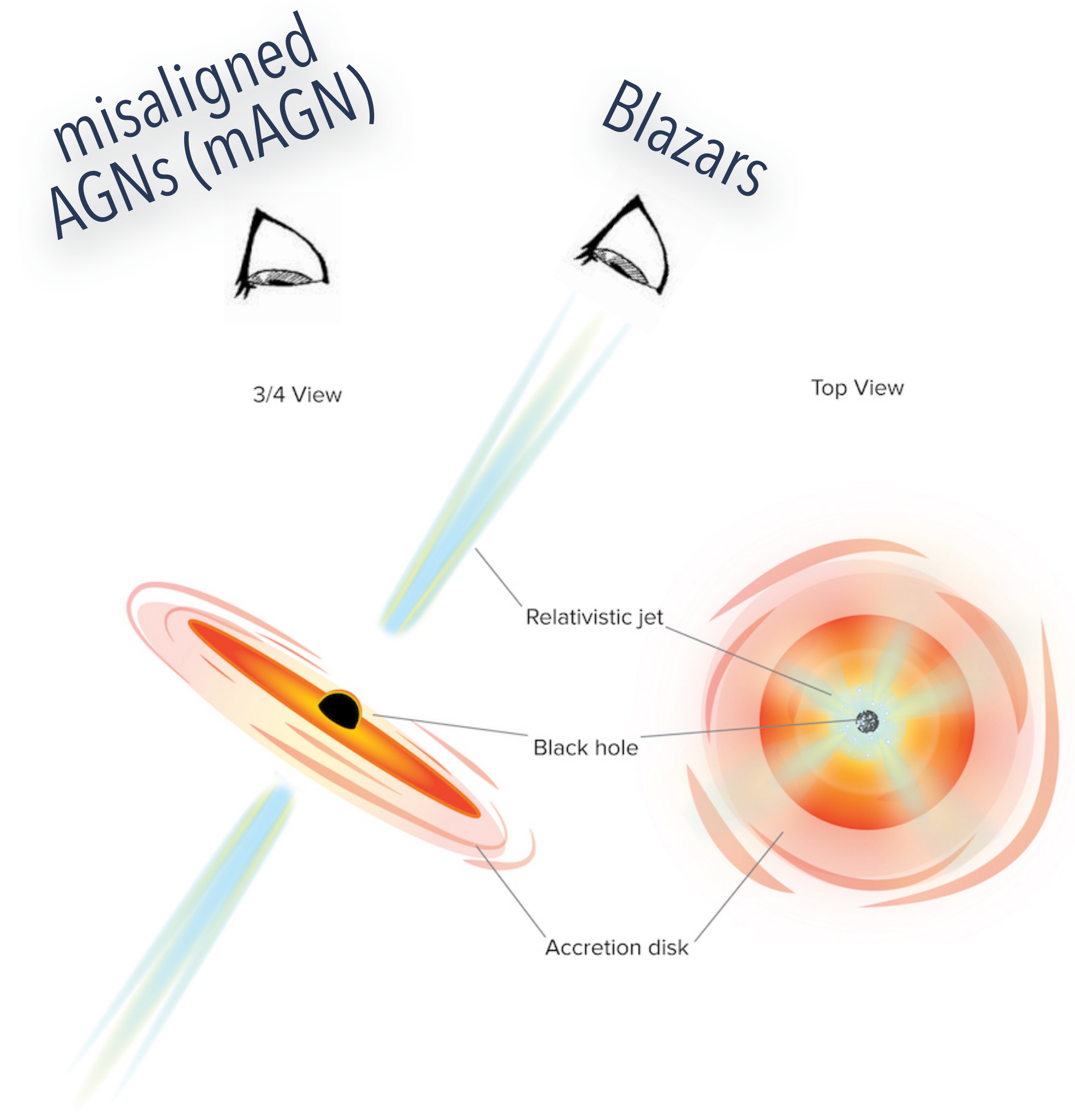

Star forming galaxies (SFG)

Millisecond pulsars (MSP)

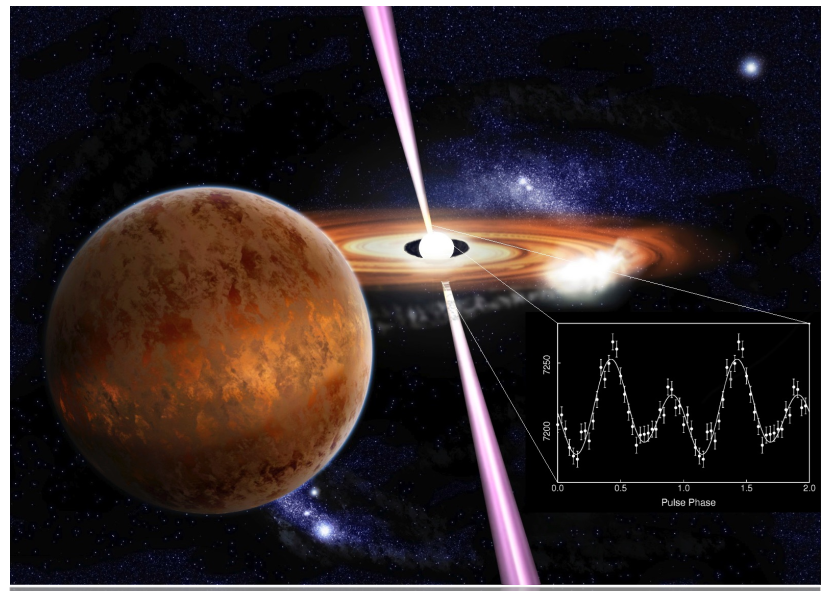

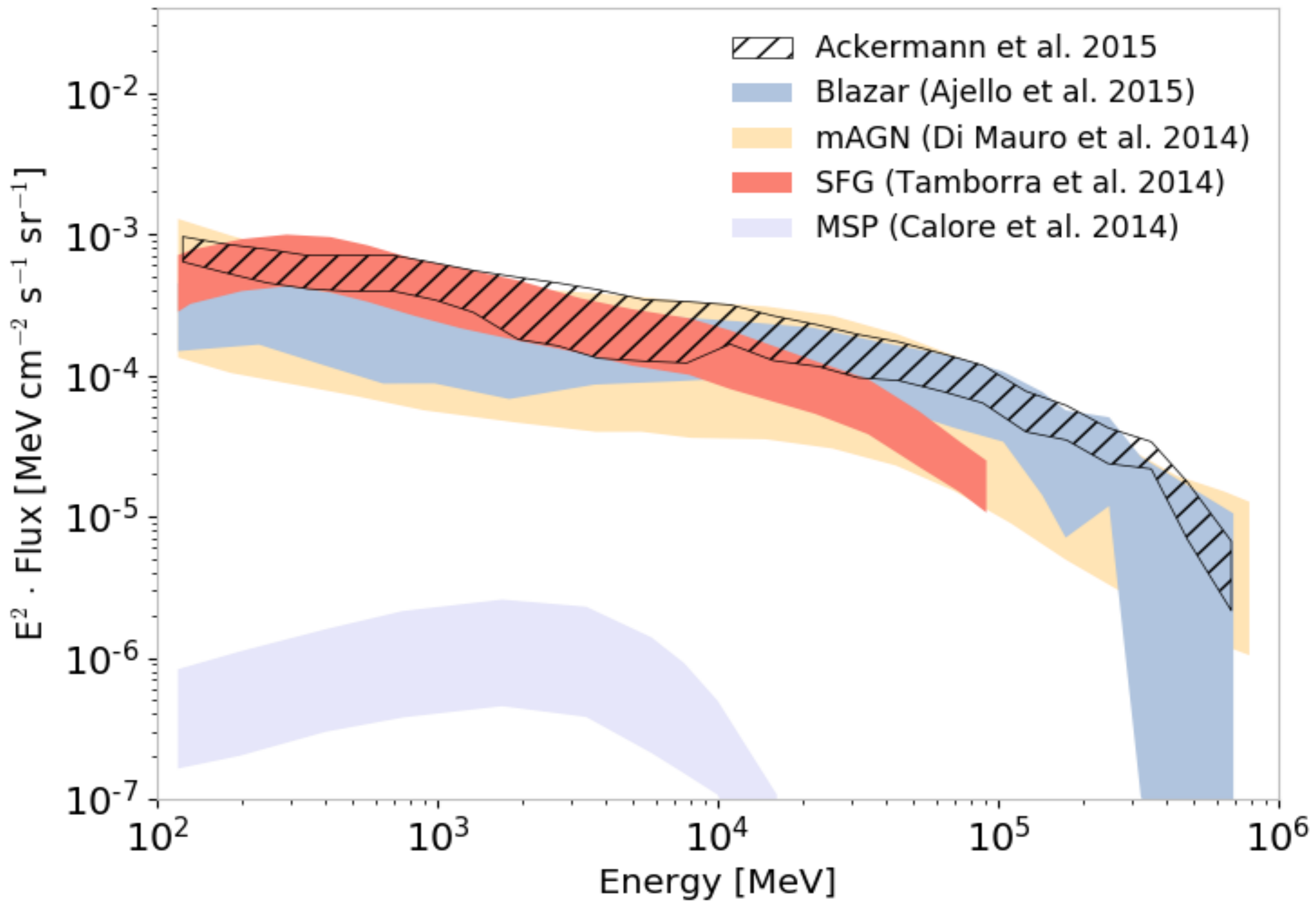

PHOTON 2019
Michela Negro

Anisotropic UGRB

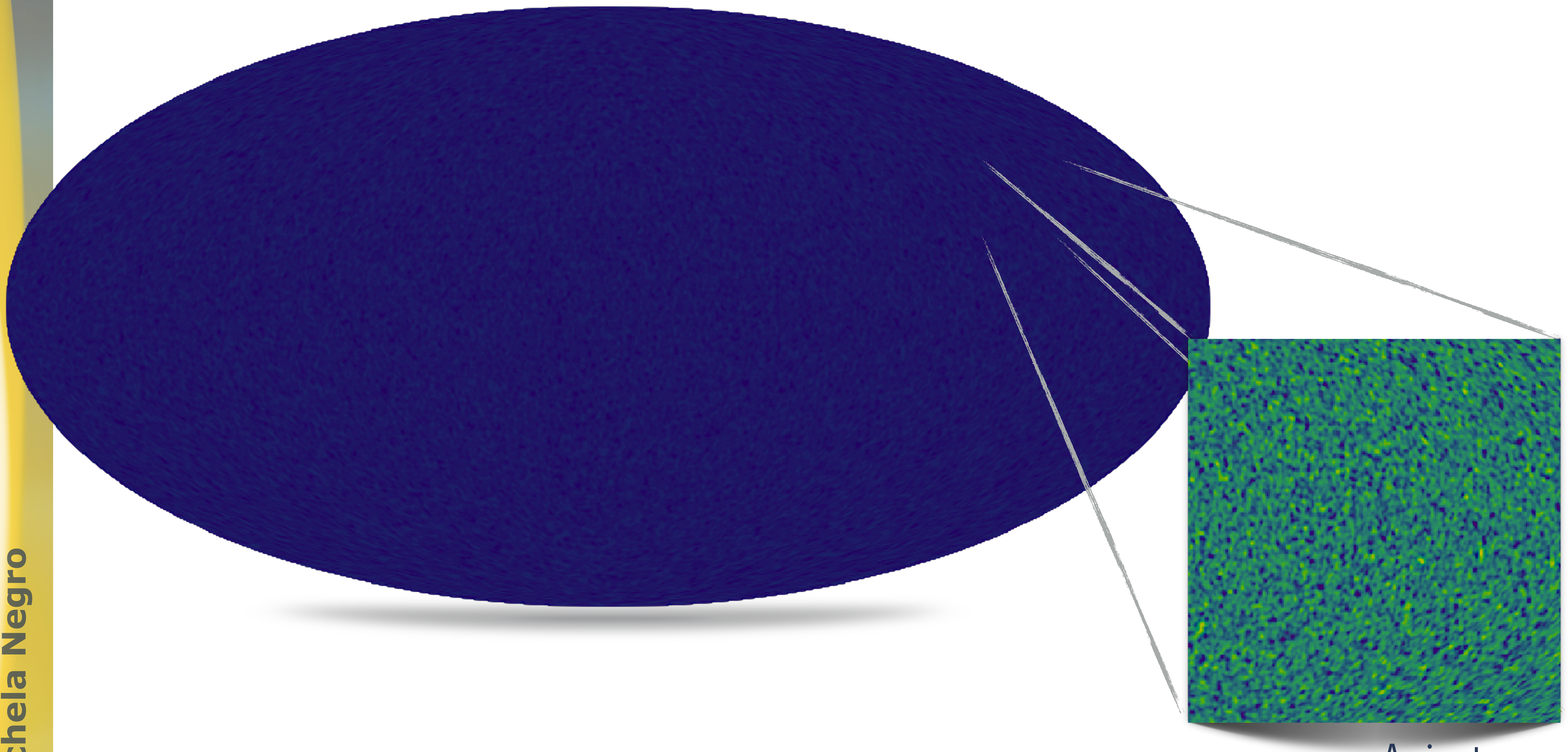

Anisotropic UGRB: autocorrelation

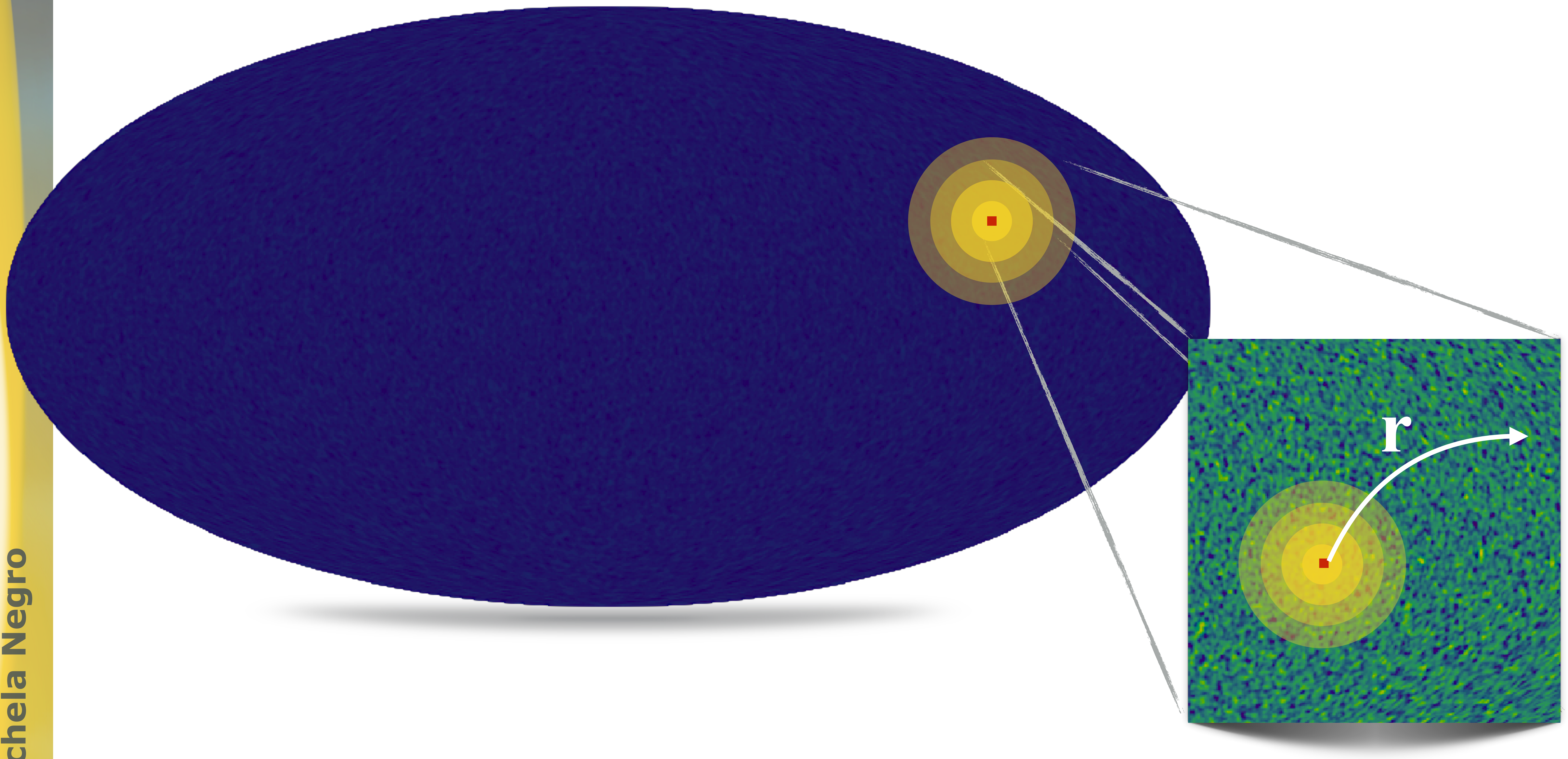

Autocorrelation angular power spectrum

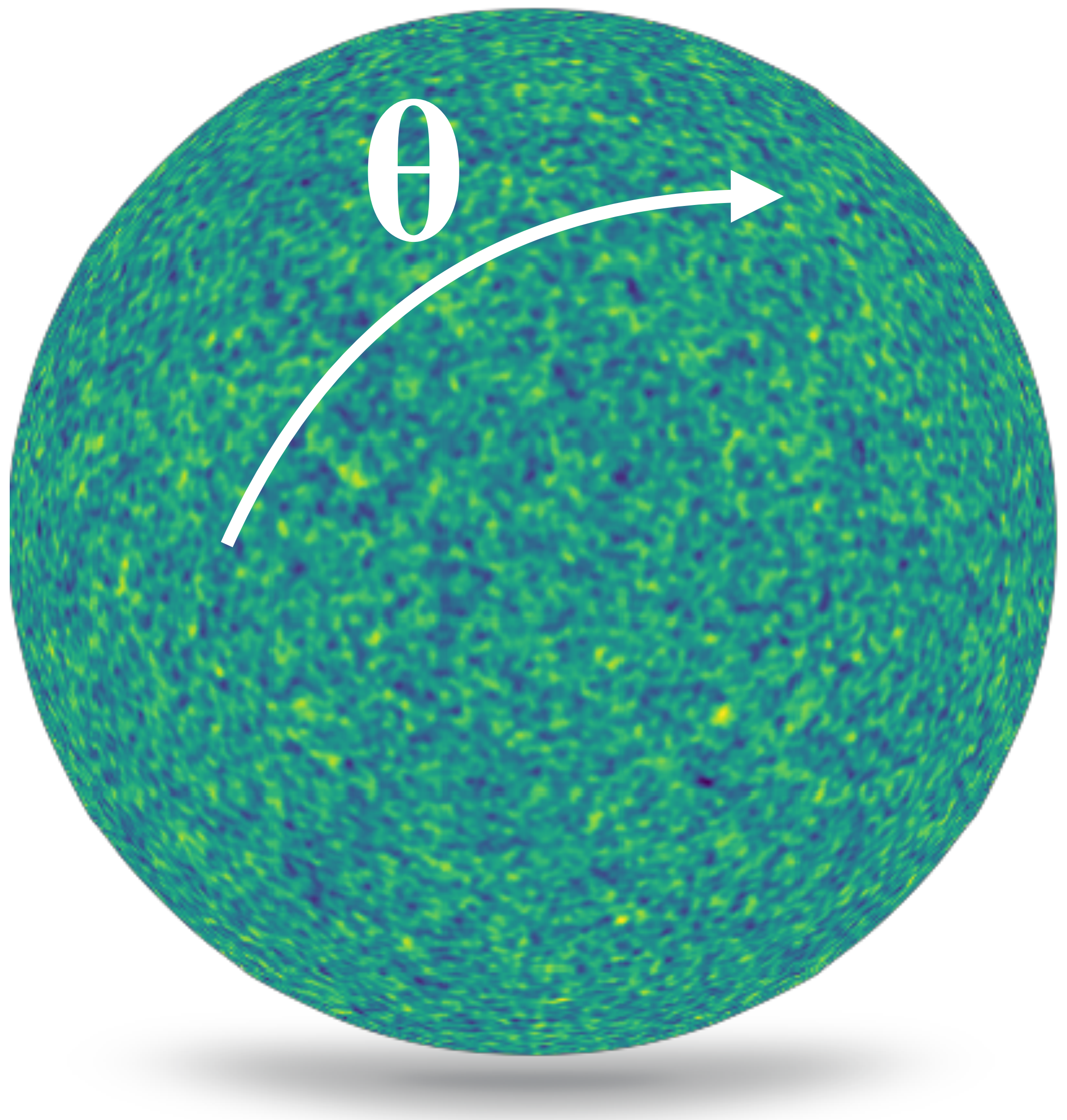

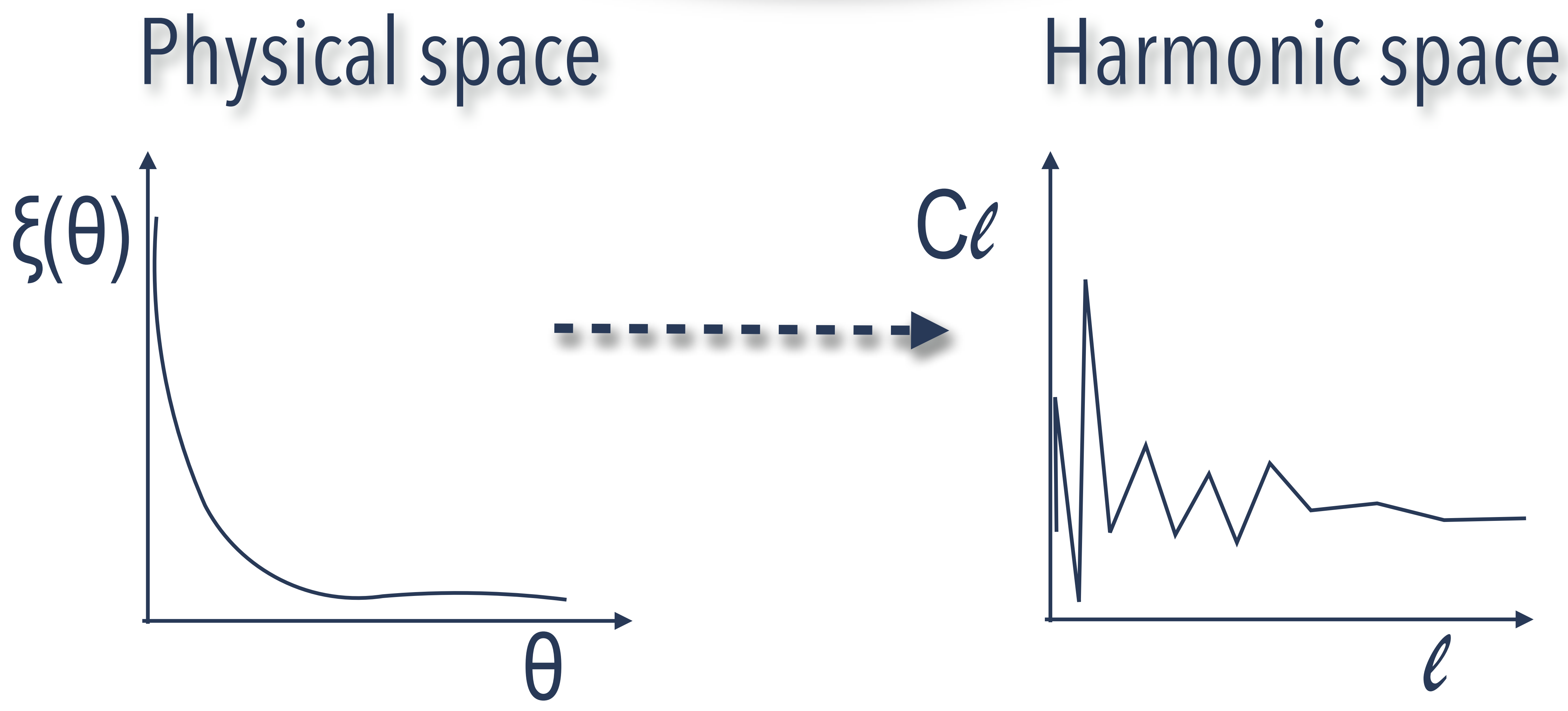

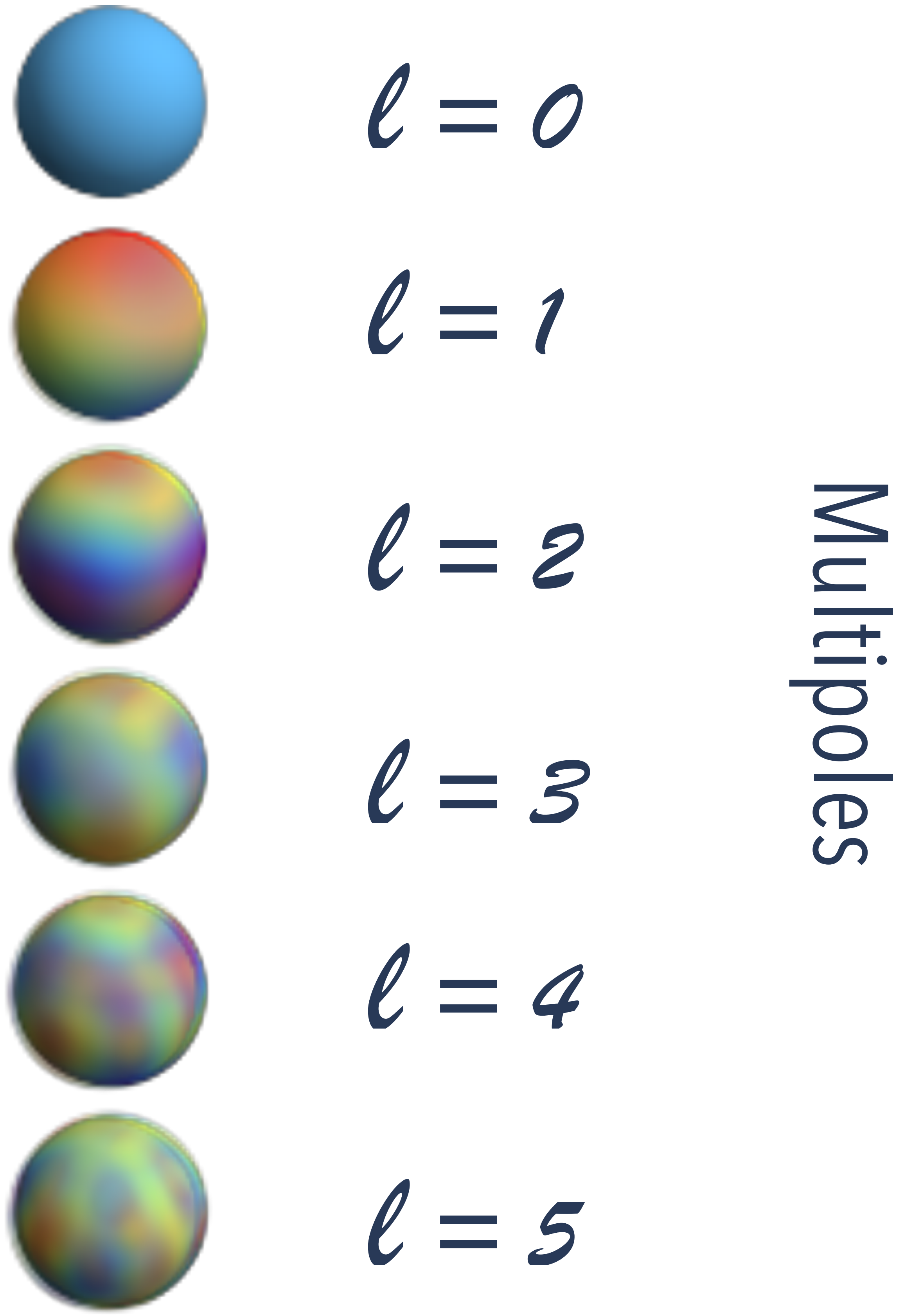

Autocorrelation angular power spectrum

Anisotropy of Isotropic point-like sources

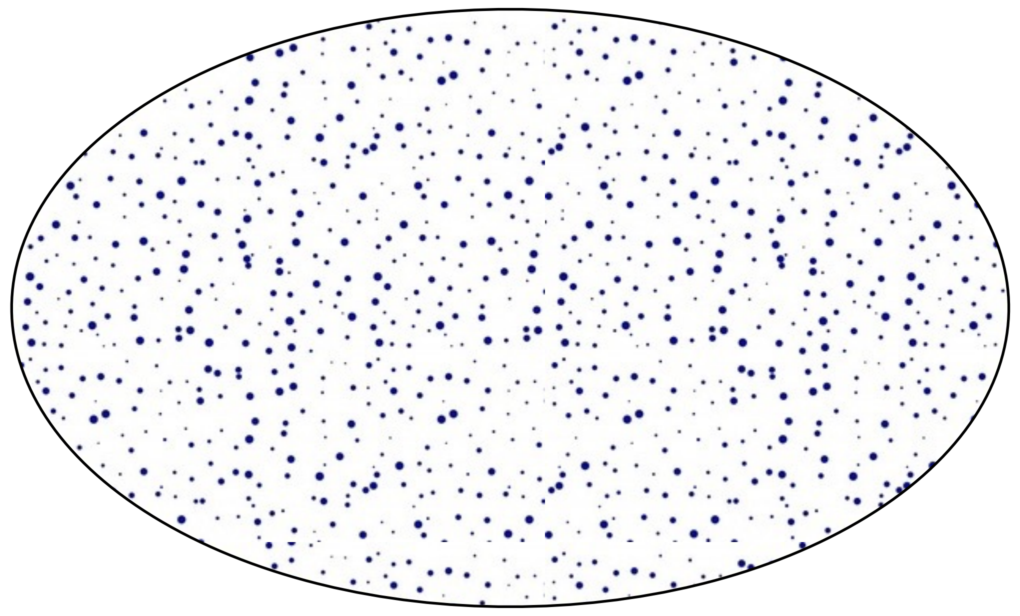

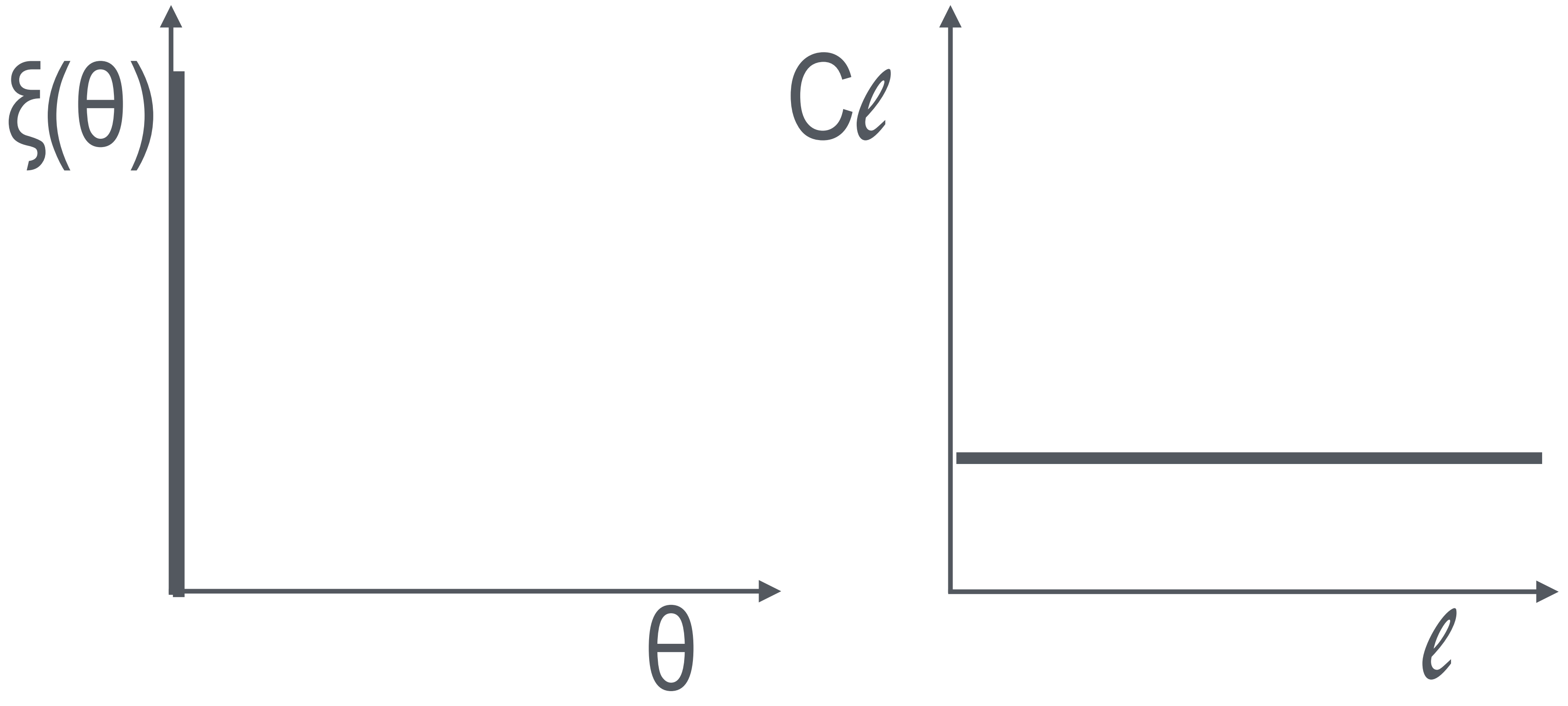

Physical space   Harmonic space

Autocorrelation angular power spectrum

Anisotropy of Isotropic point-like sources

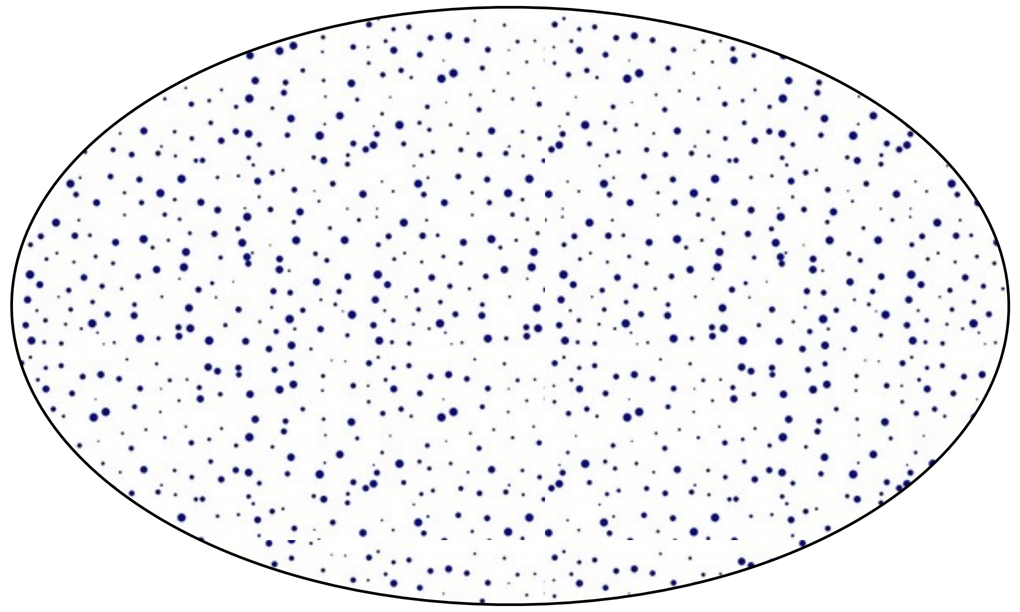

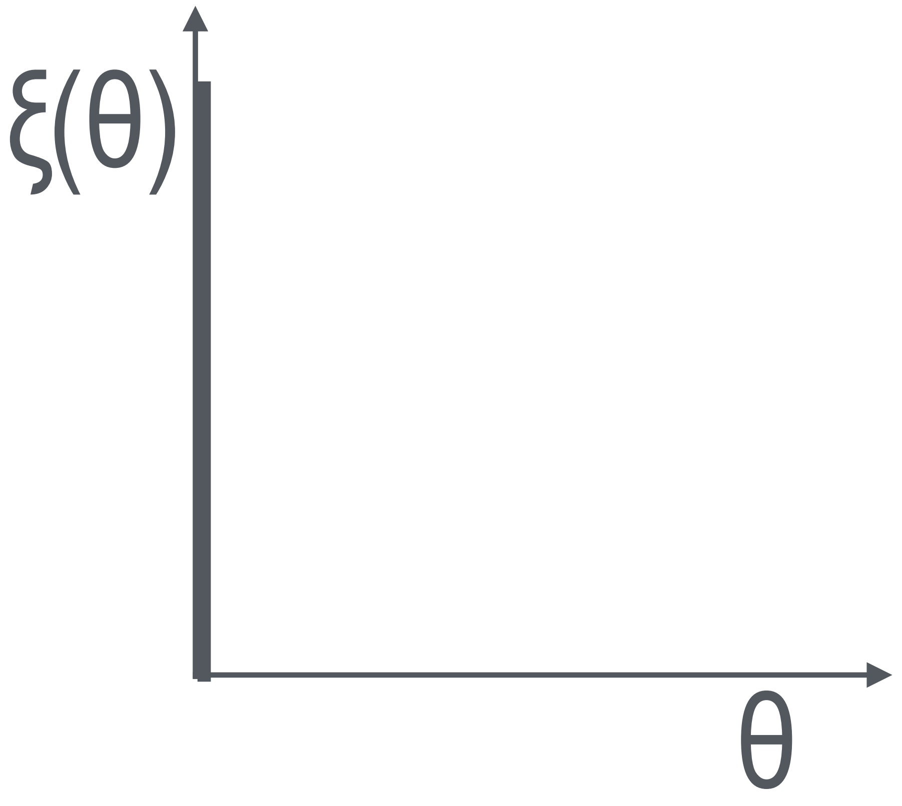

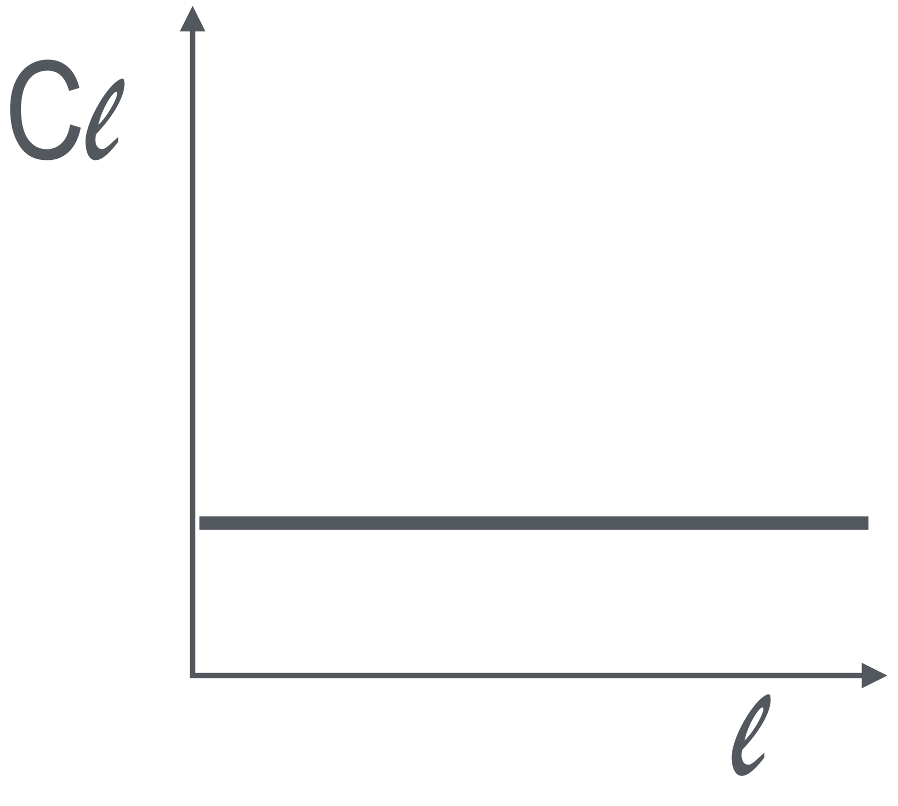

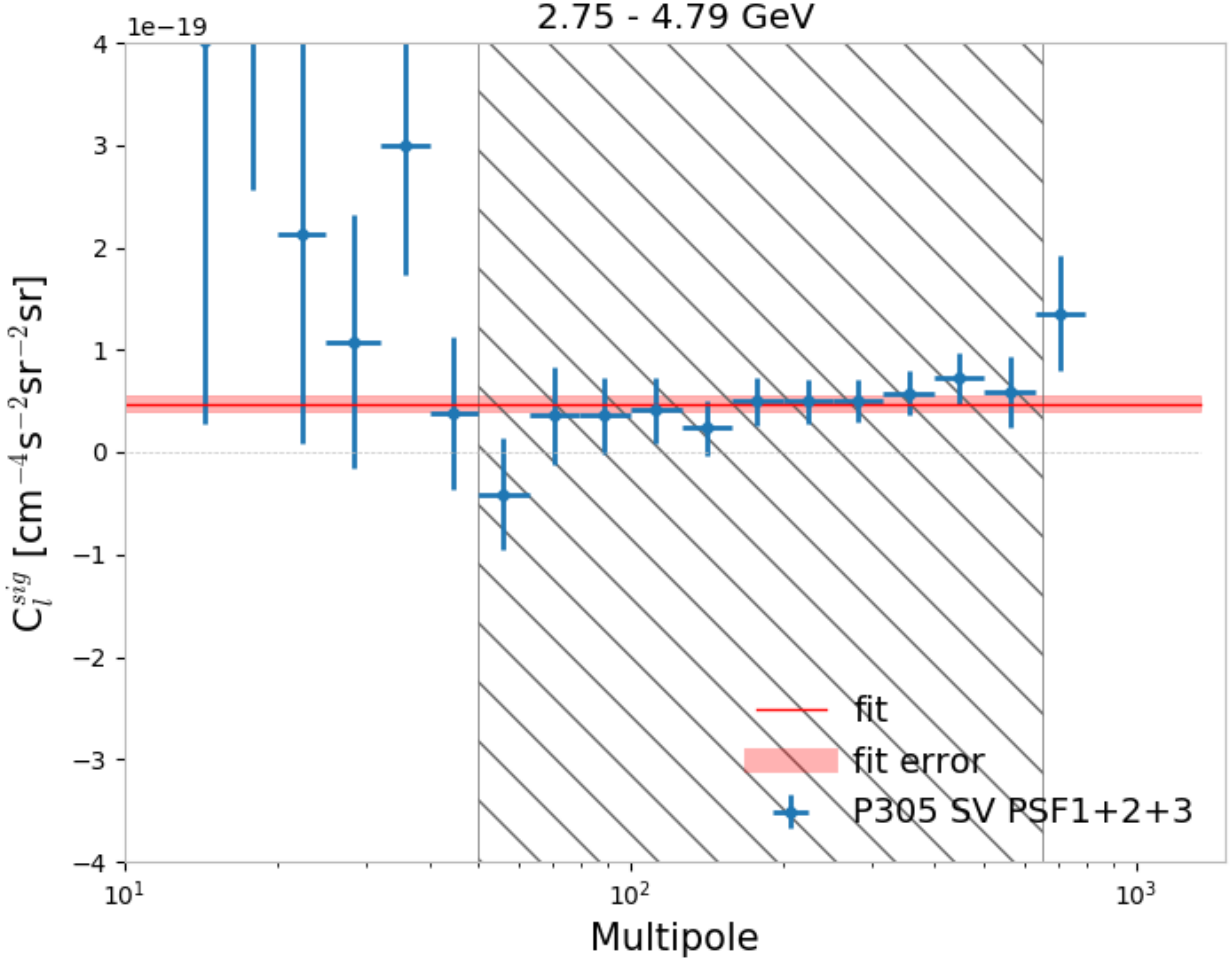

Anisotropy energy spectrum

Anisotropy of Isotropic point-like sources

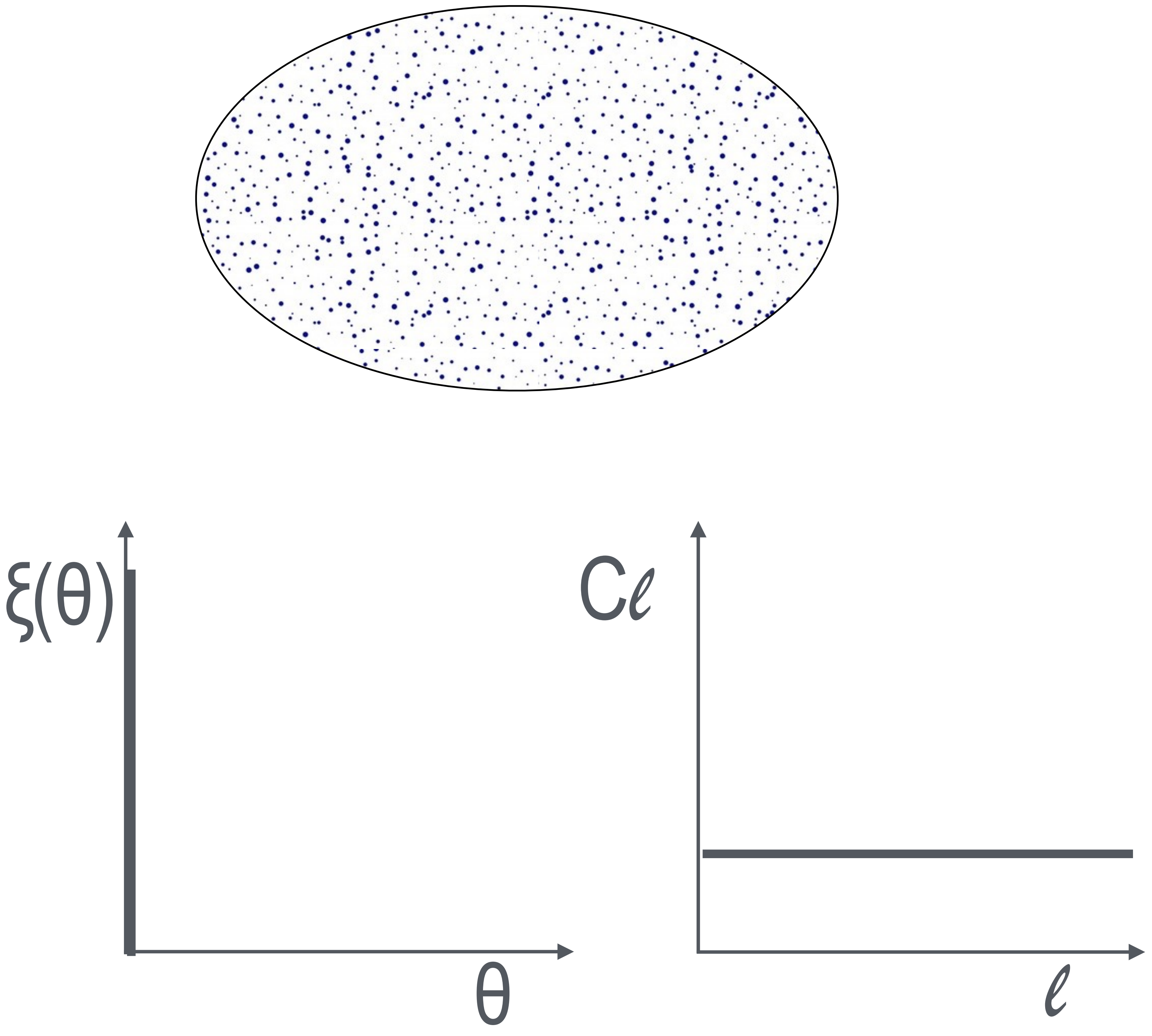

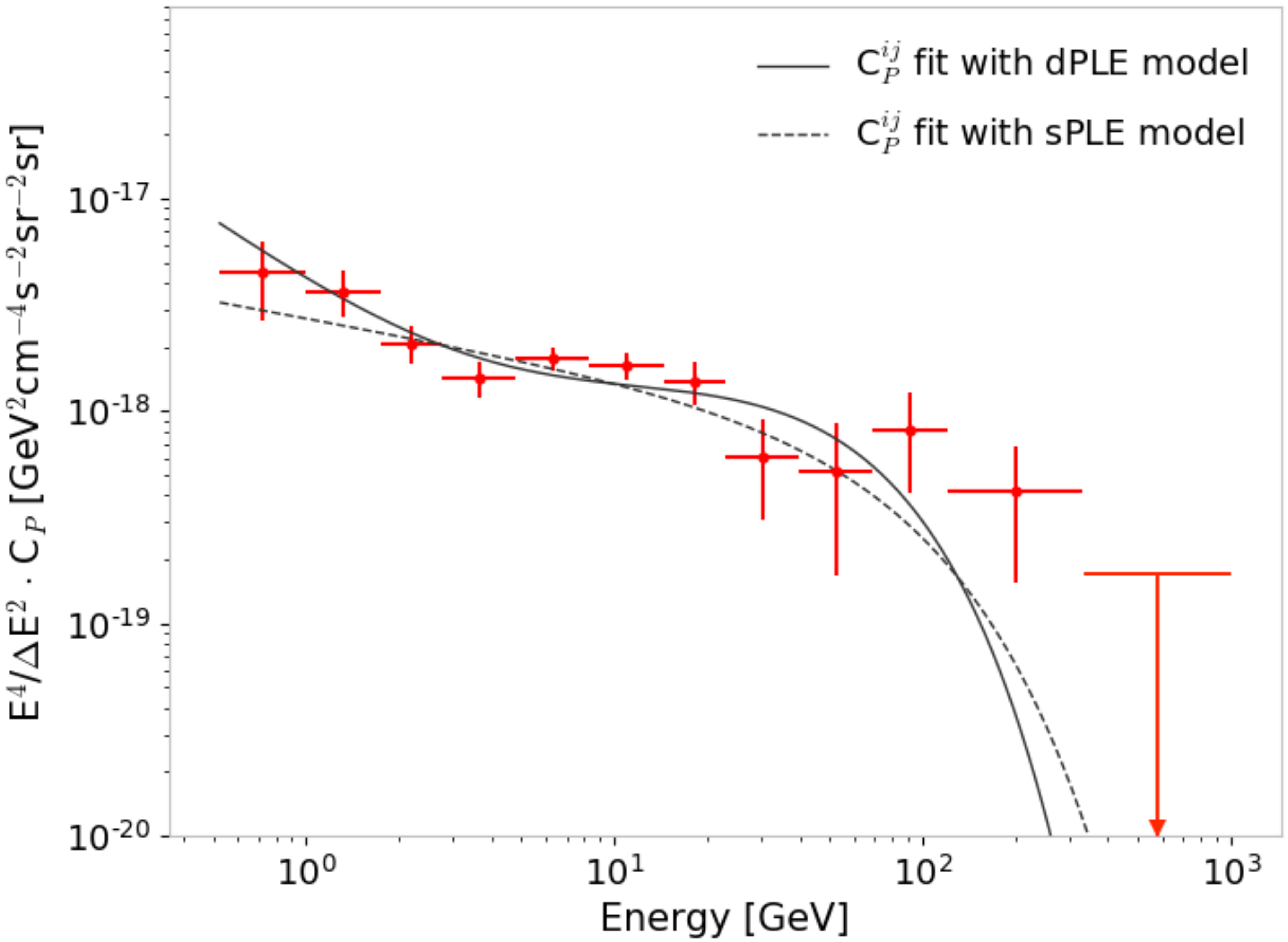

Ackermann et al. 2018

Cross-correlation of energy bins

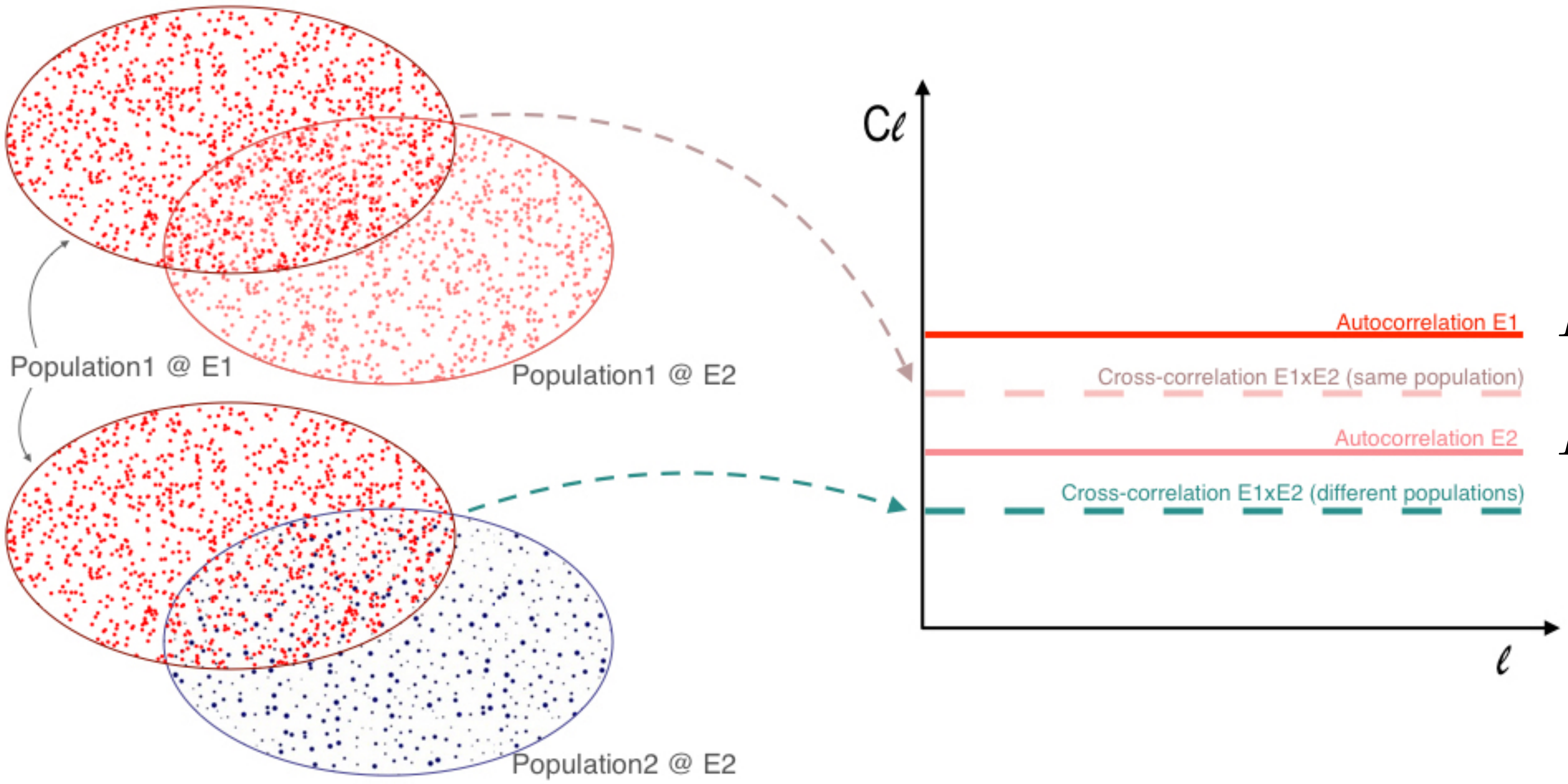

$$E_1 \times E_1 = C_P^{11}$$

$$E_2 \times E_2 = C_P^{22}$$

$$E_1 \times E_2 = C_P^{12} \leq \sqrt{C_P^{11} C_P^{22}}$$

Cross-correlation of energy bins

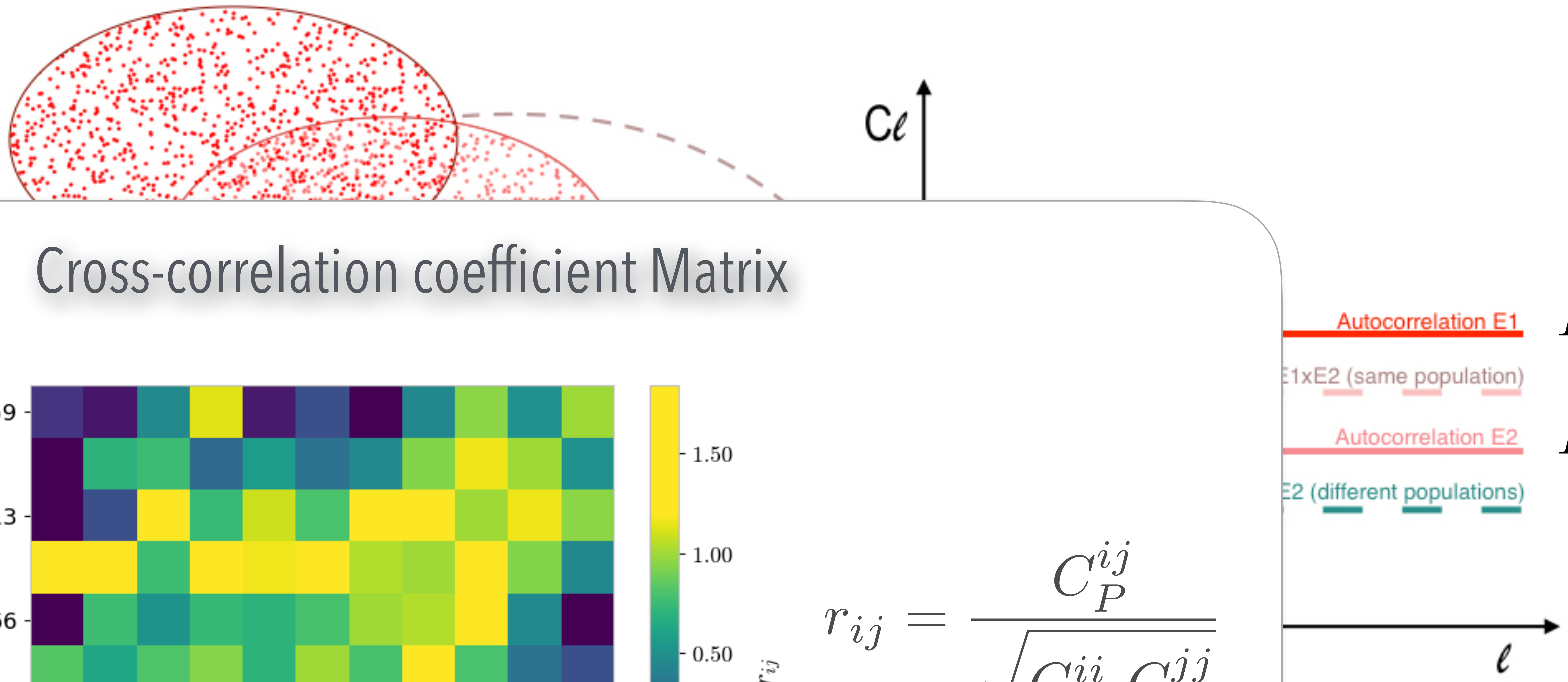

$$E_1 \times E_1 = C_P^{11}$$

$$E_2 \times E_2 = C_P^{22}$$

$$E_2 = C_P^{12} \leq \sqrt{C_P^{11} C_P^{22}}$$

Cross-correlation coefficient Matrix

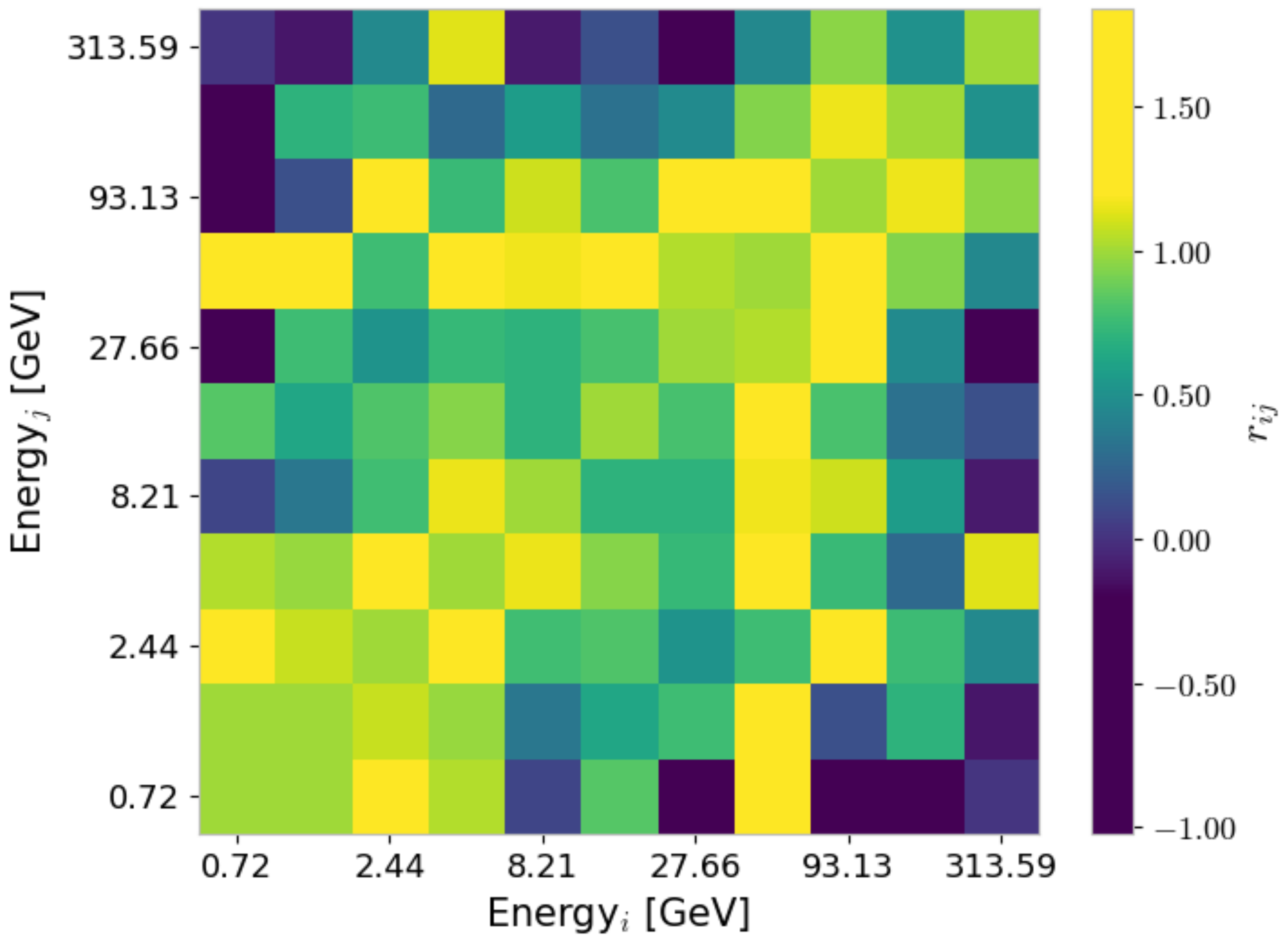

$$r_{ij} = \frac{C_P^{ij}}{\sqrt{C_P^{ii}\ C_P^{jj}}}$$

Cross-correlation of energy bins

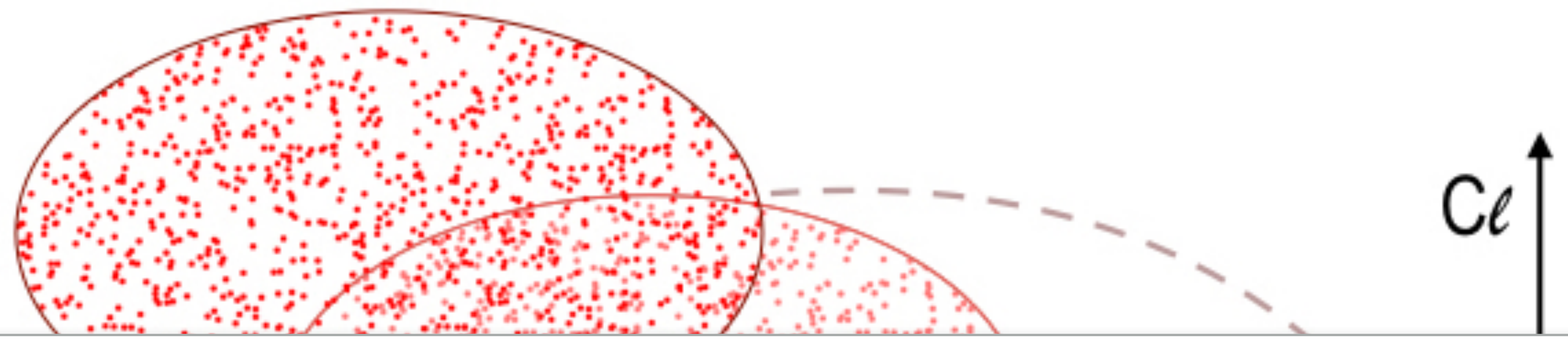

Cross-correlation coefficient Matrix

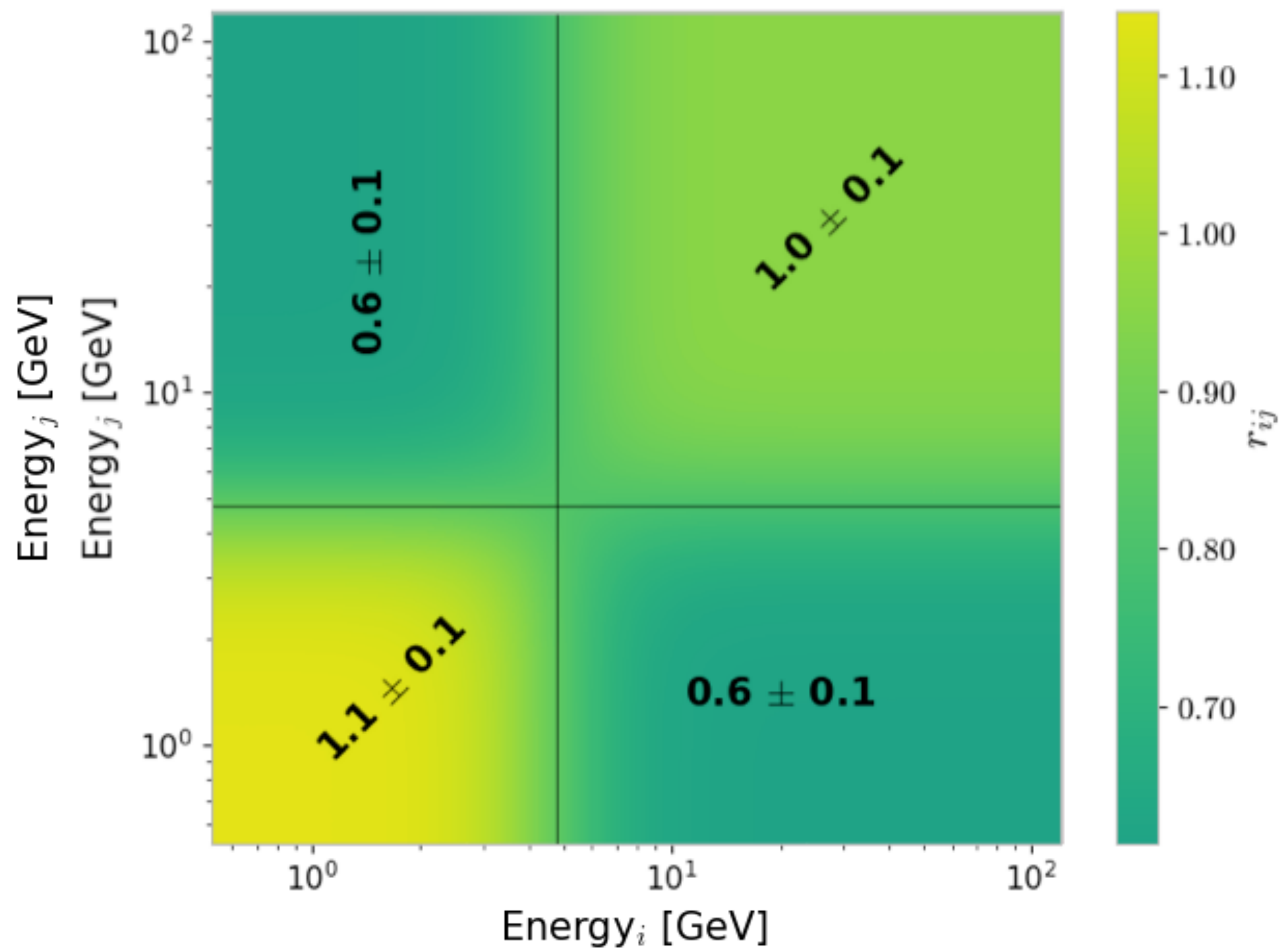

$$r_{ij} = \frac{C_P^{ij}}{\sqrt{C_P^{ii}\ C_P^{jj}}}$$

$$E_1 \times E_1 = C_P^{11}$$

$$E_2 \times E_2 = C_P^{22}$$

$$E_2 = C_P^{12} \leq \sqrt{C_P^{11} C_P^{22}}$$

Cross-correlation of energy bins

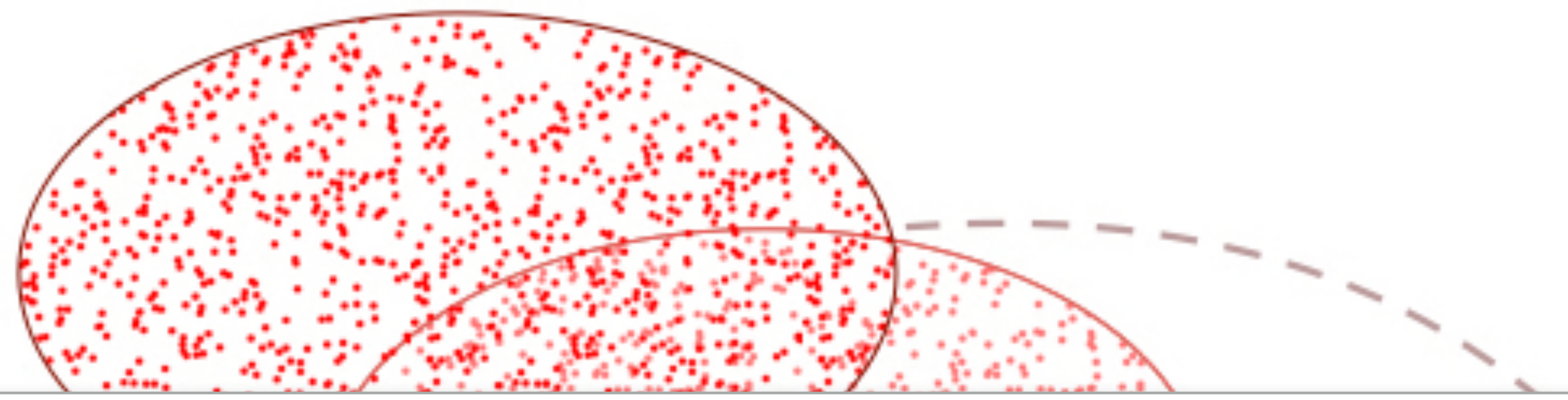

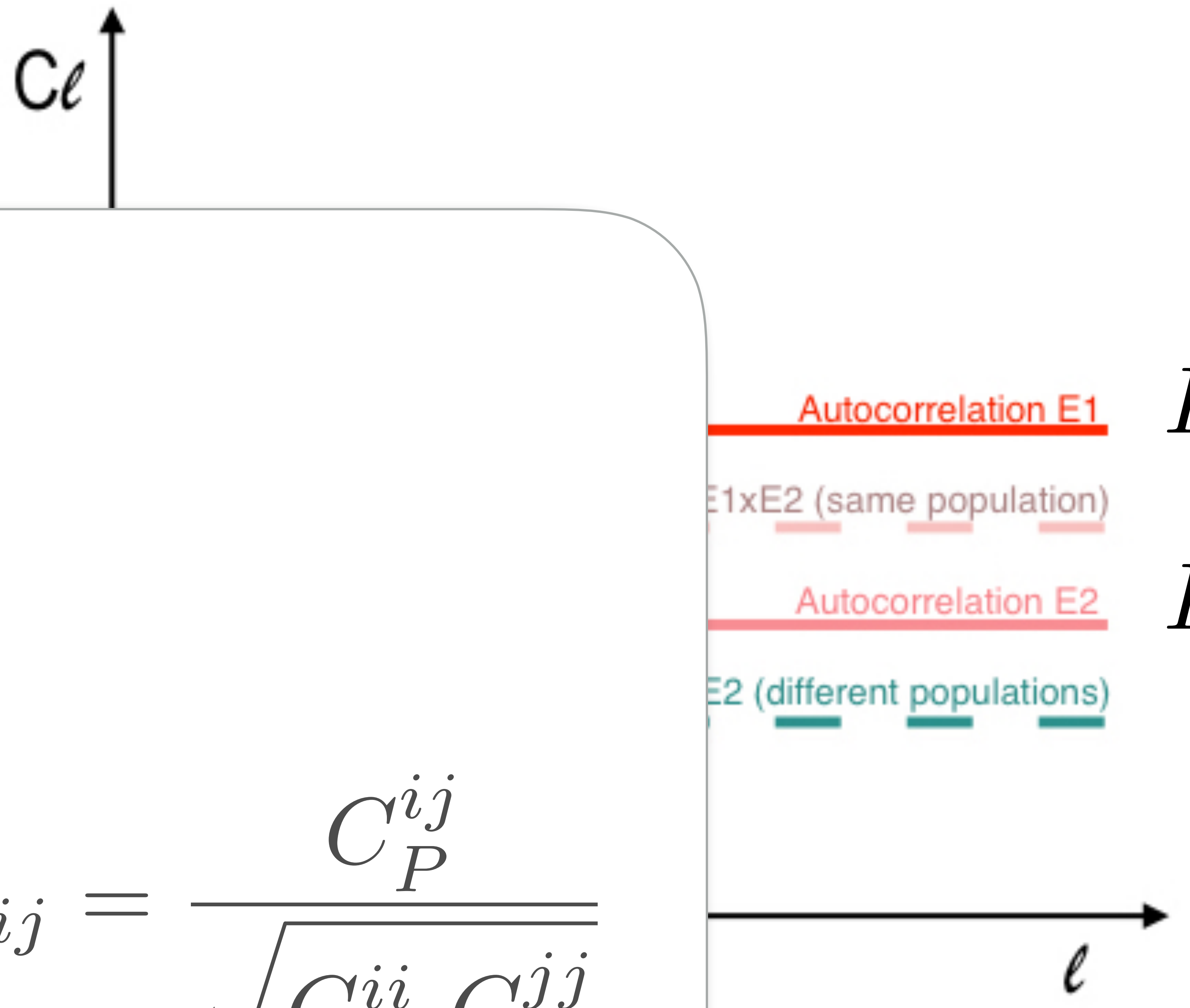

$$E_1 \times E_1 = C_P^{11}$$

$$E_2 \times E_2 = C_P^{22}$$

Cross-correlation coefficient Matrix

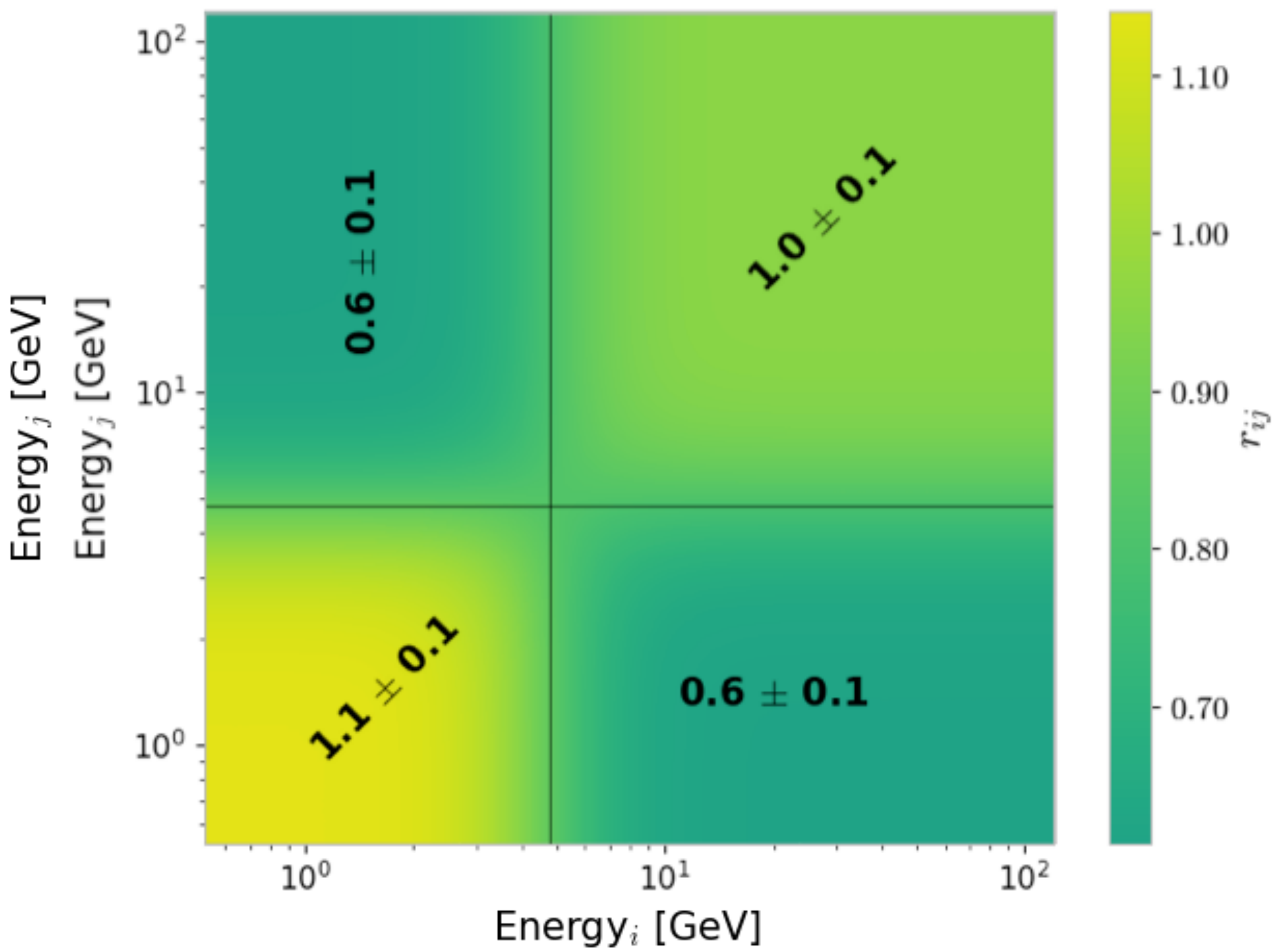

$$r_{ij} = \frac{C_P^{ij}}{\sqrt{C_P^{ii}\ C_P^{jj}}}$$

$$\leq \sqrt{C_P^{11} C_P^{22}}$$

Physical interpretation (work in progress)
- constrain source populations models
- constrain WIMP-like DM parameters

Cross-correlation with other probes

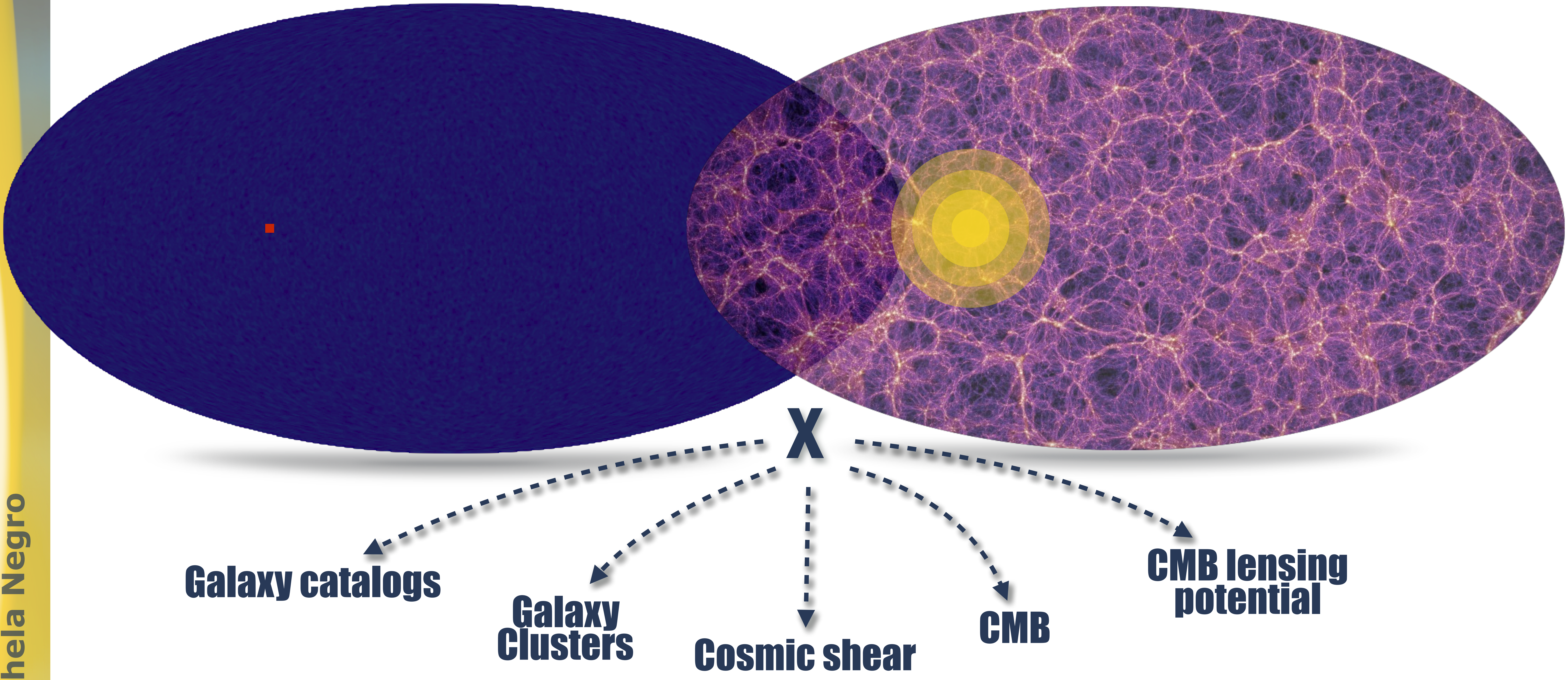

Cross-correlation with Galaxy catalogs

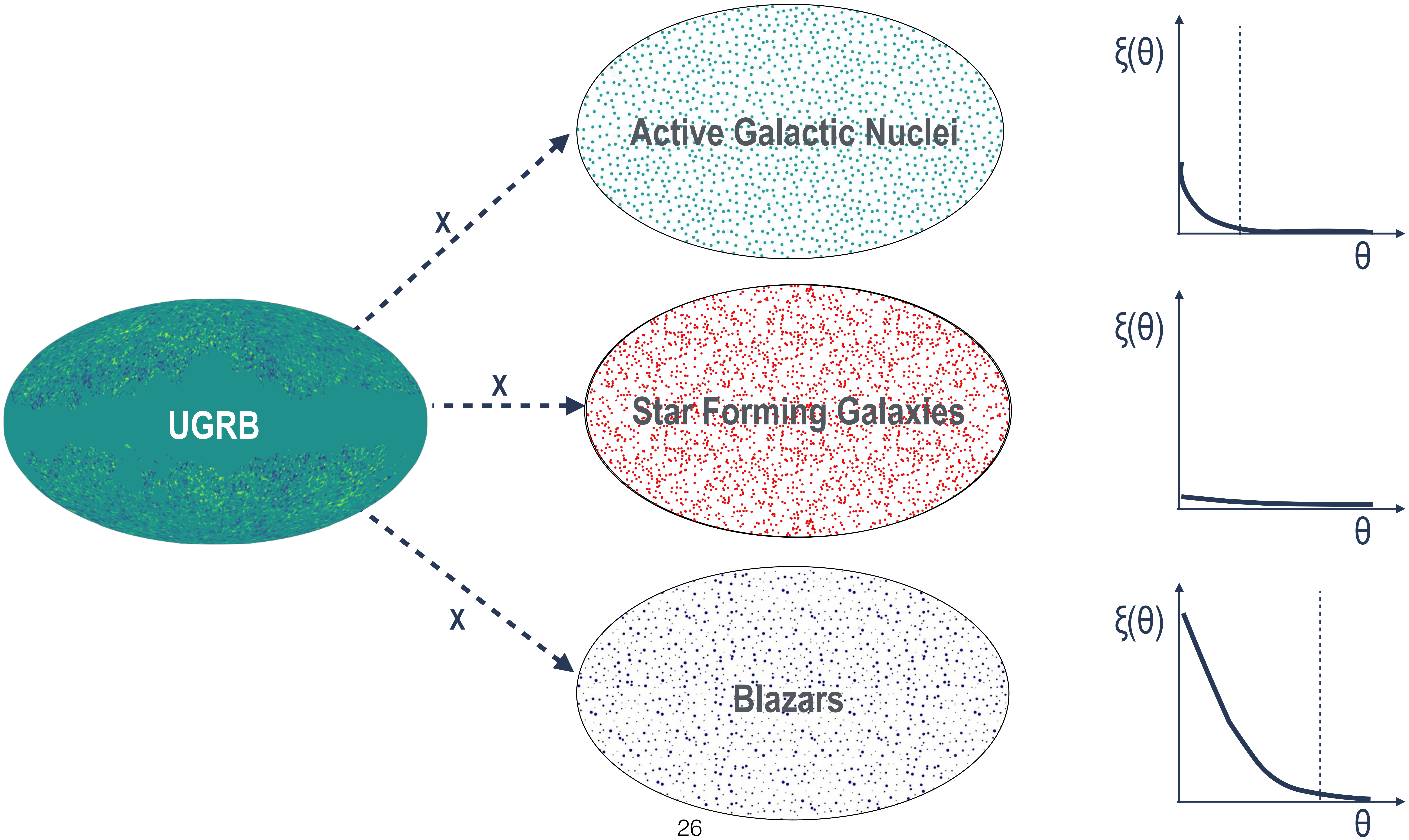

Cross-correlation with Galaxy catalogs

Investigated surveys with **spectral** (E) and **tomographic** (z) approach:

[Cuoco et al. 2017]

- **NVSS**
- **WISExSuperCOSMOS**
- **2MPZ**
- **SDSS DR12**
- **SDSS DR6 QSO**

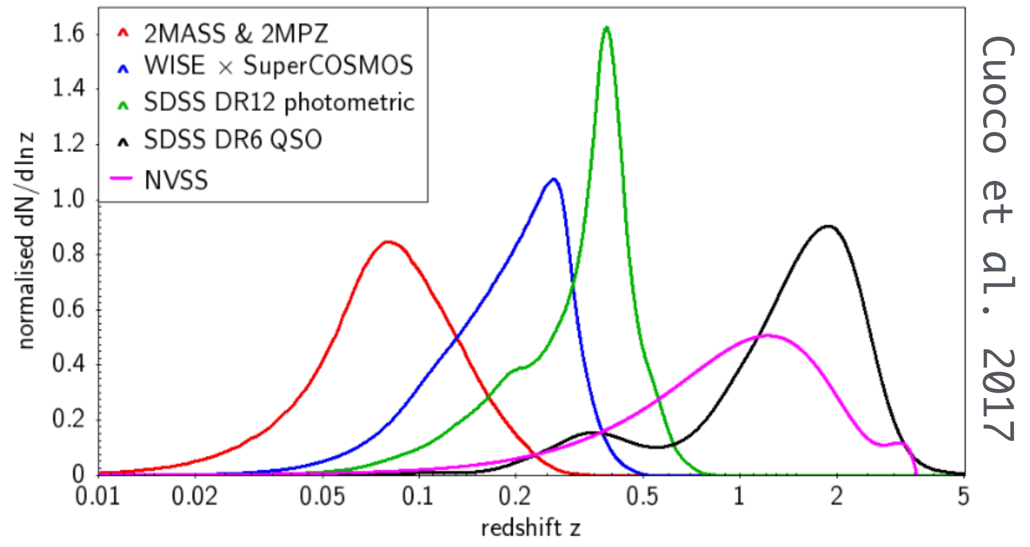

~Very high significance signal (up to 10 σ for NVSS)

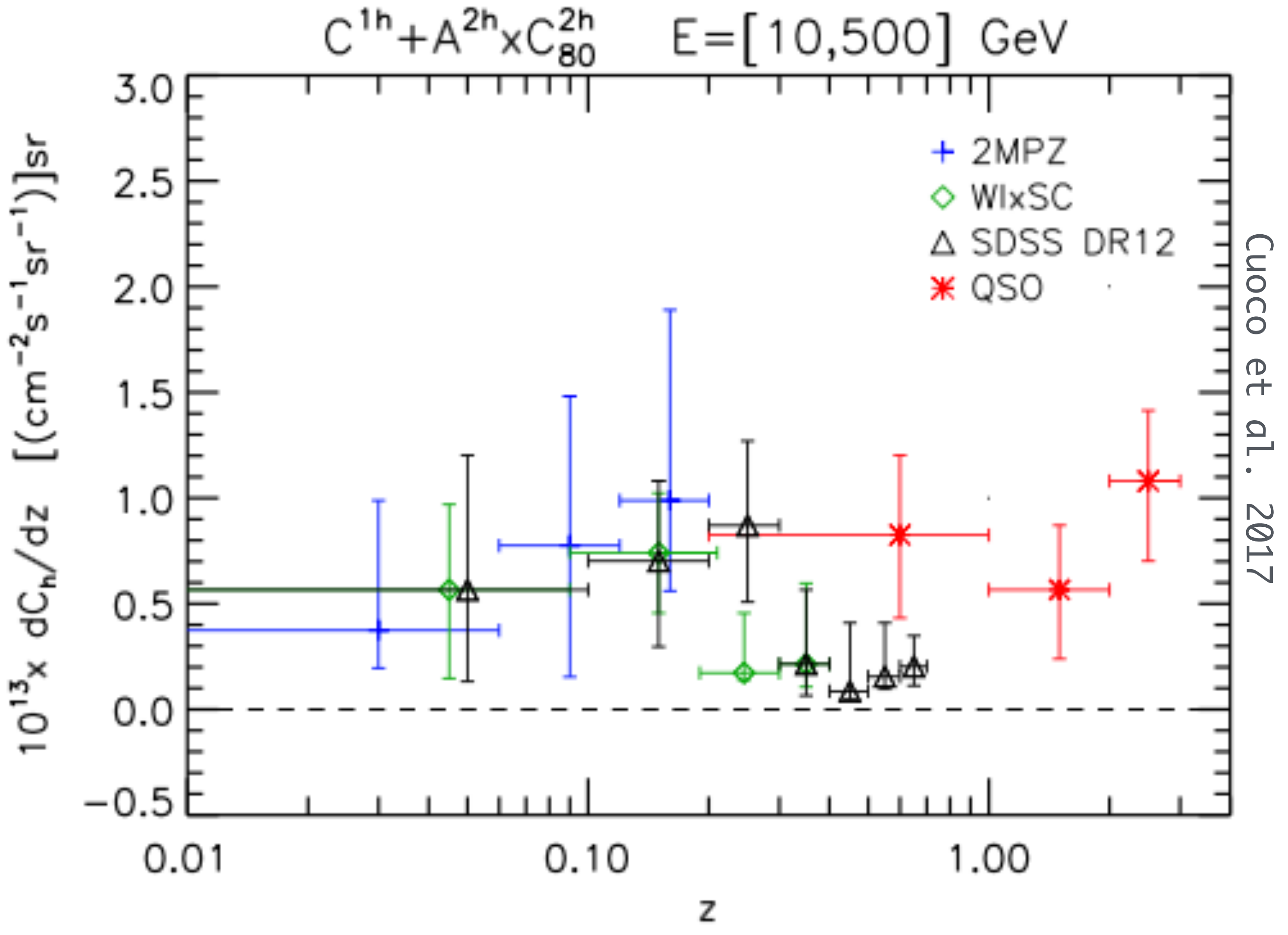

Signal varies with redshift:

UGRB produced by different types of sources

PHOTON 2019

Michela Negro

Cross-correlation with Galaxy catalogs

Beyond the **tomographic** approach for **2MPZ** catalog:

[Ammazzalorso et al. 2018]

- **redshift slicing (3 bins)**
- **B-band** luminosity slicing:
  traces the star formation activity
- **K-band** luminosity slicing:
  correlates with objects mass
- **High K - low B** (high masses + low level of star formation)**:**
  traces DM (WIMP)

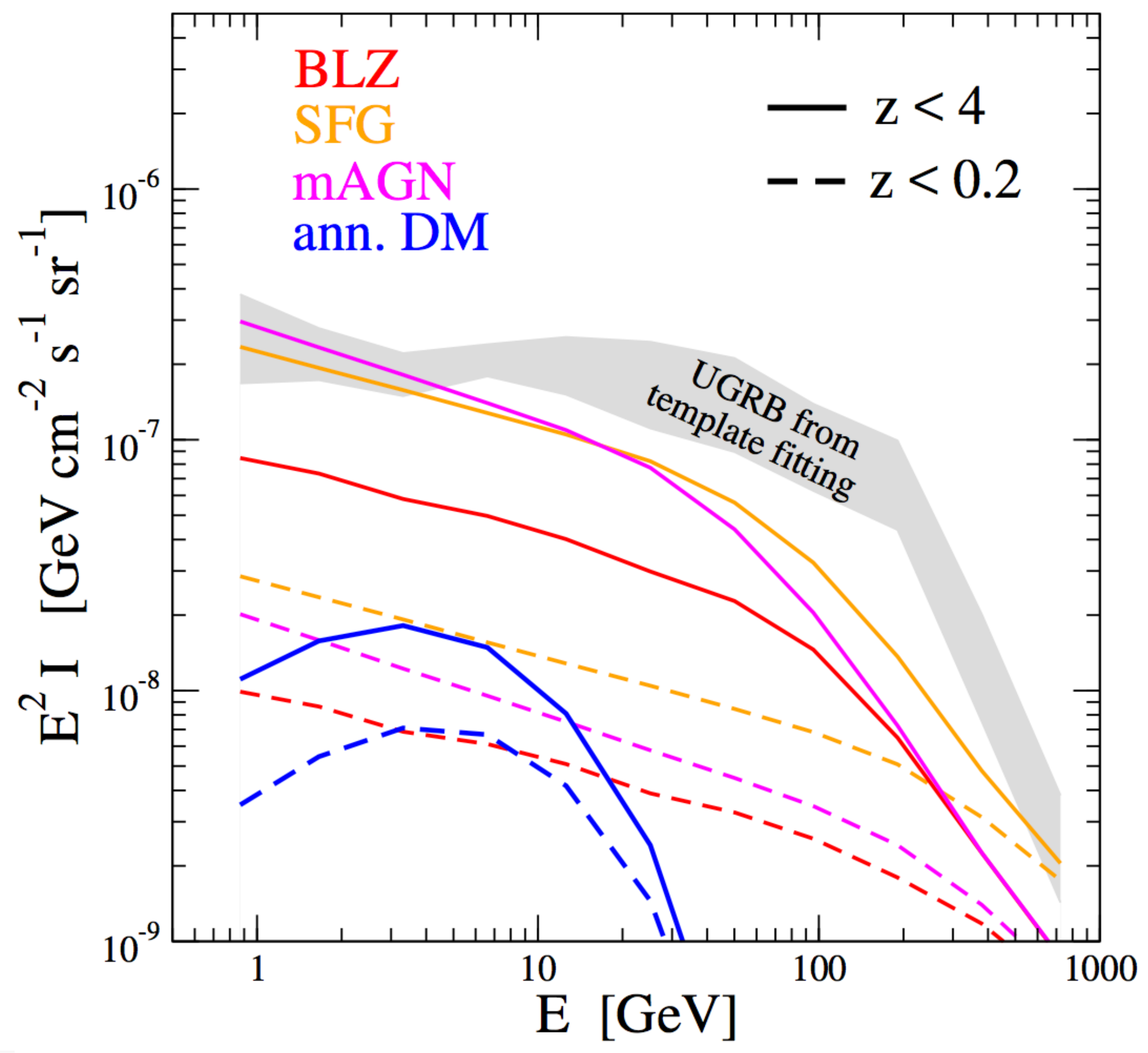

z < 0.2

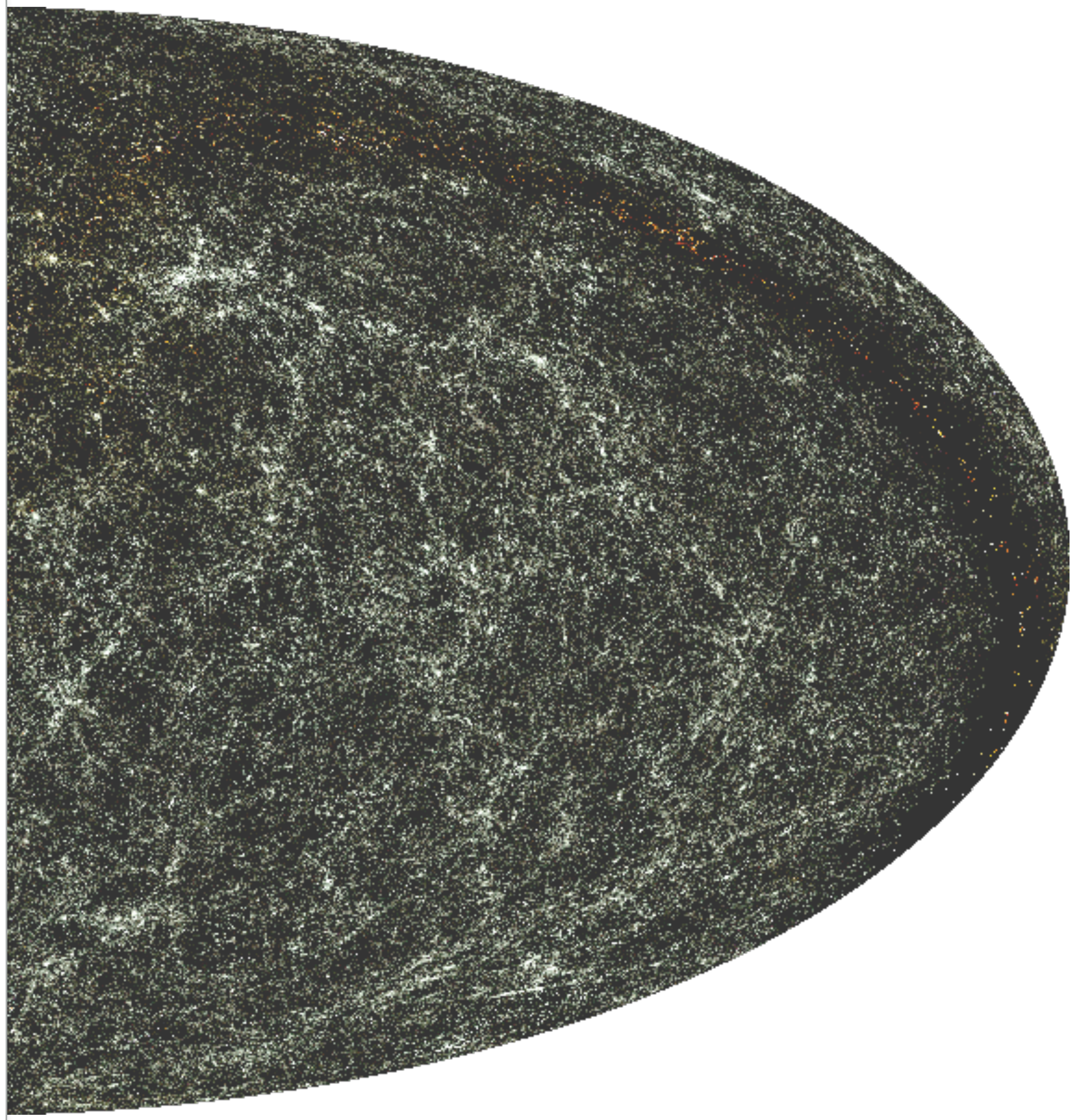

Signal dominated by **mAGNs** emissions + subdominant contribution from **blazars** and **SFGs**

Cross-correlation with Galaxy clusters

Constrain the contribution of **Intra-cluster medium** and **DM**

e.g. [Branchini et al. 2017]

- **WHL12 (158,103 clusters)**
- **redMaPPer (26,350 clusters)**
- **PlanckSZ (1,653 clusters)**

>3σ signal!

1-halo term

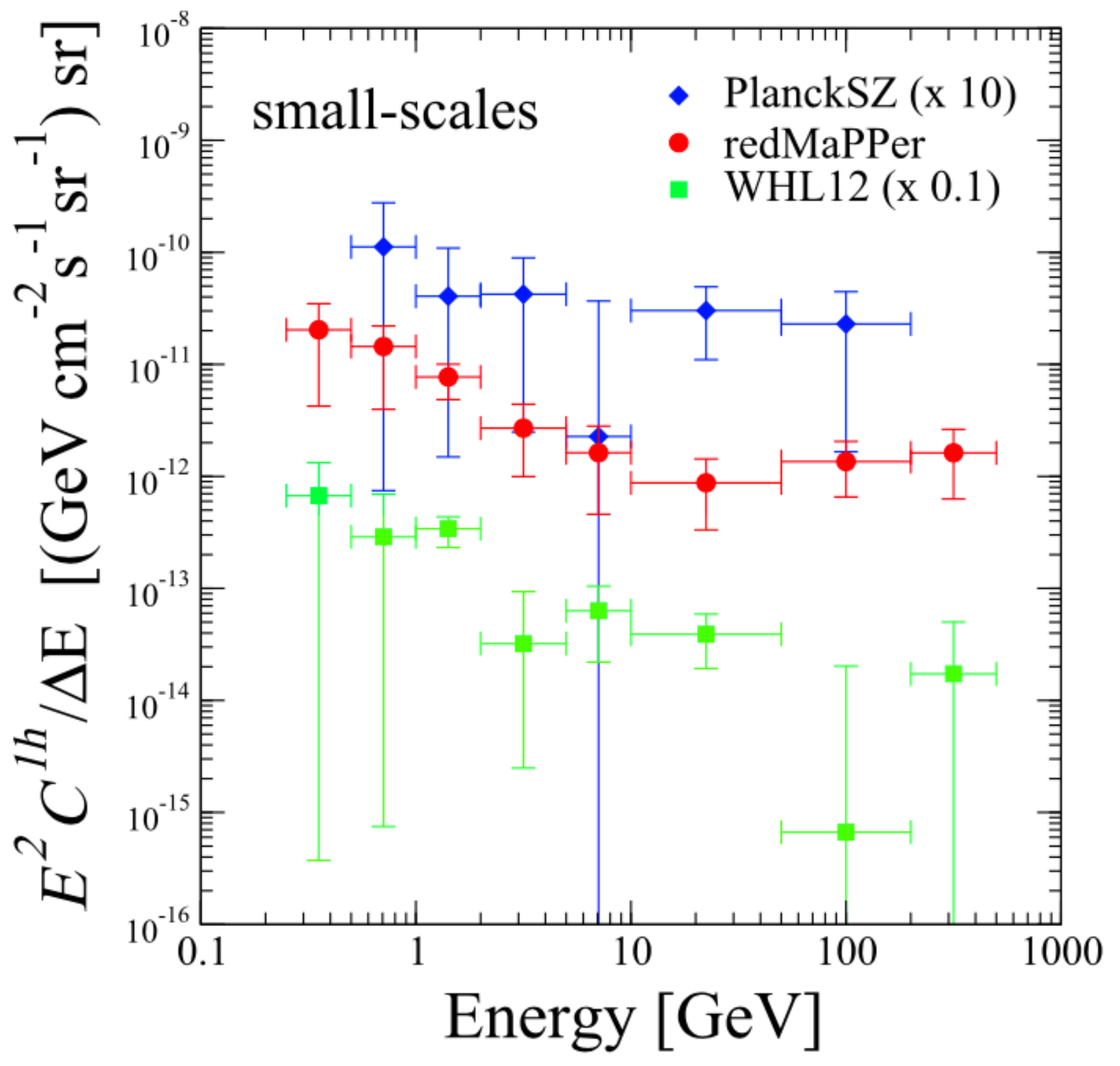

Small scales:
hard component
+ soft component

The Coma cluster of Galaxies

PHOTON 2019
Michela Negro

Cross-correlation with cosmic shear

Cosmic shear:

statistical measurement of the distortion of images due to the weak lensing

net ellipticity

mass distribution

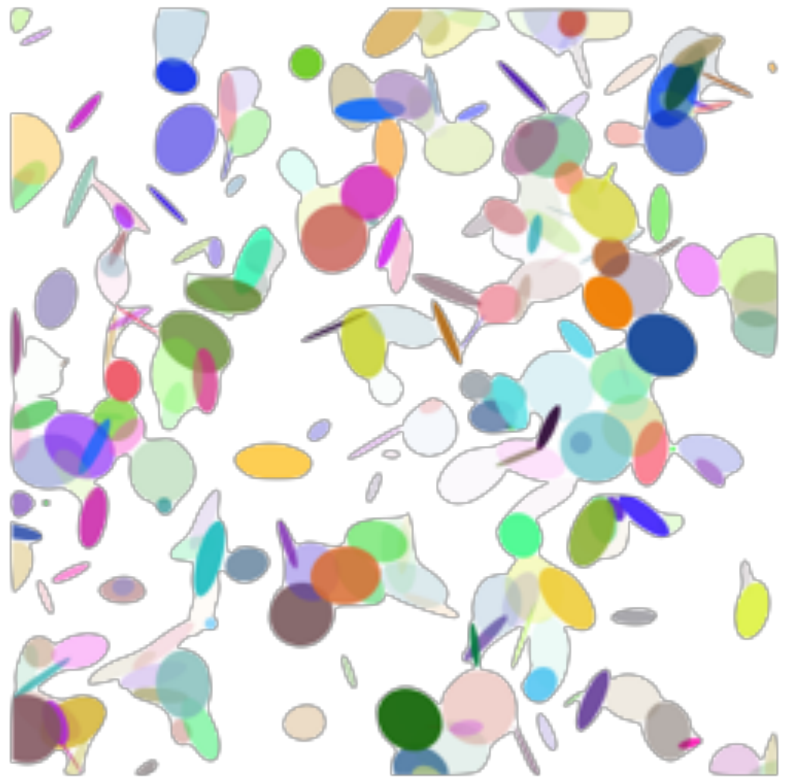

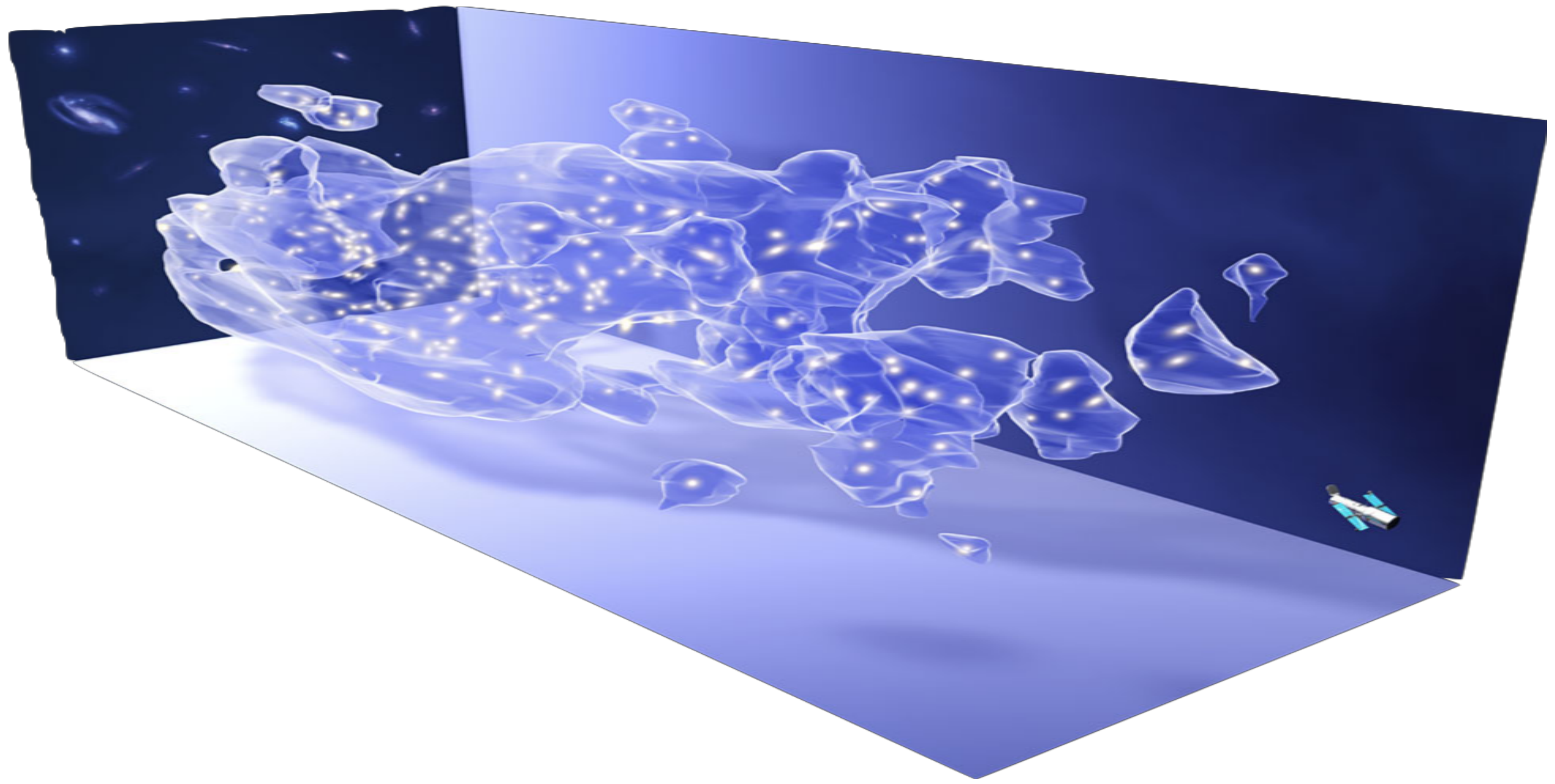

Investigated surveys with **spectral** and **tomographic** approach (proposed by Camera et al. 2013/2015):

- **CFHTLenS + RCSLenS + KiDs** [Troster et al. 2017]
- **Subaru Hyper Suprime-Cam** [Shirasaki et al. 2018]

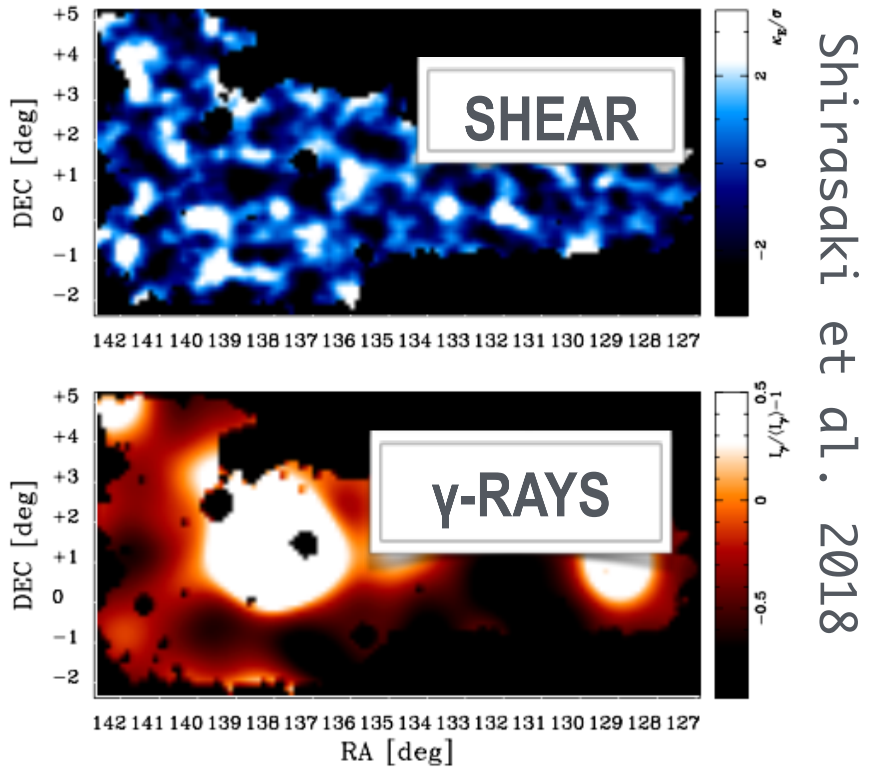

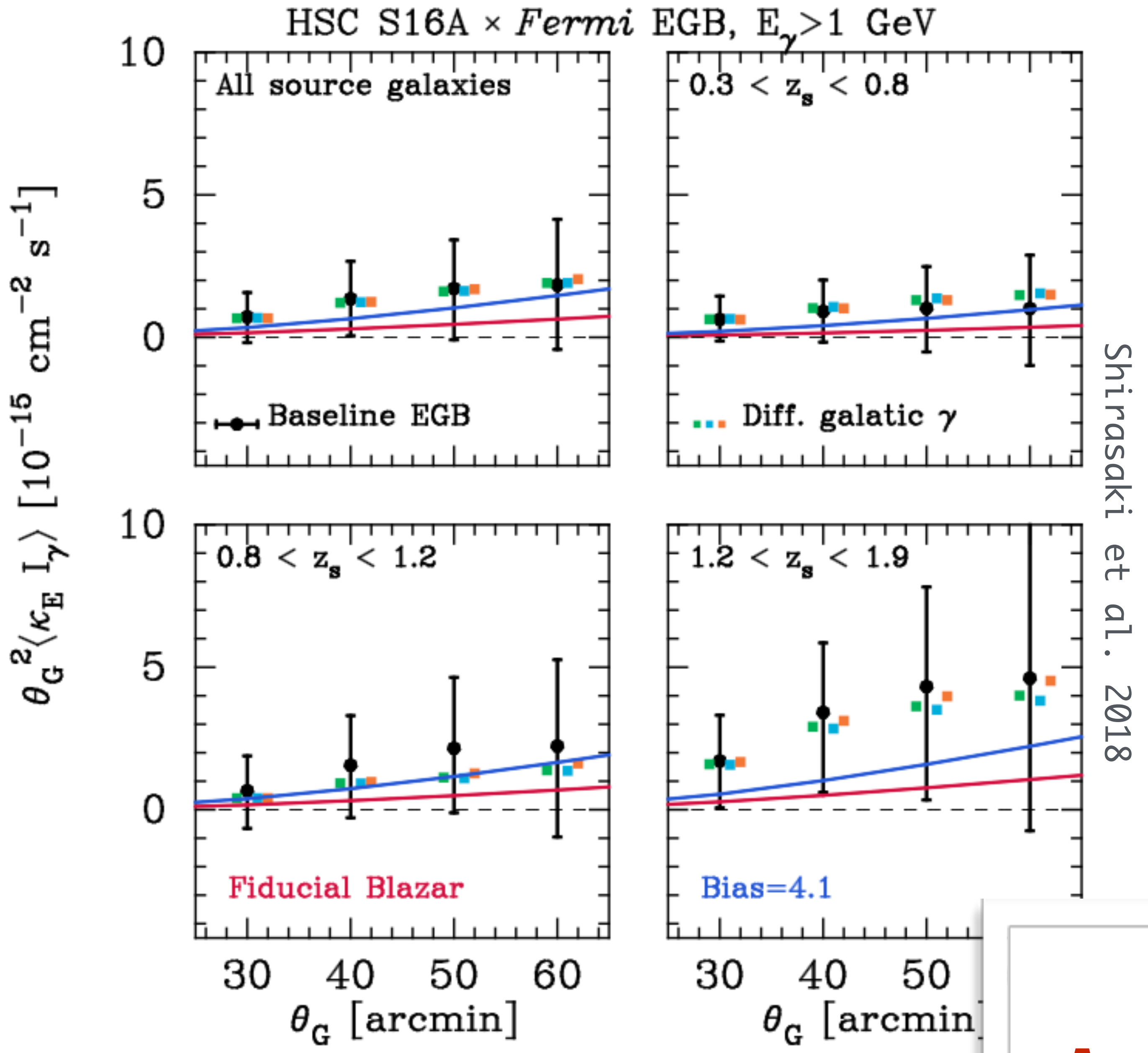

no signal detected!

STAY TUNED: Ammazzalorso et al + DES

PHOTON 2019

Michela Negro

Cross-correlation with CMB lensing

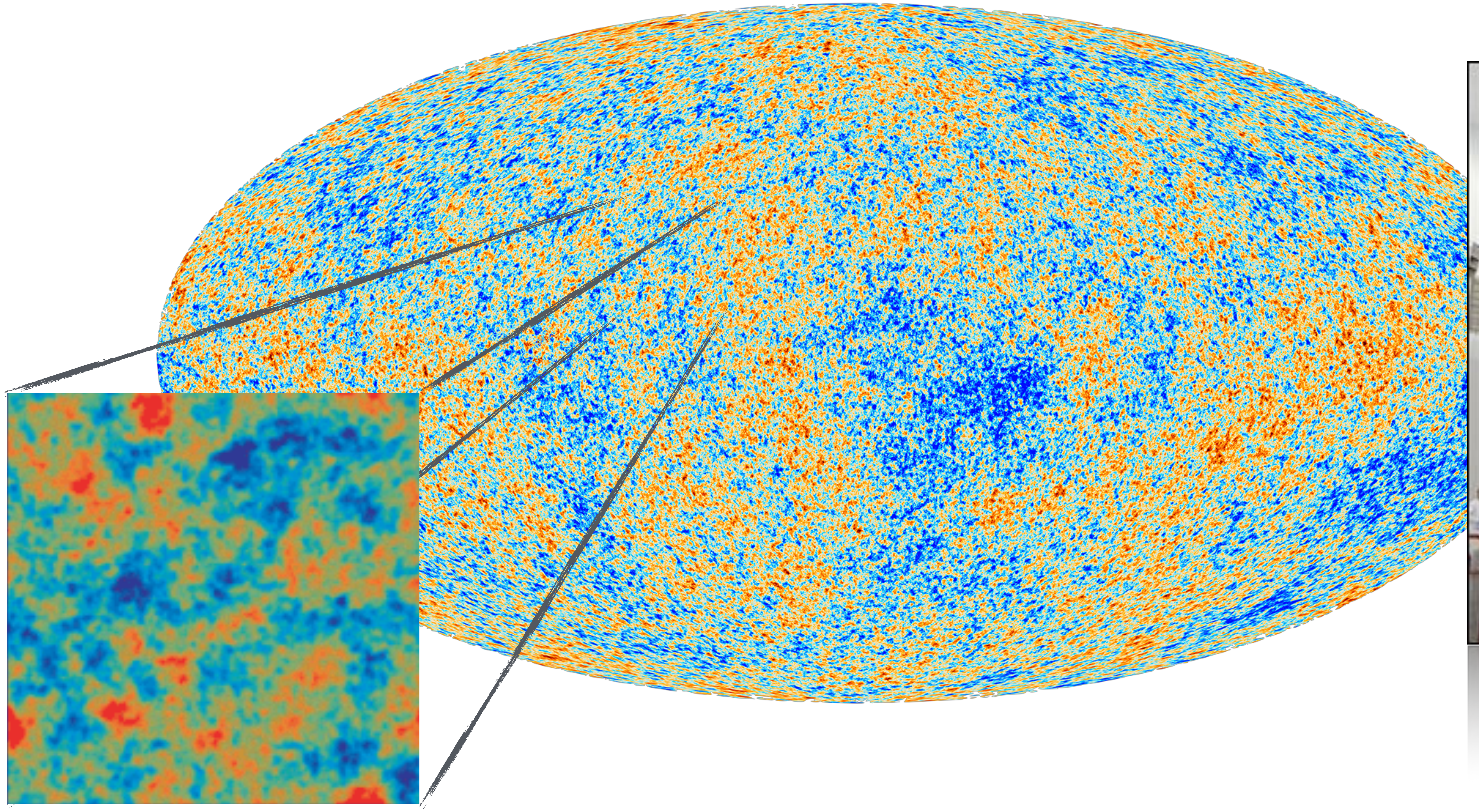

Unlensed

Planck satellite

Cross-correlation with CMB lensing

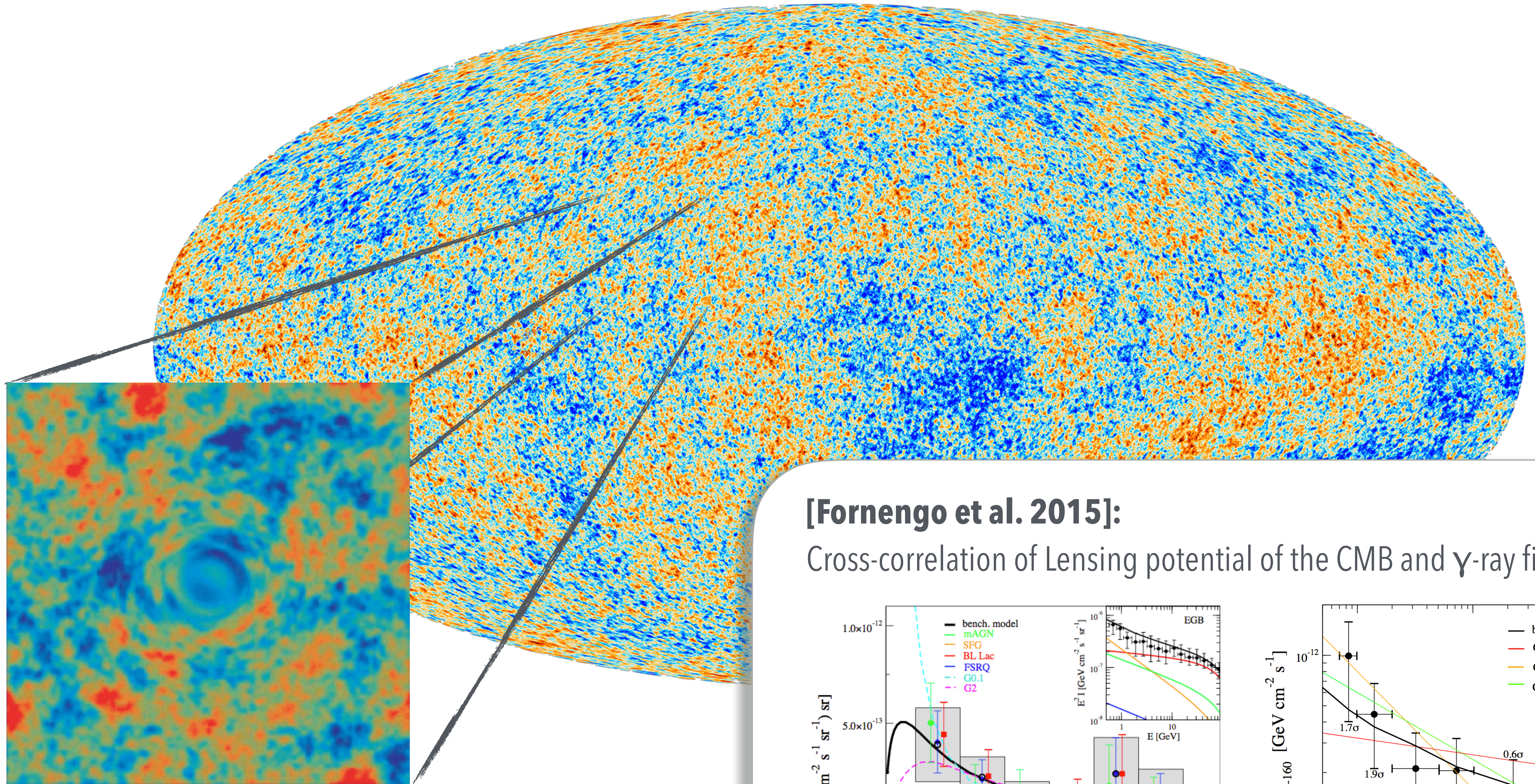

Lensed

[Fornengo et al. 2015]:

Cross-correlation of Lensing potential of the CMB and γ-ray field to investigate the LSS

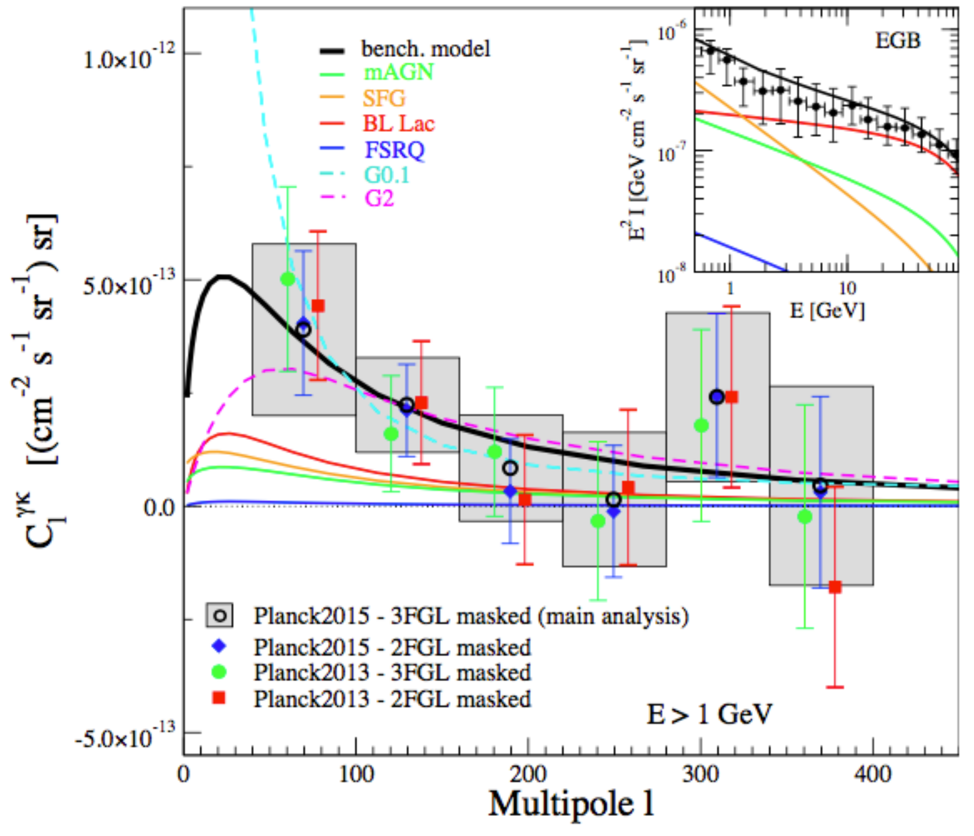

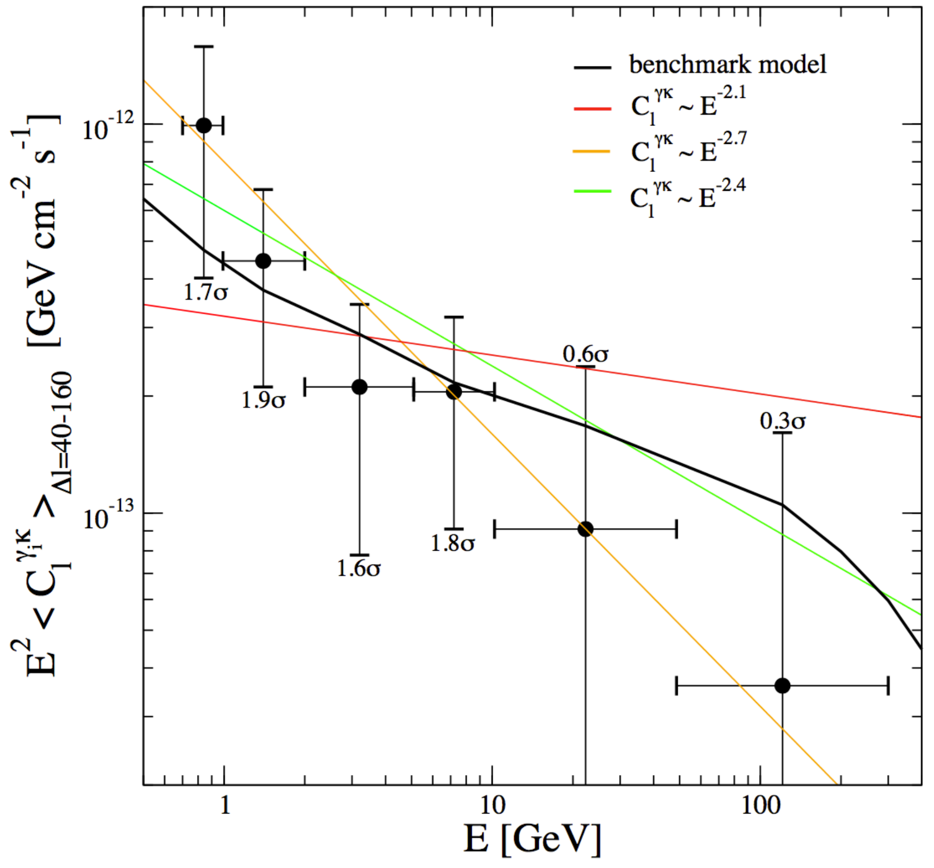

~2σ limit

Cross-correlation with CMB

Signature of the Integrated Saches-Wolfe effect

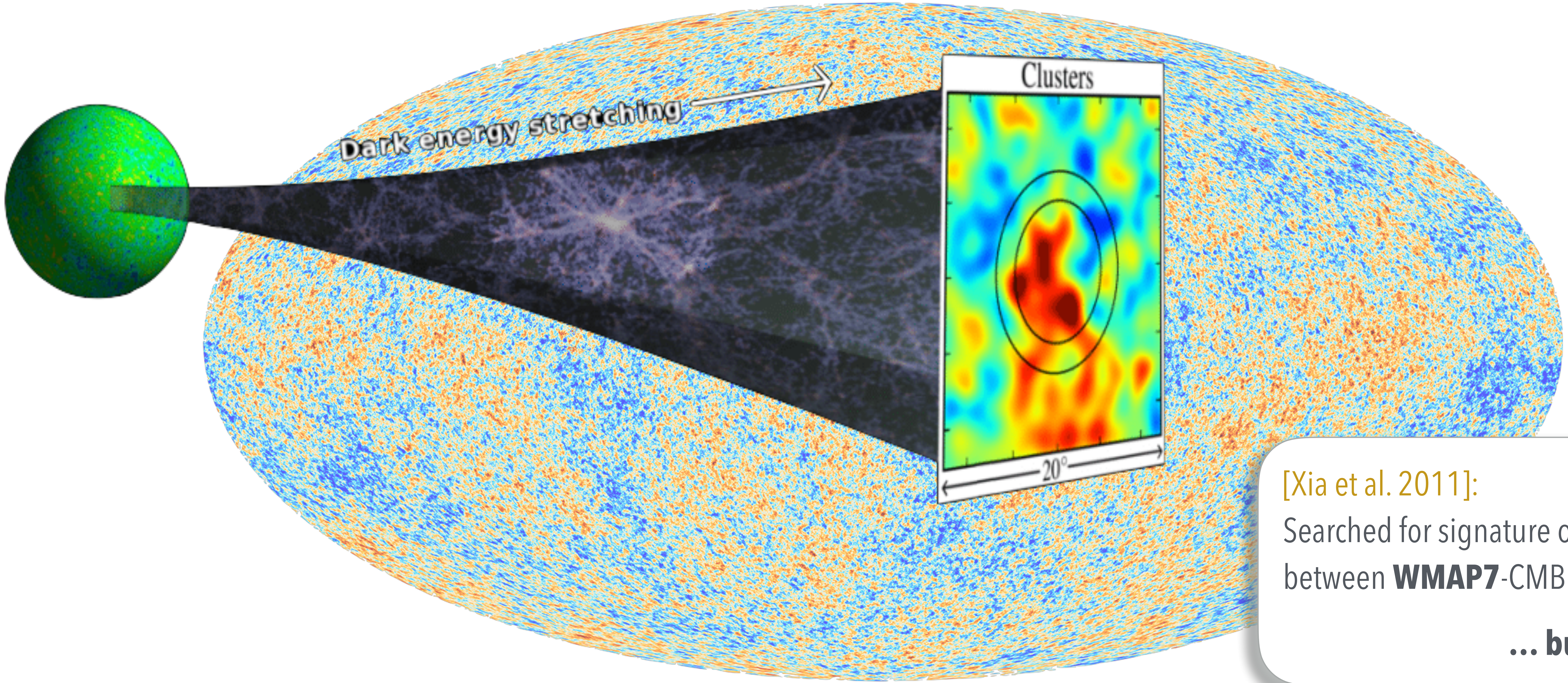

[Xia et al. 2011]:
Searched for signature of ISW in cross-correlation between **WMAP7**-CMB and 21-mo γ-ray data

... but no signal detected!

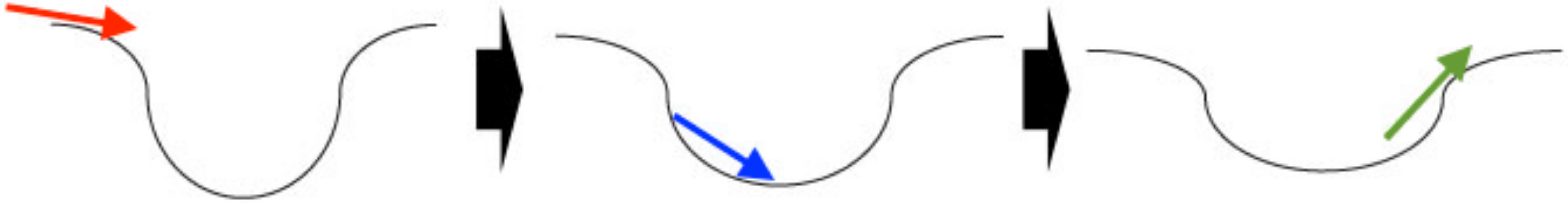

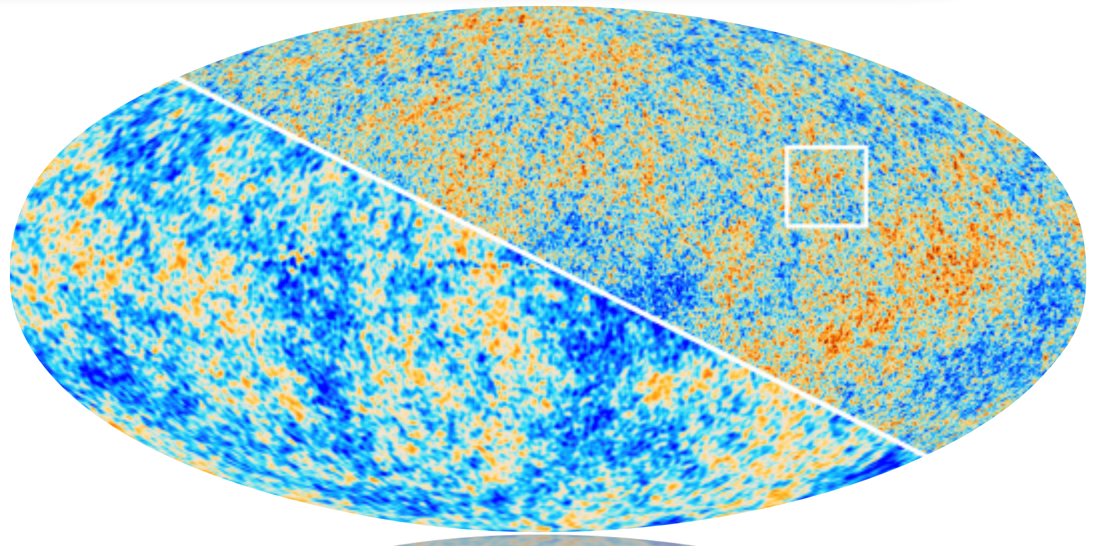

Gravitational well of galaxy supercluster: the depth shrinks as the universe (and cluster) expands

Summary and conclusions

Anisotropy of the UGRB

Complementary to Intensity spectrum estimation to unveil
the nature of the unresolved gamma-ray background

Autocorrelation

to constrain source populations models
to constrain WIMP-like DM parameters

Cross-correlation

to characterize the UGRB composition

Galaxy catalogs
Galaxy Clusters
Cosmic shear
CMB lensing
CMB

Future prospects

Study the High Energy end of the anisotropy spectrum

Čerenkov telescopes
(e.g. HAWC, CTA)

M.G. Aartsen et al.2014

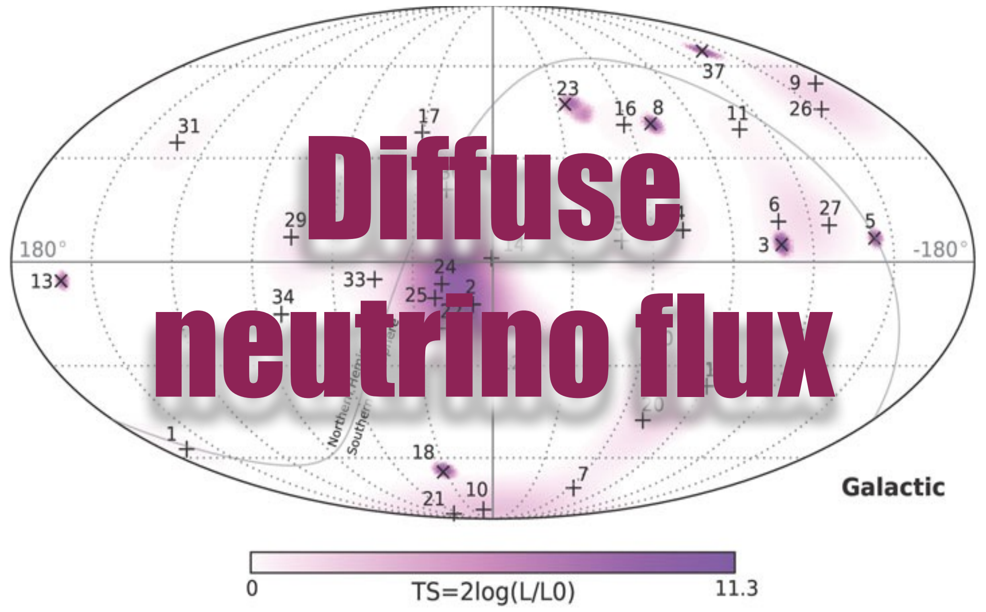

Diffuse neutrino flux

IceCube
(more with IceCube-Gen2*)

Update UGRB-Cosmic shear cross measurements

DES, LSST, Euclid

Update UGRB-CMB/CMB lensing cross measurements

Planck

* https://icecube.wisc.edu/news/view/605

PHOTON 2019

Backup

Physics Torino Department of Excellence

Istituto Nazionale di Fisica Nucleare

Fermi Gamma-ray Space Telescope

Cross-correlation signals

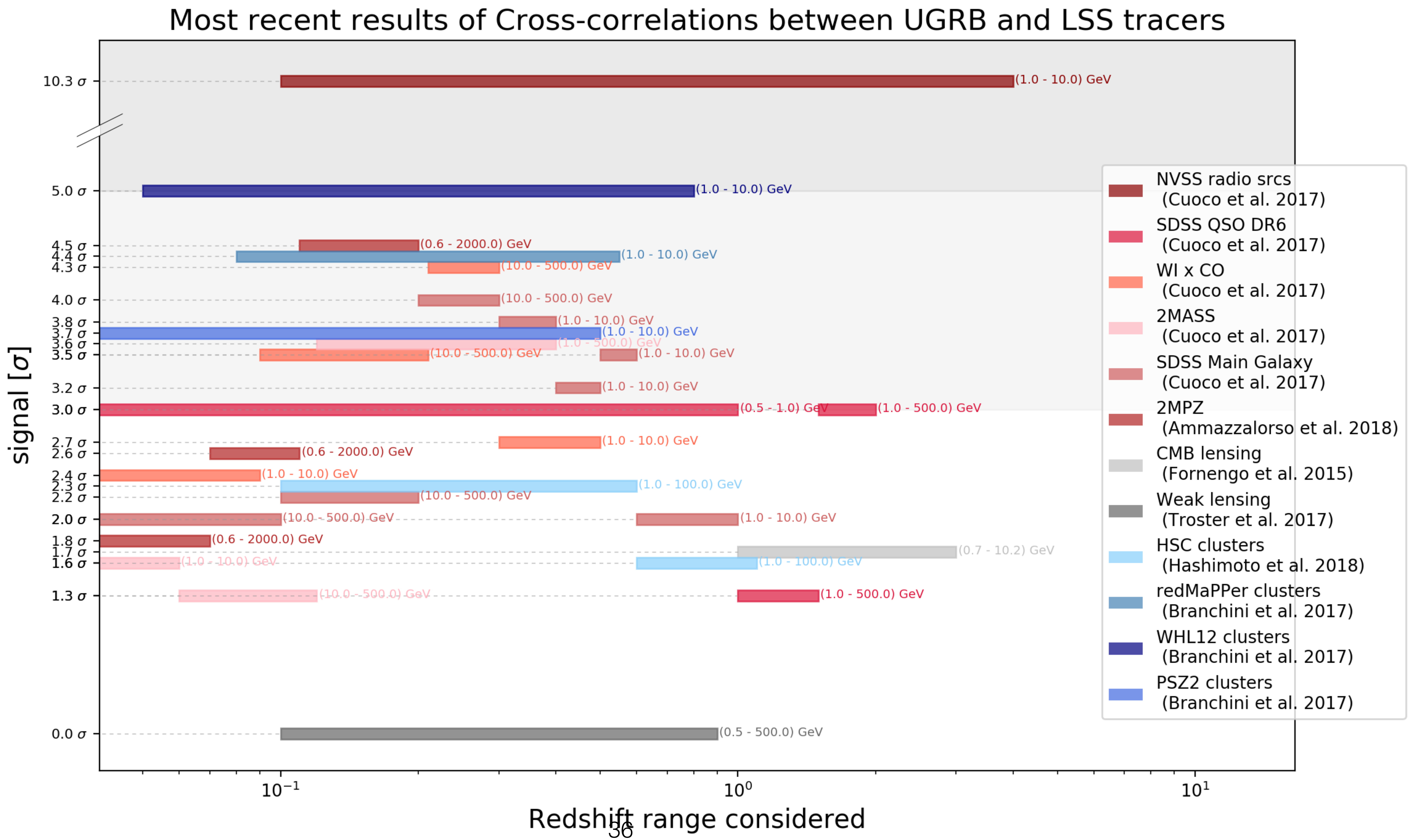

The Angular Power Spectrum - APS

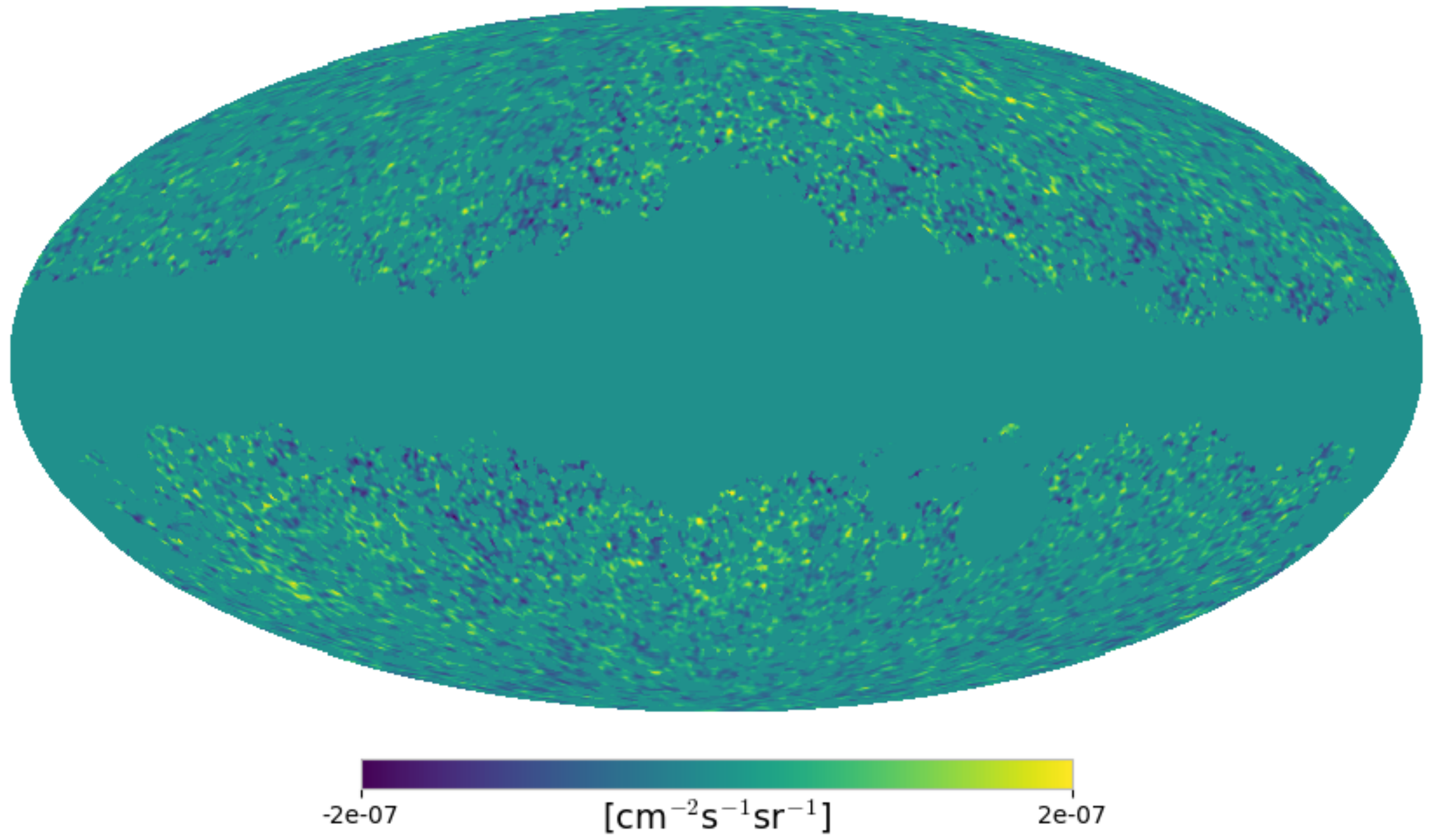

HEALPix maps (order 9, NSIDE=512)

PolSpice

$$\delta I_g(\vec{n}) = \sum_{\ell m} a_{\ell m} Y_{\ell m}(\vec{n})$$

$$C_\ell = \frac{1}{2\ell+1} \langle \sum_m a_{\ell m} a^*_{\ell m} \rangle$$

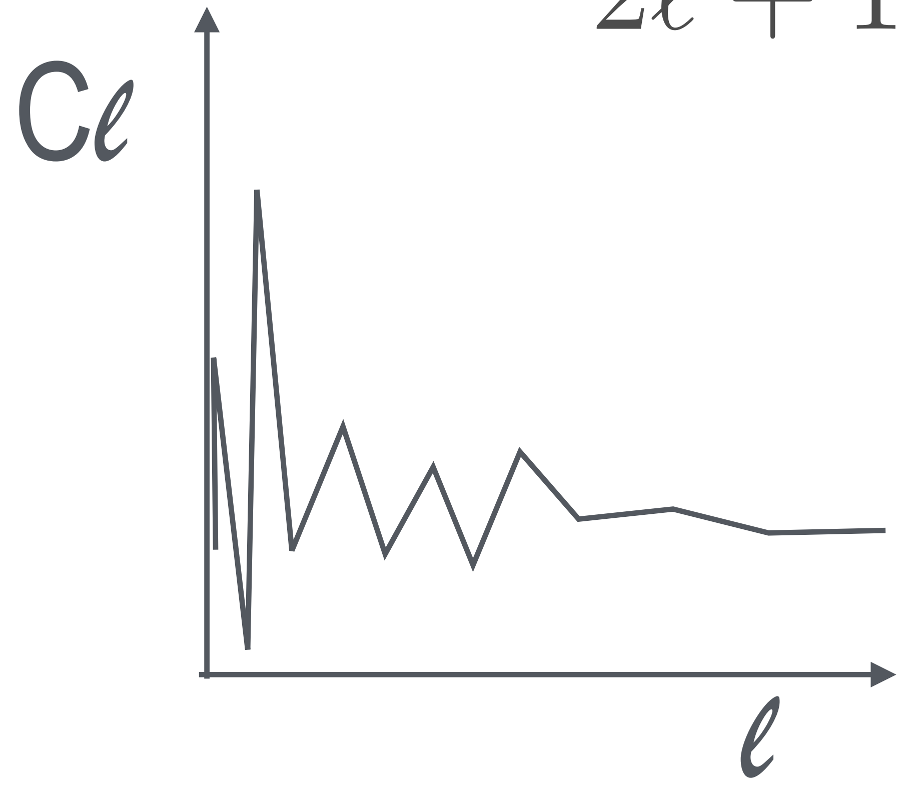

Raw APS

Corrections
- PSF
- Pixellation
- White Noise

True APS

PSF correction - The Window Functions

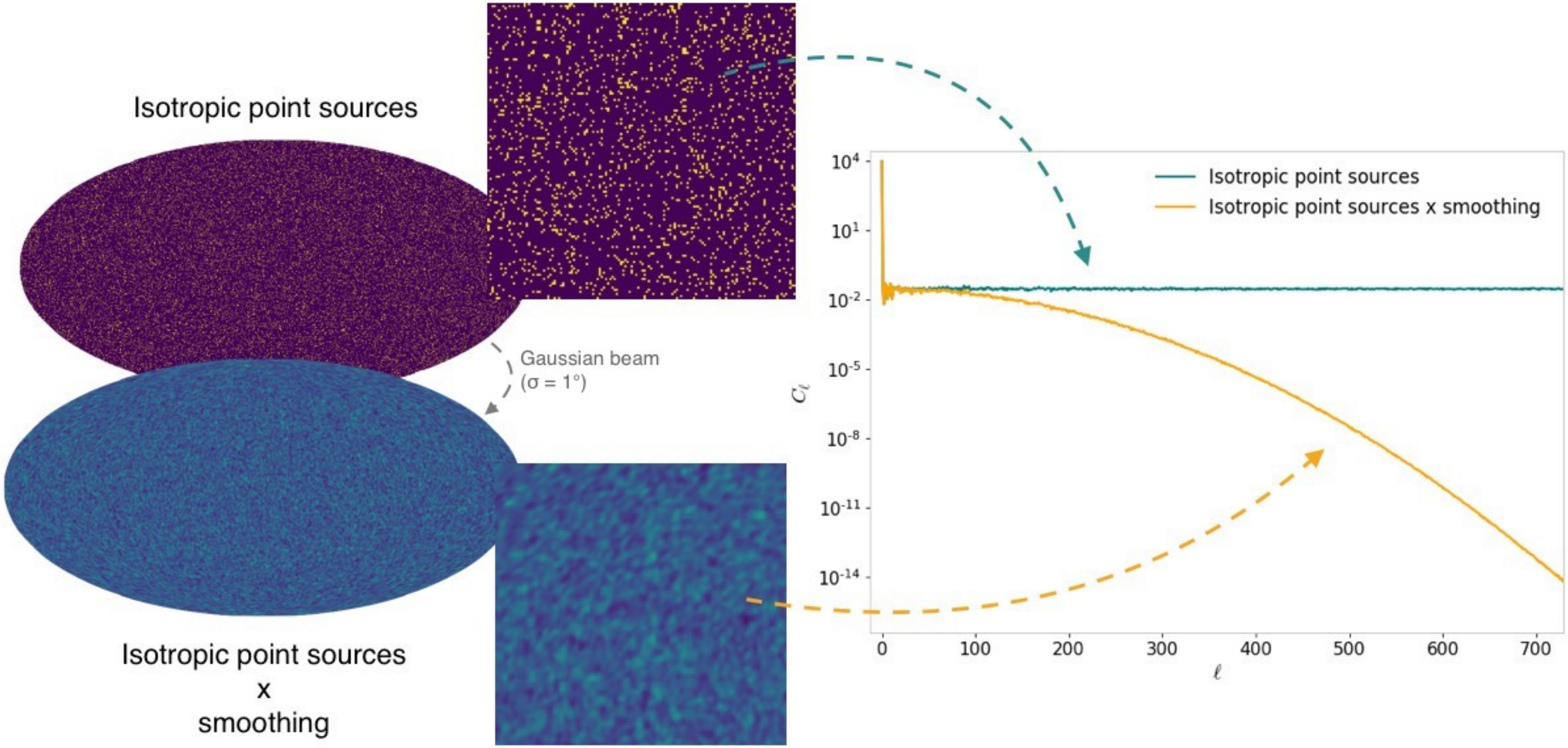

PSF correction - The Widow Functions

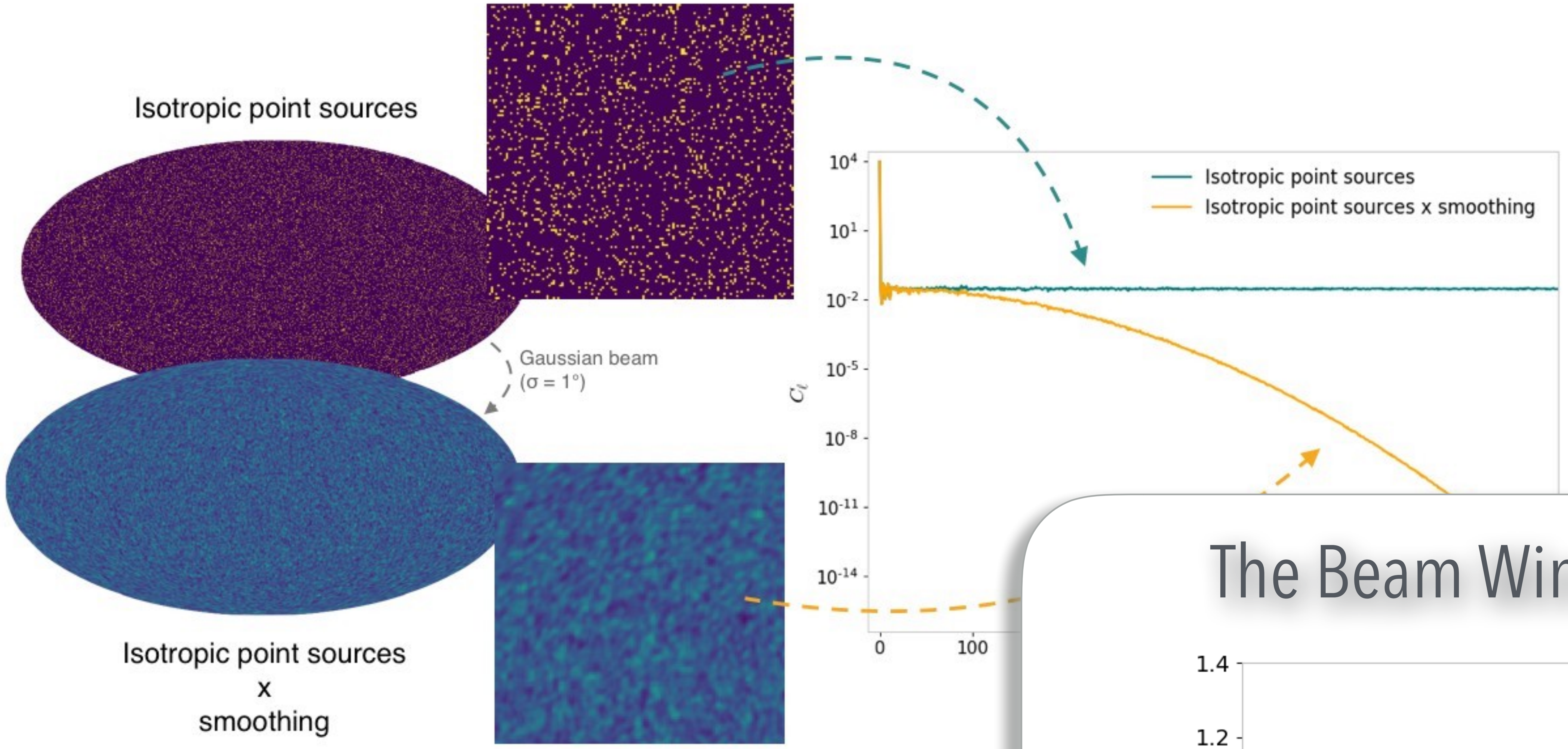

$$W^{beam}(E,\ell) = 2\pi \int_0^{\pi} P_\ell(\cos\theta)\mathrm{PSF}(\theta,E)\,\sin\theta d\theta$$

$$W_E^{beam}(\ell) = \frac{\int_{E_{min}}^{E_{max}} W^{beam}(E,\ell)\frac{dN}{dE}dE}{\int_{E_{min}}^{E_{max}} \frac{dN}{dE}dE}$$

The Beam Window Functions

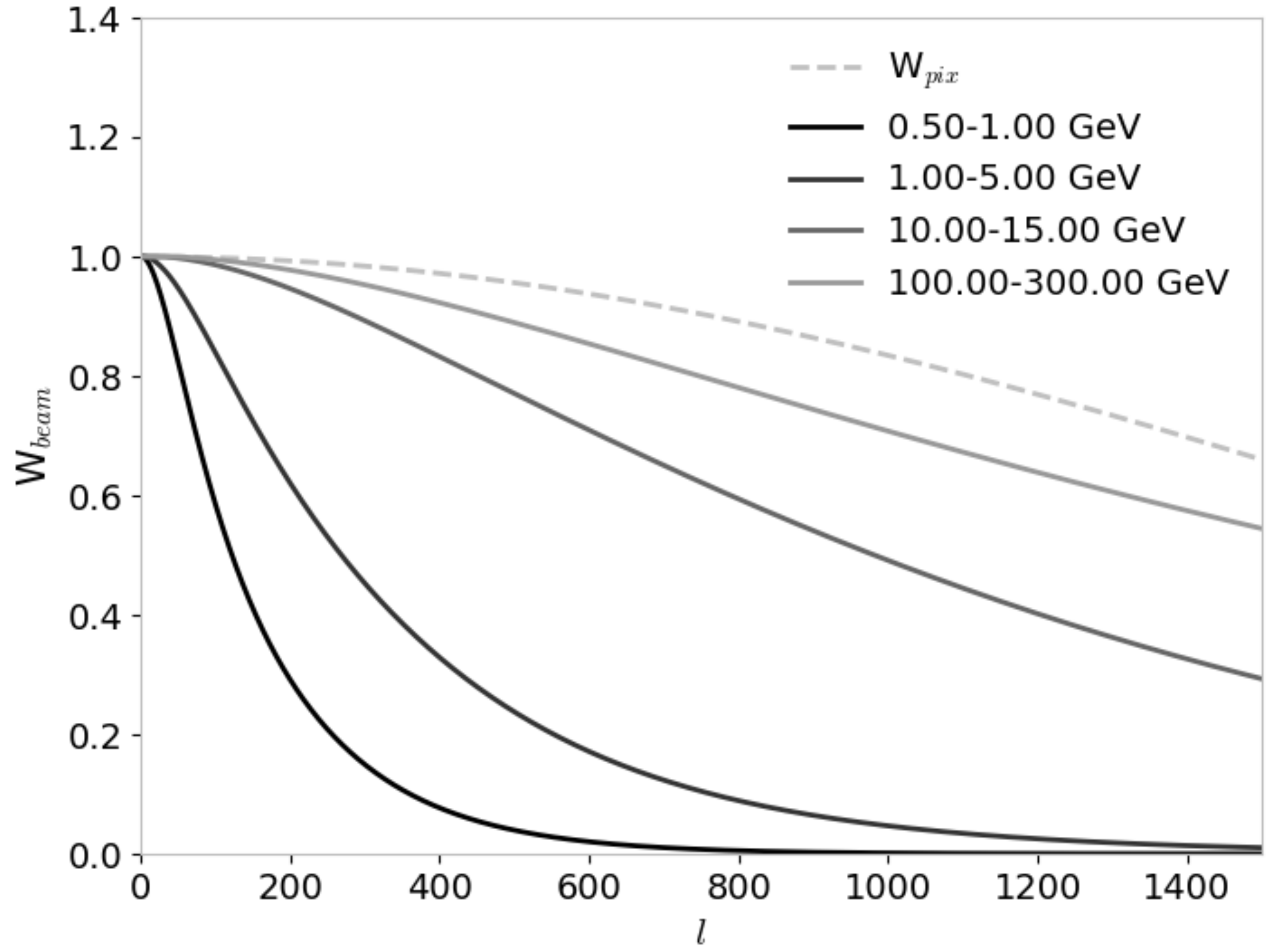

PHOTON 2019
Michela Negro

The White Noise Correction

Computed for each energy bin:

Photon counts

Exposure

$$C_N = \frac{\langle N_{\gamma,pix}/A^2_{\text{pix}} \rangle}{\Omega_{\text{pix}}}$$

Pixel area

The Standard APS estimator

$$C^{\text{sig}}_{\ell,E} = \frac{C^{\text{Pol}}_{\ell} - C_N}{W^2_{\ell,E}}$$

From the APS to the C_P

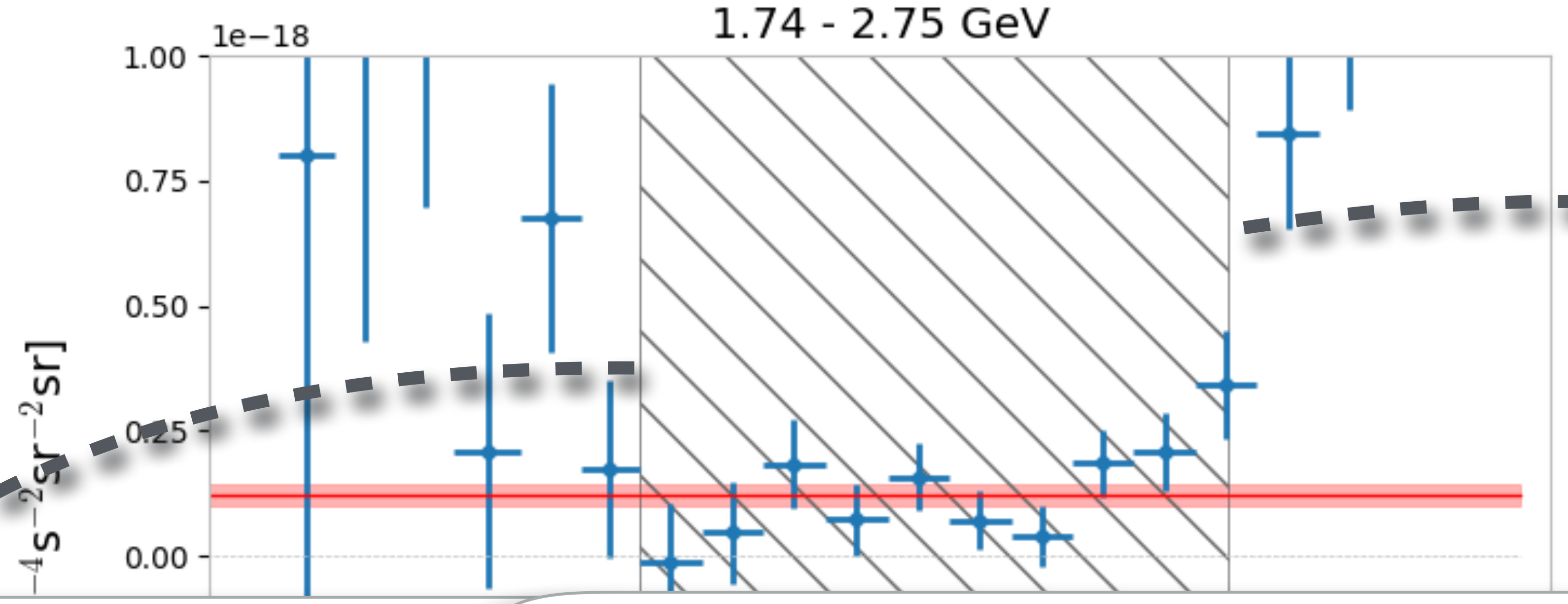

Limit at low multipoles

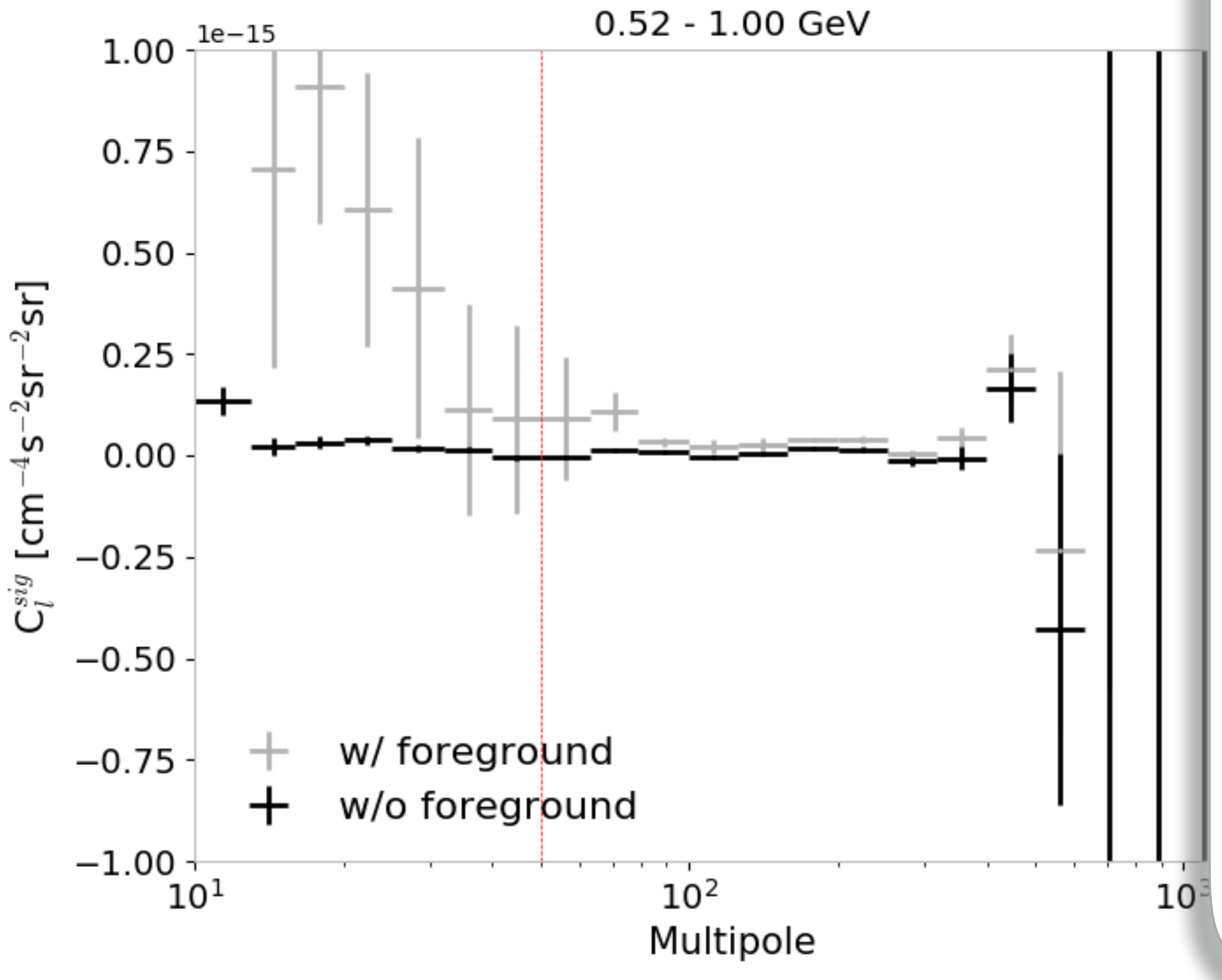

Limit at high multipoles

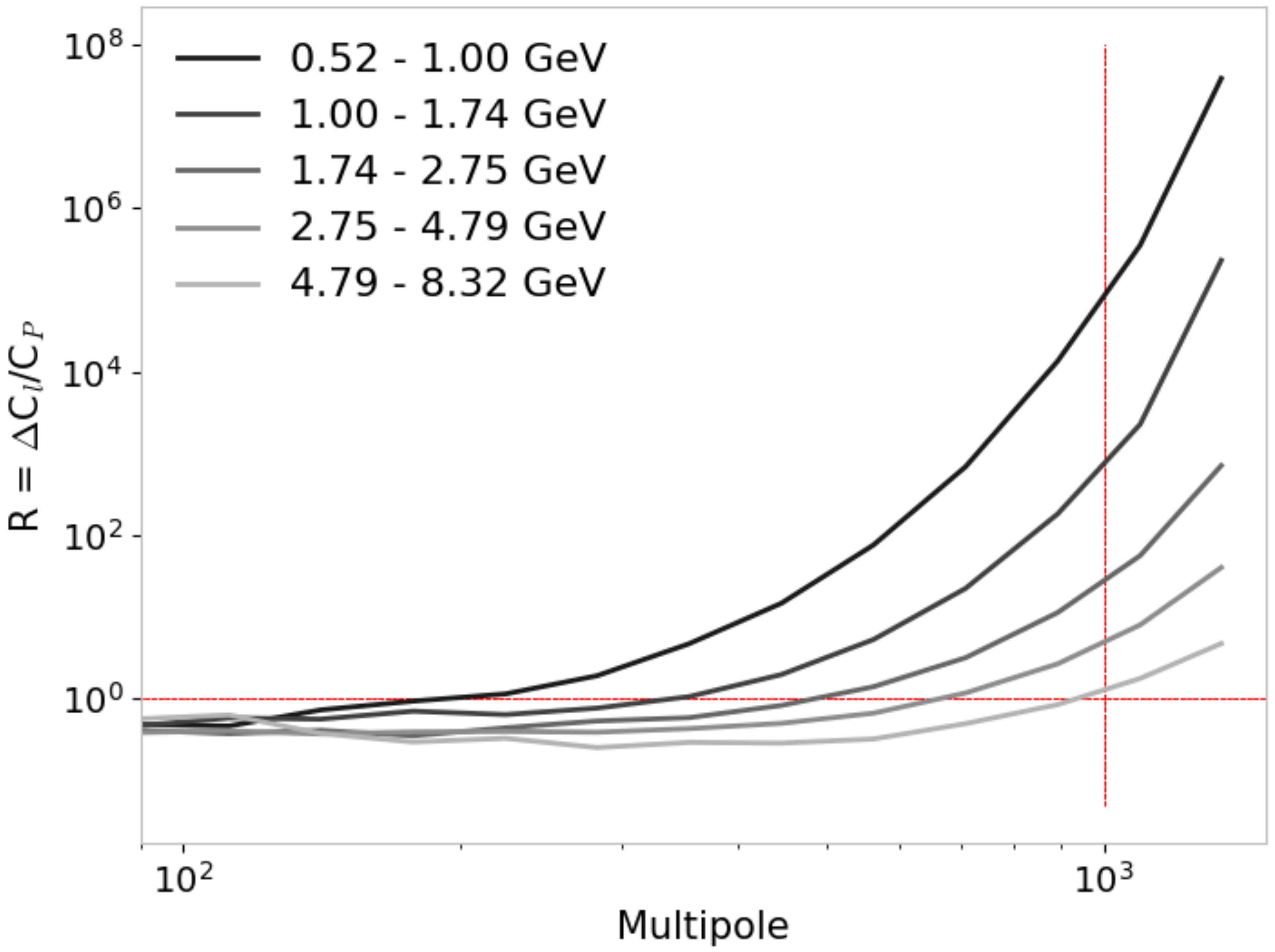

$$R(\ell_{\max}) = \frac{\Delta C_{\ell_{\max}}}{C_{\mathrm{P},\ell_{\max}}}$$

Fermi Source Catalogs

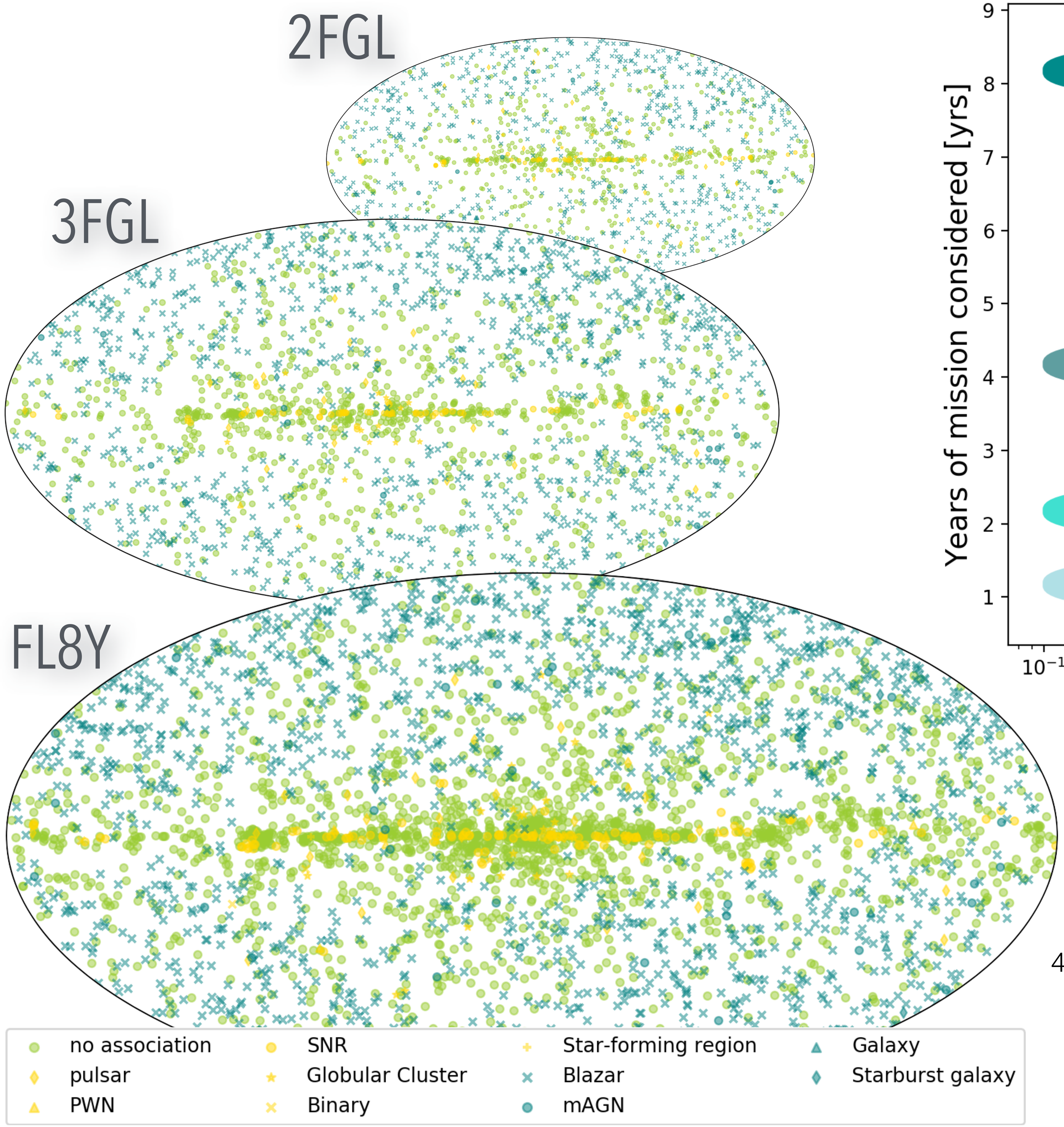

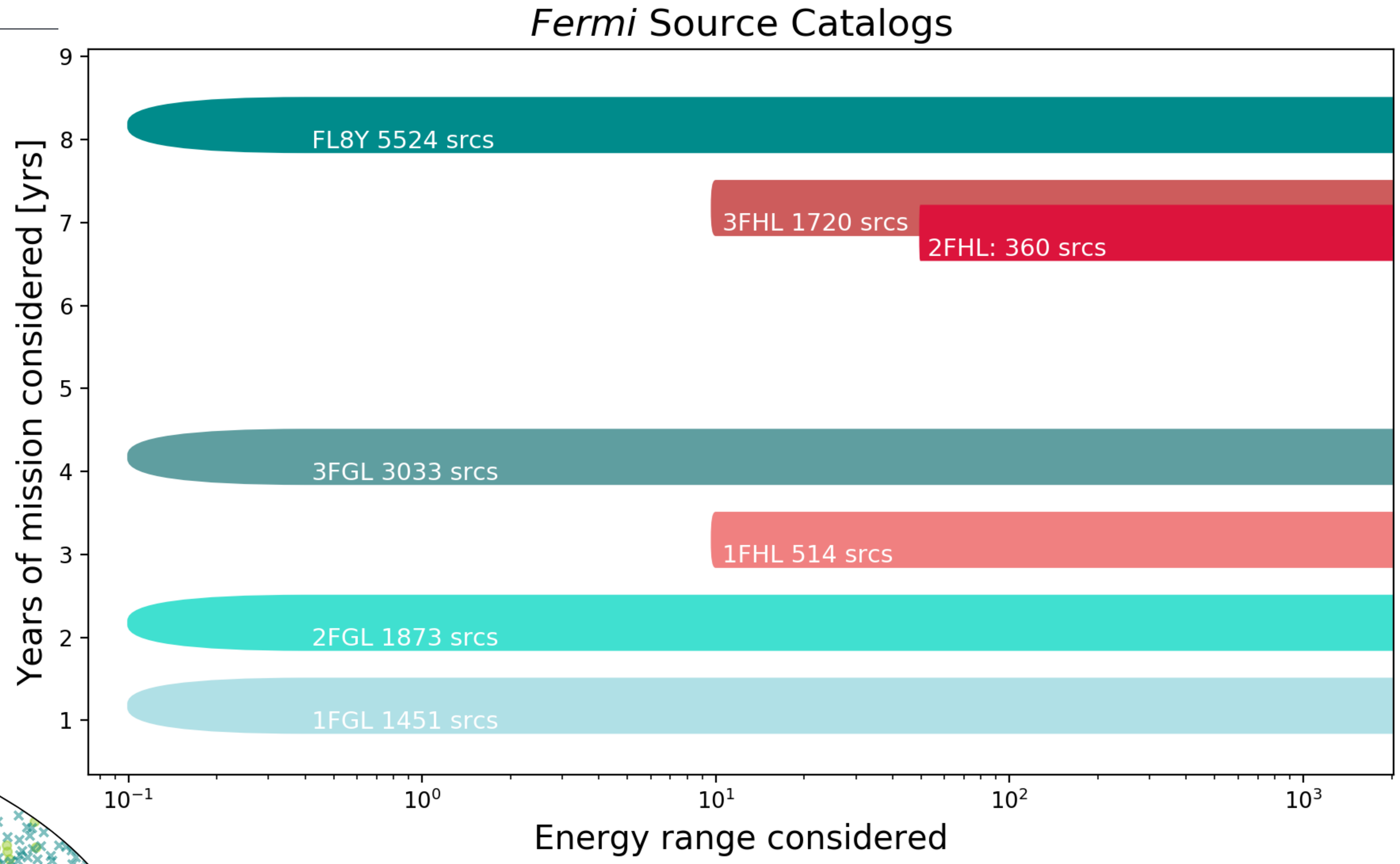

Definition of the source mask radius:

$$\frac{r_{\rm src}(\phi_{\rm src}, E_{\rm min}) - 2 \times {\rm PSF}({\rm E_{min}})}{5 \times {\rm PSF}({\rm E_{min}}) - 2 \times {\rm PSF}({\rm E_{min}})} = \frac{\log(\phi_{\rm src}) - \log(\phi_{\rm min})}{\log(\phi_{\rm max}) - \log(\phi_{\rm min})}$$

Two classes of sources

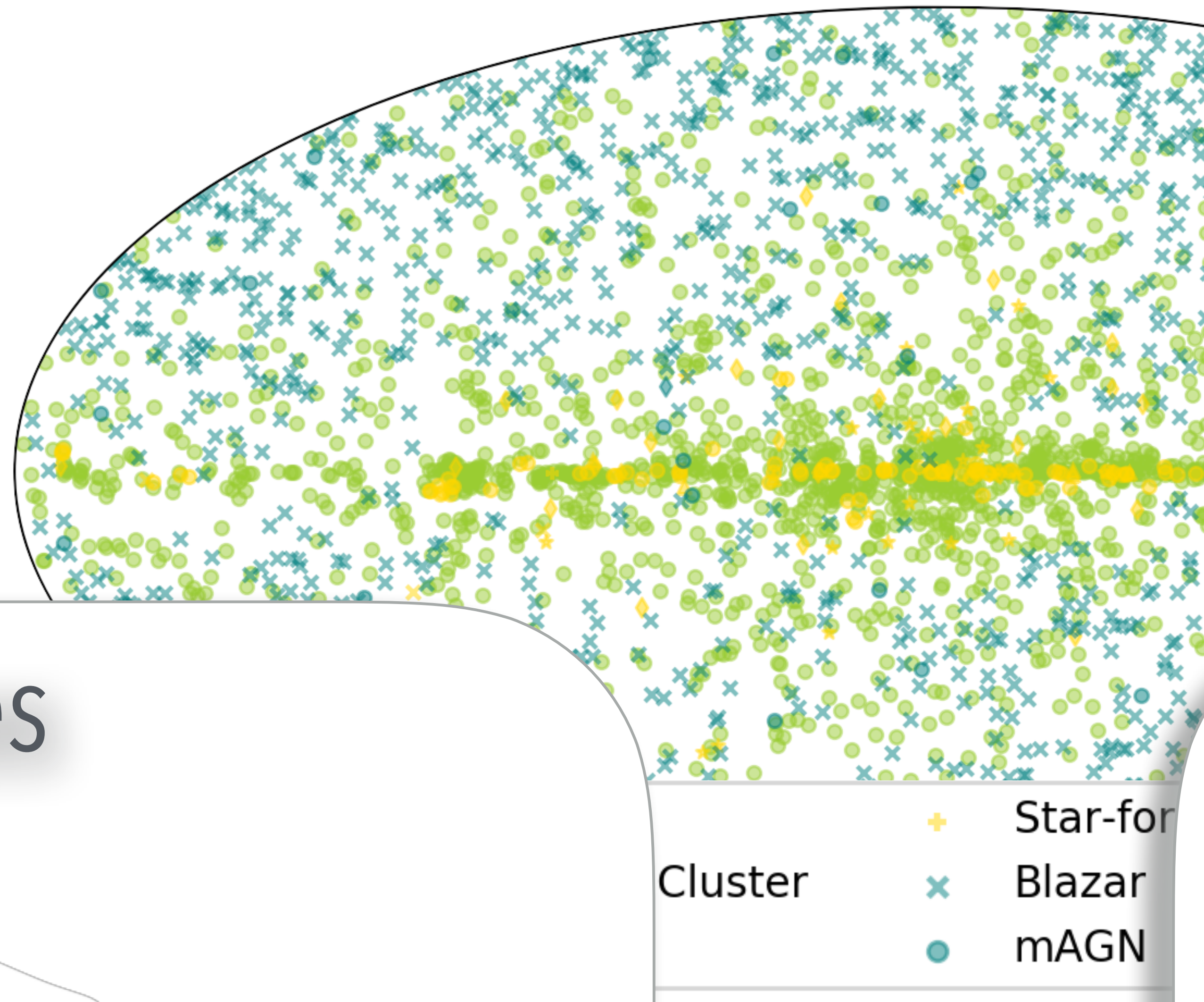

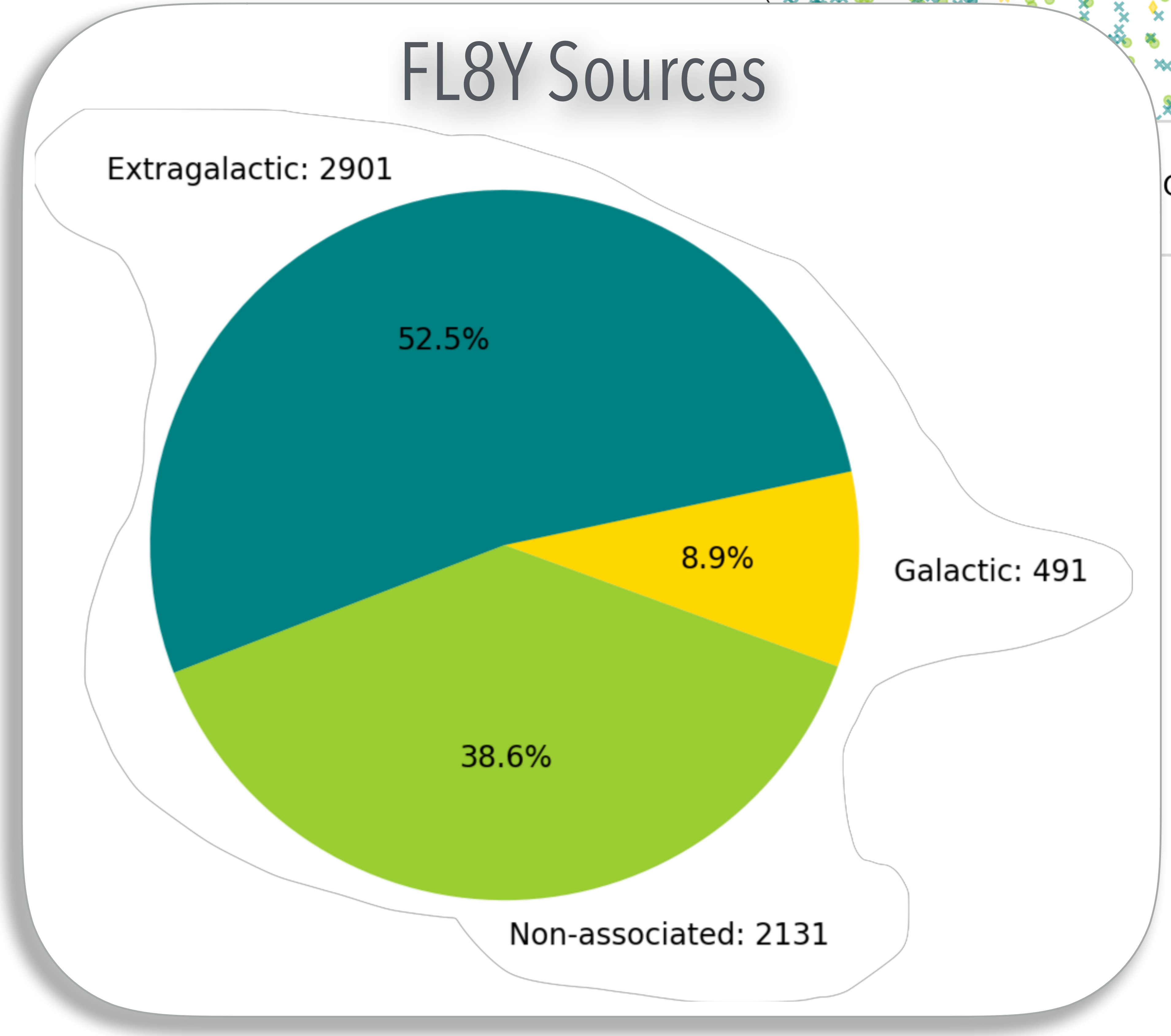

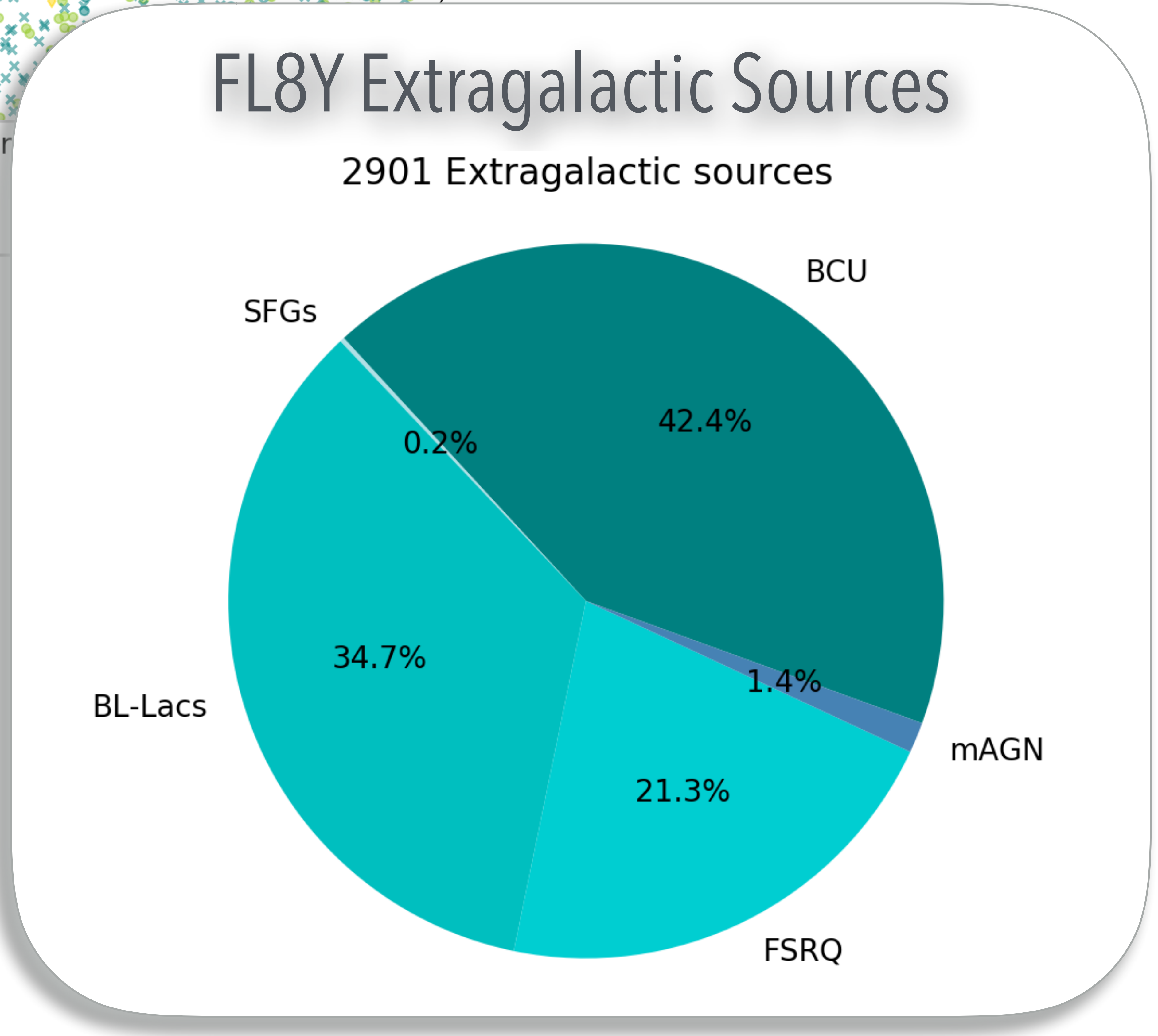

Two classes of sources

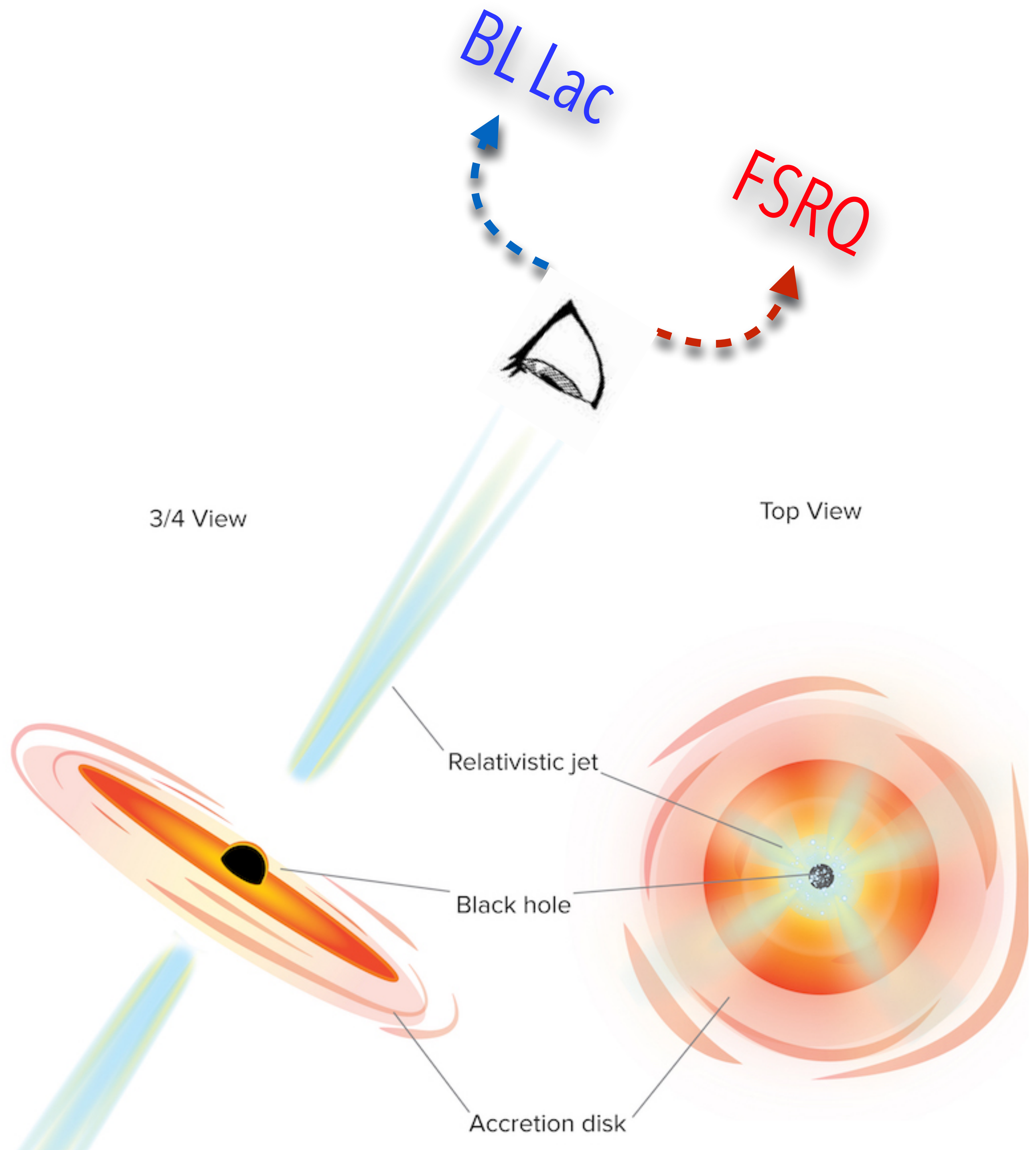

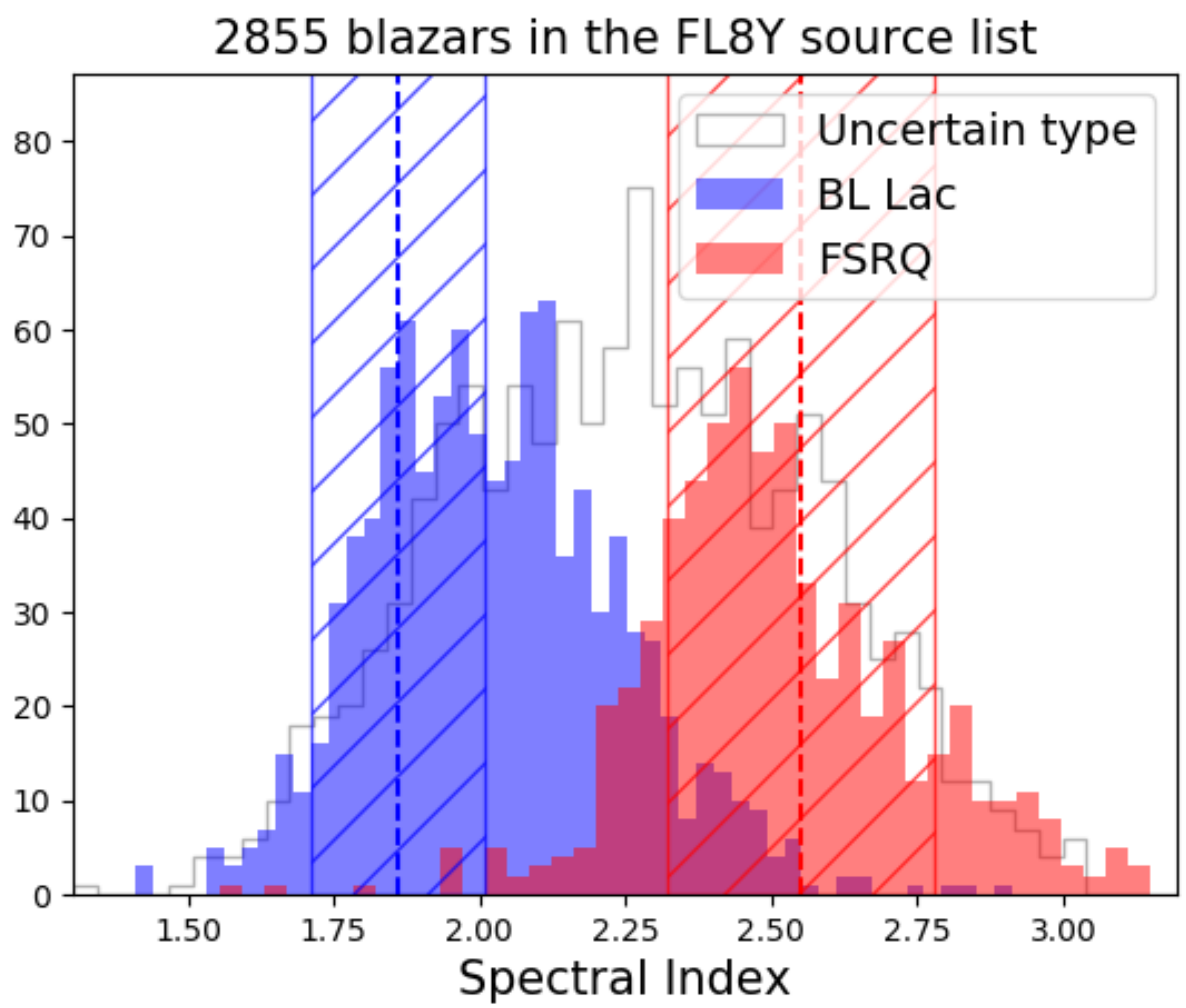

Past Measurements - Ackermann et al. 2012

Autocorrelation to constrain source populations models:

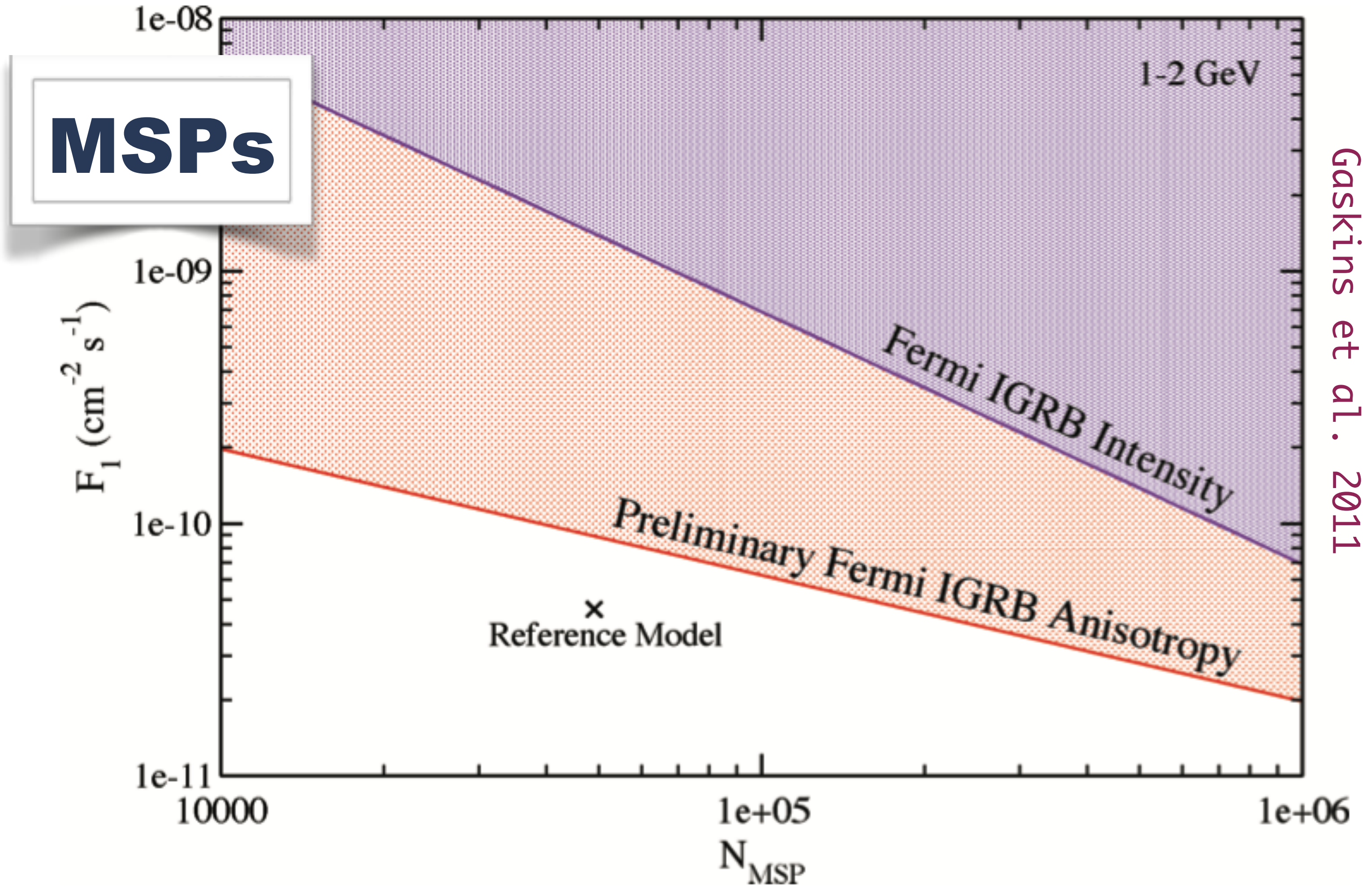

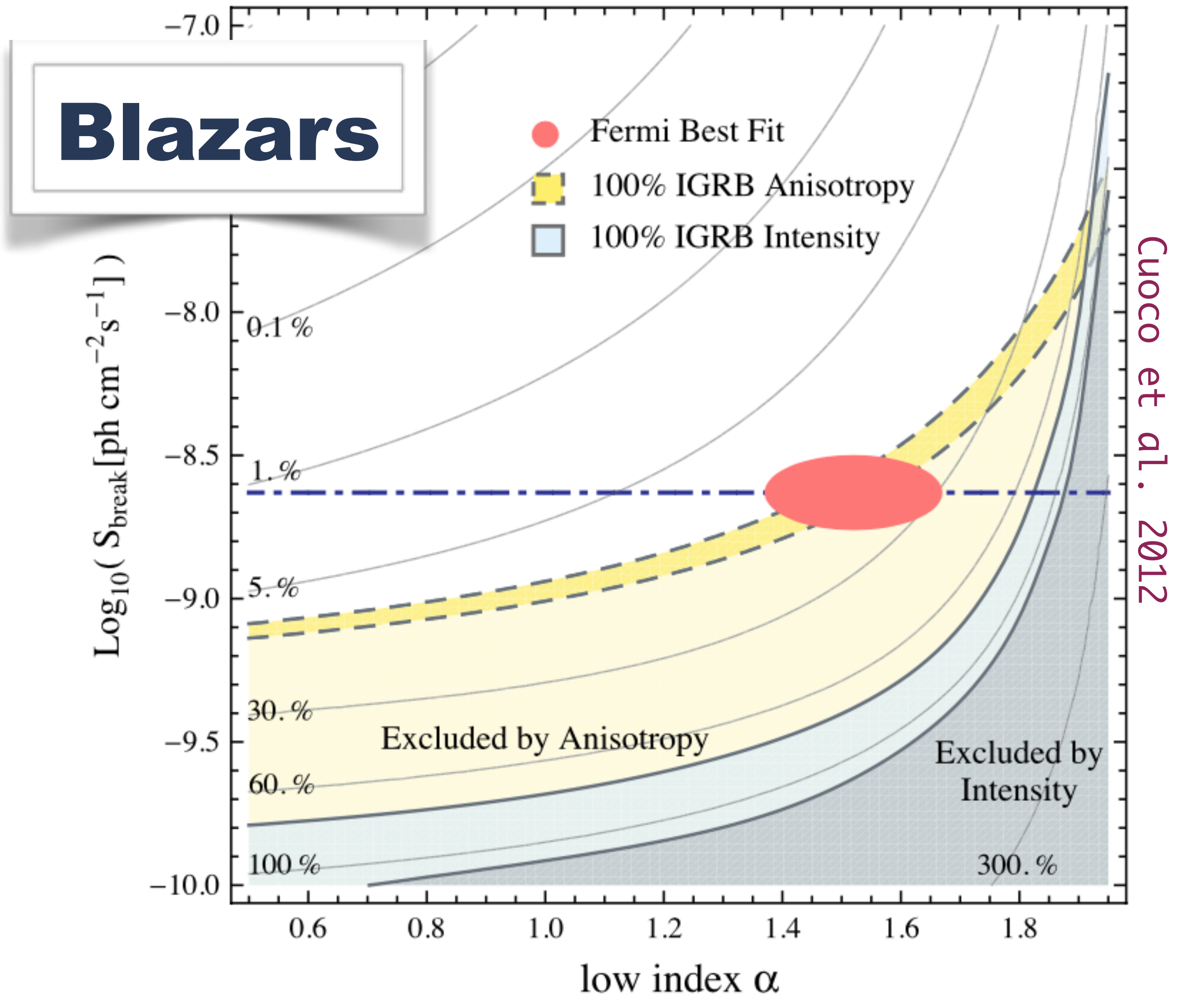

$$I = \int_0^{S_t} S \frac{dN}{dS} dS$$

$$C_P = \int_0^{S_t} S^2 \frac{dN}{dS} dS$$

Source count distribution
(the simplest model: broken power law)

- The majority of anisotropy signal: blazars
- blazars contributes to <20% of the UGRB intensity
- the 80% being due to low-intrinsic-anisotropy component

3) UGRB species do not contribute to intensity and to anisotropy at the same extent!

Zeclin et al. 2016,arXiv:1605.04256v2
Cuoco et al. 2012, arXiv:1701.06988v1

Intensity and anisotropy energy spectra

… as complementary observables of the UGRB:

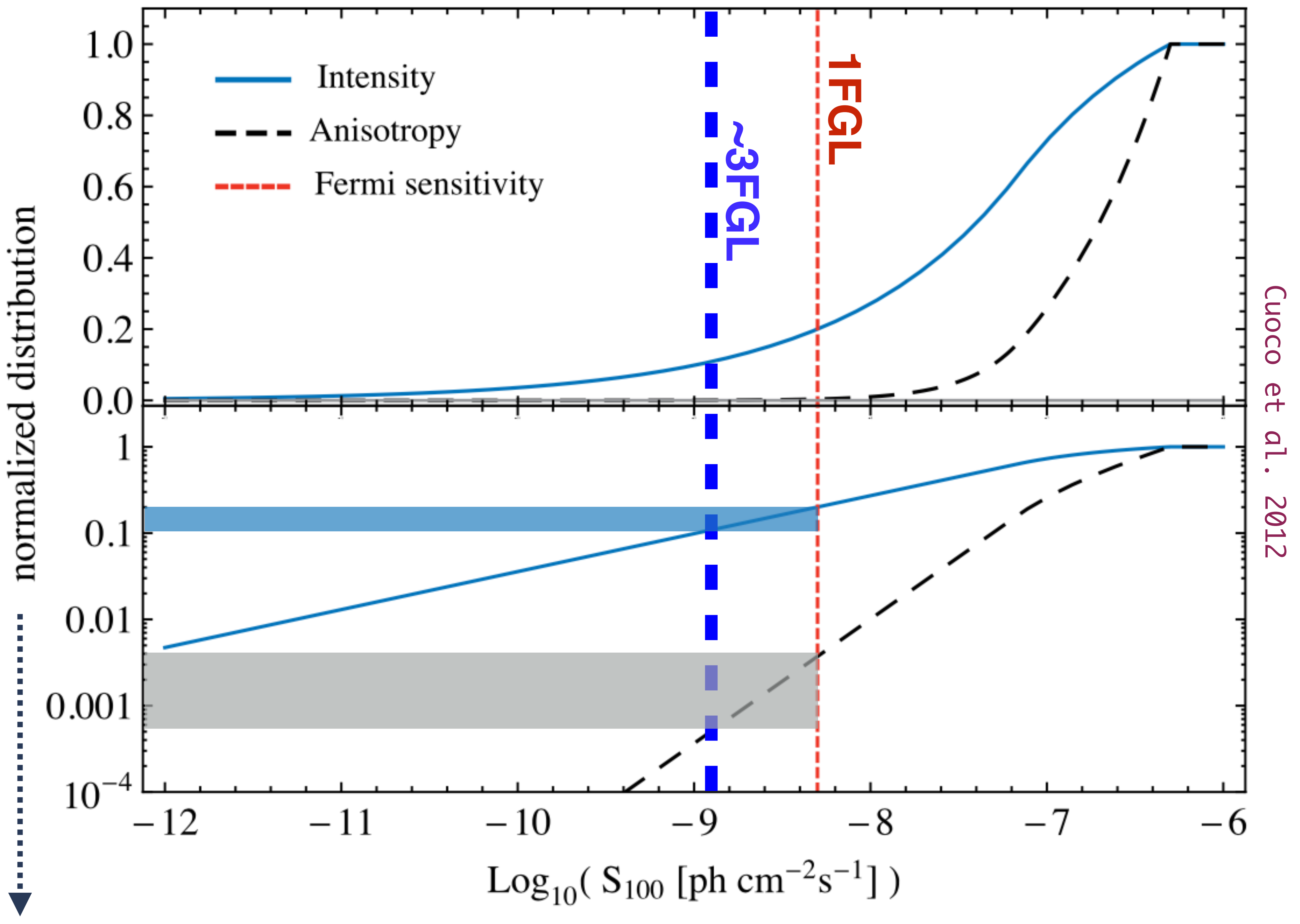

Cumulative contribution of blazar to the Intensity
and to anisotropy as a function of source intensity

The anisotropy from unresolved sources is more strongly dependent on the sensitivity limit: improved point source sensitivity have a more notable impact on the measured IGRB anisotropy.

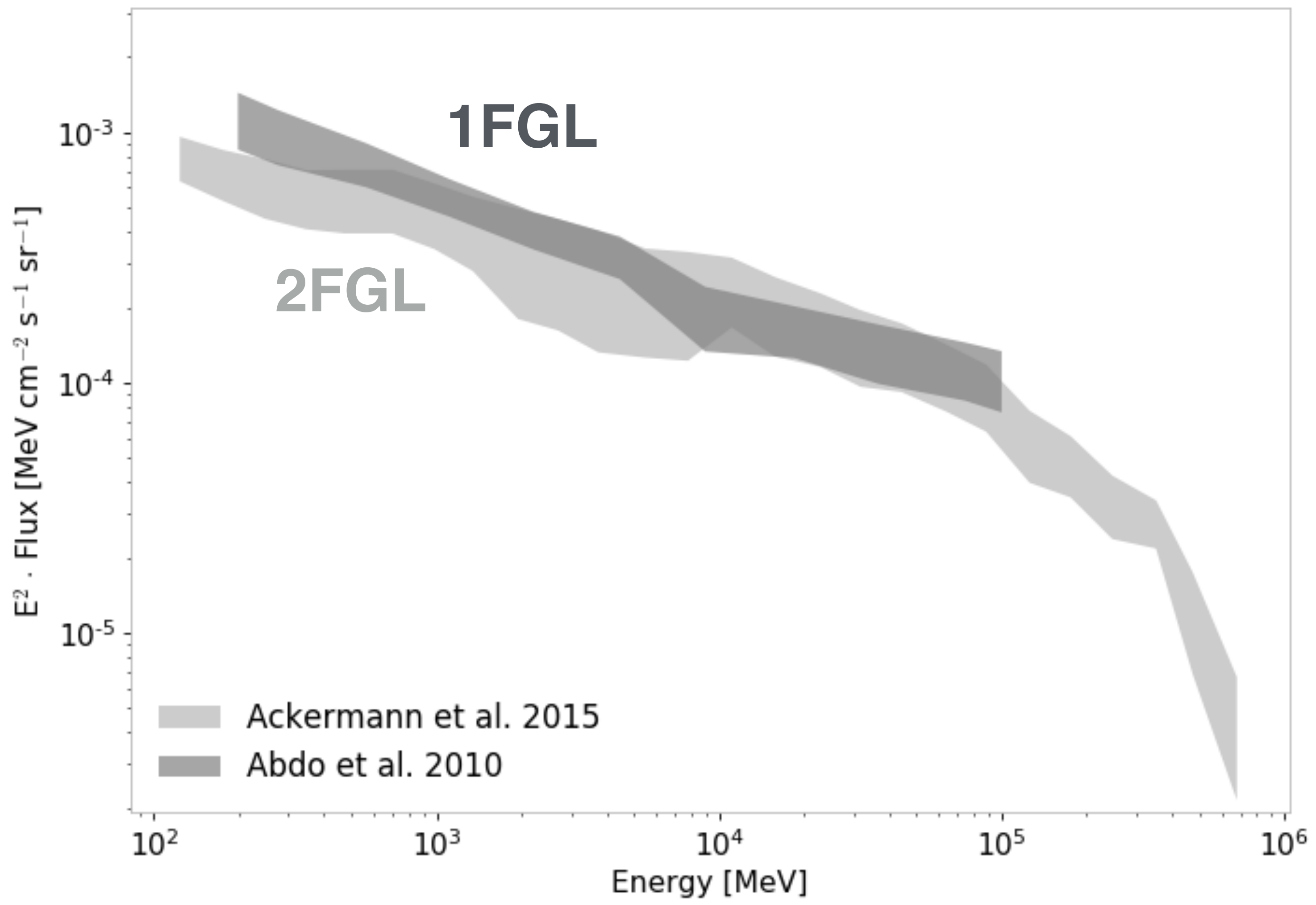

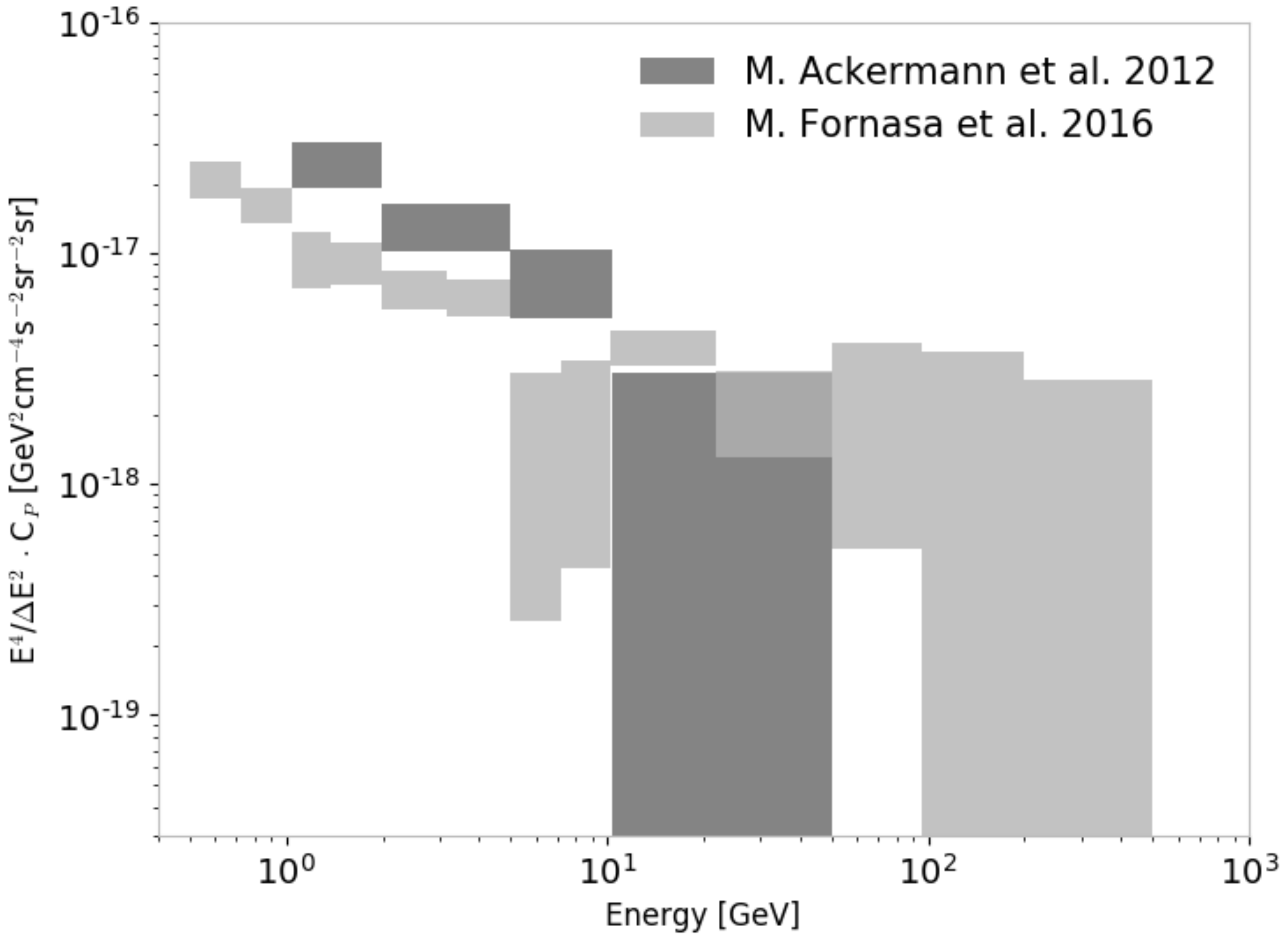

Past Measurements - Fornasa et al. 2016

Autocorrelation to constrain WIMP-like DM parameters:

Conservative exclusion limits on annihilating and decaying DM from the new APS measurement by Fornasa et al. 2016

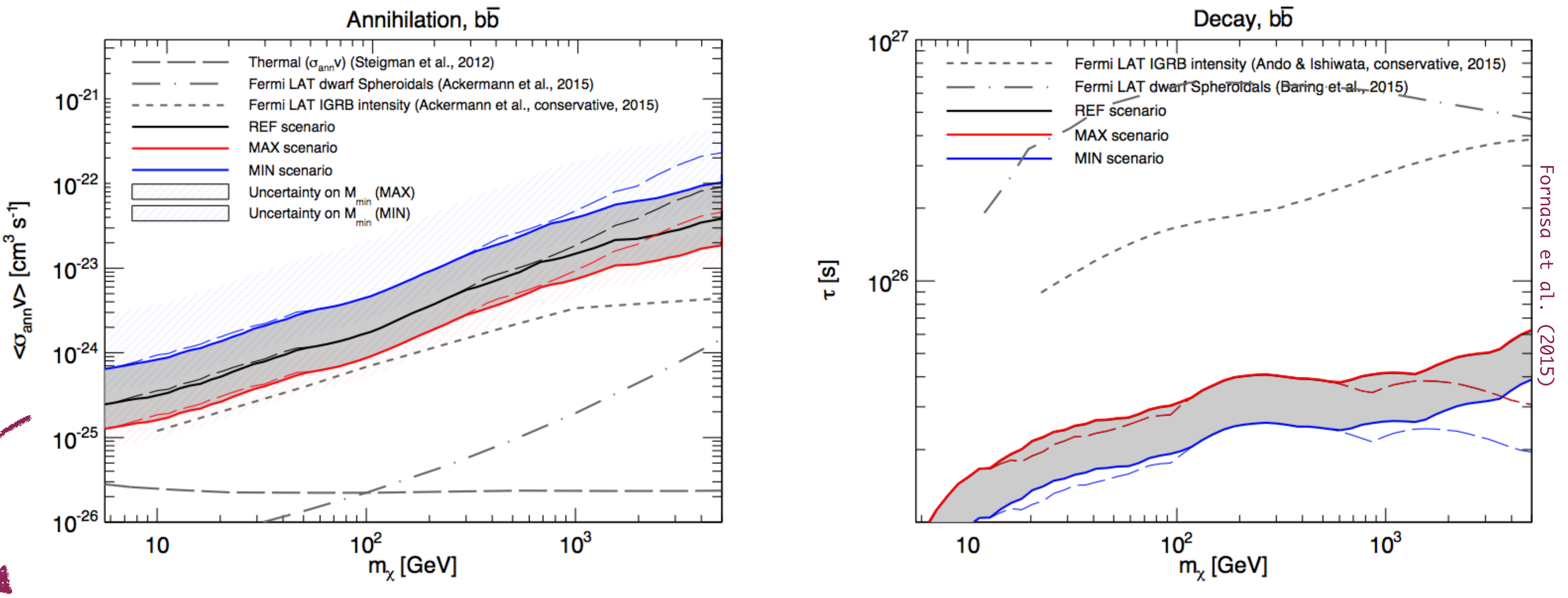

Less stringent than UGRB spectrum limit by factor of 2

PHOTON 2019
Michela Negro

Fornasa et al. 2017, arXiv:1608.07289v2

Past Measurements - Fornasa et al. 2016

Autocorrelation to investigate the UGRB composition:

Blazars VS **Blazars+new-population**:

[Abdo et al. 2017]

Preferred @ 5 σ !

Very steep!!

2.8

3.3